Publicly Accessible Penn Dissertations

2018

Human Chimeric Antigen Receptor Macrophages For Cancer Immunotherapy

Michael Klichinsky
University of Pennsylvania, mklich@pennmedicine.upenn.edu

Human Chimeric Antigen Receptor Macrophages For Cancer Immunotherapy

Abstract

Despite recent landmark advances in chimeric antigen receptor (CAR) T cell immunotherapy for the treatment of human cancer, metastatic solid tumors remain an intractable challenge. Myeloid cells are actively recruited to the tumor microenvironment (TME), where tumor associated macrophages (TAMs) are often the most abundant infiltrating immune cell. Currently, macrophage orientated immunotherapeutic approaches under clinical development in oncology seek to reduce TAM infiltration or enhance TAM phagocytosis. We hypothesized that genetically engineering human macrophages with CARs against tumor-associated antigens could redirect their phagocytic activity and lead to therapeutic efficacy with the potential for the induction of an anti-tumor T cell response.

In this thesis, we demonstrate that CD3-zeta based CARs are capable of inducing phagocytosis by human macrophages. Notably, an active intracellular CAR signaling domain was required for activity. Targeted phagocytosis and clearance of CD19+, mesothelin+, and HER2+ cells by CARs targeted against each respective antigen was significantly superior to that by control untransduced (UTD) macrophages. Importantly, CAR macrophages were capable of polyphagocytosis and serial phagocytosis of tumor cells.

We demonstrate that primary human monocyte derived macrophages, which are resistant to most viral vectors, are efficiently transduced by the chimeric-fiber adenoviral vector Ad5f35. Ad5f35 transduced primary human CAR macrophages demonstrated targeted phagocytosis, with phagocytic activity dependent on both the CAR and antigen densities. CAR, but not UTD, macrophages led to potent dose-dependent killing of tumor cells in vitro and led to tumor regression and improved overall survival in murine xenograft models of human cancer.

Macrophage transduction with Ad5f35 leads to a broad gene expression change, an interferon signaling signature, and induction of a classically activated M1 phenotype. CAR macrophages upregulated co-stimulatory ligand and antigen processing/presentation genes and led to enhanced T cell stimulation in vitro and in vivo. Lastly, CAR, but not UTD, macrophages showed a broad resistance for M2 conversion in response to immunosuppressive cytokines.

In conclusion, human CAR macrophages display targeted tumor phagocytosis, lead to improved overall survival in xenograft models, and demonstrate enhanced T cell stimulation. Taken together, these data show that CAR macrophages are a novel cell therapy platform for the treatment of human cancer.

Degree Type
Dissertation

Degree Name
Doctor of Philosophy (PhD)

Graduate Group
Pharmacology

First Advisor
Saar Gill

Second Advisor
Carl H. June

Keywords

car macrophage, chimeric antigen receptor, chimeric antigen receptor macrophage, macrophage

Subject Categories

Allergy and Immunology | Immunology and Infectious Disease | Medical Immunology | Pharmacology

HUMAN CHIMERIC ANTIGEN RECEPTOR MACROPHAGES FOR CANCER IMMUNOTHERAPY

Michael Klichinsky

A DISSERTATION

in

Pharmacology

Presented to the Faculties of the University of Pennsylvania

in

Partial Fulfillment of the Requirements for the

Degree of Doctor of Philosophy

2018

Supervisor of Dissertation   Co-Supervisor of Dissertation

_____   _____

Saar Gill, MD PhD   Carl H. June, MD

Assistant Professor of Medicine   Richard W. Vague Professor in

                                                           Immunotherapy

Graduate Group Chairperson

_____

Julie A. Blendy, PhD, Professor of Pharmacology

Dissertation Committee

Gregory Beatty, MD, PhD, Assistant Professor of Medicine

Vladimir R. Muzykantov, MD PhD, Professor of Pharmacology

Daniel Powell, PhD, Associate Professor of Pathology and Laboratory Medicine

Wenchao Song, PhD, Professor of Pharmacology

DEDICATION

To my best-friend and wife: Mila Furman

To my loving family: Svetlana, Edward, and Paula Klichinsky

ACKNOWLEDGMENT

ABSTRACT

HUMAN CHIMERIC ANTIGEN RECEPTOR MACROPHAGES FOR CANCER

IMMUNOTHERAPY

Michael Klichinsky, PharmD

Saar Gill, MD PhD

Carl H. June, MD

Despite recent landmark advances in chimeric antigen receptor (CAR) T cell

immunotherapy for the treatment of human cancer, metastatic solid tumors remain an

intractable challenge. Myeloid cells are actively recruited to the tumor microenvironment

(TME), where tumor associated macrophages (TAMs) are often the most abundant

infiltrating immune cell. Currently, macrophage orientated immunotherapeutic

approaches under clinical development in oncology seek to reduce TAM infiltration or

enhance TAM phagocytosis. We hypothesized that genetically engineering human

macrophages with CARs against tumor-associated antigens could redirect their

phagocytic activity and lead to therapeutic efficacy with the potential for the induction of

an anti-tumor T cell response.

In this thesis, we demonstrate that CD3-zeta based CARs are capable of inducing

phagocytosis by human macrophages. Notably, an active intracellular CAR signaling

domain was required for activity. Targeted phagocytosis and clearance of CD19+,

mesothelin+, and HER2+ cells by CARs targeted against each respective antigen was

significantly superior to that by control untransduced (UTD) macrophages. Importantly,

CAR macrophages were capable of polyphagocytosis and serial phagocytosis of tumor cells.

We demonstrate that primary human monocyte derived macrophages, which are resistant to most viral vectors, are efficiently transduced by the chimeric-fiber adenoviral vector Ad5f35. Ad5f35 transduced primary human CAR macrophages demonstrated targeted phagocytosis, with phagocytic activity dependent on both the CAR and antigen densities. CAR, but not UTD, macrophages led to potent dose-dependent killing of tumor cells *in vitro* and led to tumor regression and improved overall survival in murine xenograft models of human cancer.

Macrophage transduction with Ad5f35 leads to a broad gene expression change, an interferon signaling signature, and induction of a classically activated M1 phenotype. CAR macrophages upregulated co-stimulatory ligand and antigen processing/presentation genes and led to enhanced T cell stimulation *in vitro* and *in vivo*. Lastly, CAR, but not UTD, macrophages showed a broad resistance for M2 conversion in response to immunosuppressive cytokines.

In conclusion, human CAR macrophages display targeted tumor phagocytosis, lead to improved overall survival in xenograft models, and demonstrate enhanced T cell stimulation. Taken together, these data show that CAR macrophages are a novel cell therapy platform for the treatment of human cancer.

TABLE OF CONTENTS

LIST OF TABLES

LIST OF ILLUSTRATIONS

CHAPTER 1. Introduction

Overview

Immunotherapy has been solidified as one of the pillars in modern cancer treatment. In particular, chimeric antigen receptor (CAR) T cells have demonstrated unprecedented efficacy in relapsed and refractory hematologic malignancy. Despite the success in leukemia, lymphoma, and myeloma, the response to T cell based adoptive cellular therapy in metastatic solid tumors has been minimal. Though the mechanism of resistance is not clearly understood, the role of the tumor microenvironment, consisting of the non-neoplastic cells within a tumor, is likely paramount to the inhibitory effect tumors have on tumor reactive T cells. Studies have shown that macrophages are a key component of the tumor microenvironment and aid in the development of all known hallmarks of tumor development, invasion, and metastasis. Accordingly, macrophages are often the most abundant leukocyte in the microenvironment of common human solid tumors.

Given the active recruitment of myeloid cells to tumors, we hypothesized that genetically engineering macrophages with chimeric antigen receptors may be an effective approach to attacking cancer. In essence, the mechanism of the approach can be described with the "Trojan Horse" analogy – in which the tumor recruits macrophages to feed its pro-tumoral and immune-suppressive milieu, but the engineered macrophages are rewired to attack the tumor in response to surface bound tumor associated antigens. Furthermore, given that macrophages are sentinel cells of the immune system and professional antigen

presenting cells (APCs), they have the potential to initiate an adaptive immune response against tumor neoantigens via the process of antigen processing and presentation.

In this thesis, we explore the concept of rewiring macrophage activity through genetic manipulation. We test the hypothesis that phagocytosis can be programmed via chimeric antigen receptor introduction into human macrophages. We evaluate the anti-tumor potential of CAR macrophages targeted against relevant human tumor associated antigens in relevant in vitro and in vivo models of human cancer. Importantly, this work utilizes primary human monocyte derived macrophages, and thus has immediate potential for translation into clinical studies.

Finally, we assess the role of phenotype on the activity of ex vivo differentiated CAR macrophages and assess the potential for passive induction of the anti-tumor pro-inflammatory macrophage phenotype by using an immunostimulatory viral vector. Furthermore, the potential for downstream subversion of CAR macrophage phenotype toward a tumor-promoting M2 state in response to immunosuppressive cytokines is assessed.

The data presented and discussed in this thesis introduce, for the first time, the concept of targeting cancer with chimeric antigen receptor macrophages. By genetically manipulating macrophages, we show that these innate immune cells can be bestowed with adaptive specificity. Given the importance of immunotherapeutic approaches to the treatment of human cancer, and the paramount medical need in the setting of metastatic

solid tumors, the therapeutic approach presented in this thesis introduces a novel cellular

immunotherapeutic platform with direct translational potential for human disease.

Cancer, the immune system, and the role of macrophages

Cancer

The discovery of the language that encodes life – DNA – unlocked our understanding of the mechanism by which information is processed and transmitted both horizontally (cell division) and vertically (reproduction). Insight into the replication and fidelity of the genetic code provides insight into the mechanisms of Darwinian evolution and one of the most complex diseases in modern man – cancer. The mechanisms for the development of cancer are fundamentally rooted in Darwinian evolution. Random mutations provide for genetic diversity. The human haploid genome is composed of 3.2×10^9 nucleotides, and our DNA replication machinery has an error rate of approximately 1×10^{-8} – one error per every hundred million bases replicated. DNA replication machinery has built-in error detection and correction mechanisms, with a proof-reading and correction rate of approximately 99%. Taken together, these estimates suggest that the error rate of human DNA replication is approximately 1×10^{-10} – one error per every ten billion bases replicated. On average there are 0.32 mutations per every genome replication event.

Though environmental factors such as carcinogen exposure or rare inherited mutations enhance the risk of cancer formation by accelerating mutation rate, the occurrence of cancer is a matter of stochasticity and probability. If there are 0.32 uncorrected mutations per each genomic replication, and the average adult human body is estimated to be composed of trillions of cells, there is a clear potential for the random occurrence of a

non-synonymous mutation in genes that allow for the uncontrolled proliferation and avoidance of apoptosis that lead to cancer. The necessity for non-synonymous and non-biochemically inert mutations in proto-oncogenes and tumor suppressor genes for the induction of cancer further reduce the likelihood of transformation by several orders of magnitude. While these rough estimates and considerations are fundamental to the understanding of cancer, the real test is in the epidemiology of the disease.

As of 2015, 38.4% of men or women will develop and receive a cancer diagnosis in their lifetimes. In 2018, there are an estimated $1.7x10^6$ new cases of cancer in the United States alone, with an approximately $6.1x10^5$ cancer deaths. In 2018, the most common cancers in the US are (from most to least frequent): breast cancer, lung cancer, prostate cancer, colon and rectal cancer, melanoma, bladder cancer, non-Hodgkin lymphoma, kidney cancer, endometrial cancer, leukemia, pancreatic cancer, thyroid cancer, and liver cancer.

Logically, the incidence of cancer increases with age, and as the median lifespan of our population increases, so does the incidence of cancer. Despite a continuing trend of increased numbers of cancer diagnoses, the overall rate of cancer deaths in the United States has decreased by 25% between 1990 and 2014 – highlighting the progress that has been made in early detection, surgical technique, radiotherapy, and pharmacologic treatment.

While the acquisition of multiple, random, synergistic mutations in proto-oncogenes and tumor suppressor genes underlies all cancers, the term cancer encompasses a broad family of diverse diseases with unique characteristics, pathologies, and responses to

treatment. Hanahan and Weinberg proposed a number of characteristics which underlie the development of cancer, including: self-sufficiency in growth signals, insensitivity to anti-growth signals, evasion of programmed cell-death, limitless replicative potential, sustained angiogenesis, and tissue invasion/metastasis (Hanahan & Weinberg 2000).

While the initial transformation of a normal cell into a neoplastic cell is a cell-intrinsic event, the impact of surrounding normal tissue on the development of the tumor is of paramount importance to the growth, survival, immune evasion, invasion, and metastasis of tumors. The term "tumor microenvironment" (TME) describes the infiltrating milieu of non-neoplastic cells within a tumor, including stromal cells, fibroblasts, endothelial cells, podocytes, and leukocytes. In this thesis, we describe the role of macrophages in the tumor microenvironment, methods by which they exert protumor function, and approaches to harness their effector function against cancer.

The tumor microenvironment and cancer immunity

As neoplastic cells grow, they require the orchestration of a complex series of events in order to form tumors – a phenomenon which neoplastic cells cannot perform on their own. Organs are composed of various tissues and cell types performing independent roles which complement each other's functions. In addition, cells within an organ are constantly communicating via various feedback and regulatory mechanisms. Tumors, like organs, consist of a variety of cell types in addition to neoplastic cells, with the

6

specific subtypes of normal cells present and their relative abundances varying amongst tumor types and individual patients. The TME is composed of a heterogenous mixture of the following non-neoplastic cells: monocytes, macrophages, myeloid precursors, myeloid derived suppressor cells, granulocytes, granulocyte precursors, cytotoxic T cells, regulatory T cells, NK cells, plasma cells, fibroblasts, stromal cells, mesenchymal stem cells, endothelial cells, podocytes, and others.

Given that cancer is a disease founded on genetic mutation, non-synonymous mutations in protein-coding genes have the potential to produce neoantigens. Early studies in the laboratory of Robert Schreiber showed that cells of the immune system, specifically T cells, have the potential to react against tumor cells carrying neoantigens via MHC-I peptide complex recognition and cytolysis by CD8+ cytotoxic T lymphocytes. Schreiber demonstrated that tumors readily engrafted in genetically engineered immunodeficient mice, but often failed to grow in immunocompetent mice of the same genetic background in the same period of time. In addition, when CD8+ T cells were genetically inhibited or pharmacologic depleted in immunocompetent mice, tumor engraftment and growth improved. These results suggest that while tumors consist of host self-cells, and self-tolerance is established in the thymus during early development, mutated neoantigens hold the potential to break self-tolerance and allow immune recognition of tumor neoantigens. In fact, this finding let to Schreiber's theory of immunoediting, suggesting that Darwinian evolution is, again, at work in the development of cancer – only cells that are able to avoid immune recognition survive the elimination phase of immunoediting, and eventually outgrow following an equilibrium phase. Alternatively, or in addition to

immunoediting, tumors can shut down neoantigen reactive T cell attack by mechanisms including MHC-I downregulation, production of immunosuppressive cytokines, physical T cell exclusion, and induction of T cell exhaustion via augmented checkpoint interactions such that the T cells are unable to exert immune selective pressure on the tumor (Dunn et al. 2004; Dunn et al. 2002; Schreiber et al. 2011).

The concept of immune evasion and immunoediting is considered one of the hallmark enabling characteristics of cancer, along with genomic instability and mutation. In fact, the genomic mutation frequency in cancer correlates with better outcomes and better response to immunotherapy, solidifying the concept that more mutations result in more neoantigens and an increased likelihood for T cell mediated attack. Furthermore, there is abundant evidence that an increased CD8 T cell infiltration in the TME results in better overall survival in a number of different human cancers. Conversely, there is an inverse relationship between macrophage infiltration and overall survival and response to immunotherapy – more macrophages are associated with a poor prognosis. Below, we discuss the biology of macrophages and the means by which they promote tumor progression.

The role of macrophages in cancer

Macrophages are highly plastic cells, capable of adapting to diverse tissues and environmental stimuli. The fact that monocytes/macrophages can extravasate, traffic, and

persist within diverse and hypoxic tissues, and have the potential to exert both pro-inflammatory and anti-inflammatory effects, makes them the perfect candidate immune cell for tumors to recruit. Tumors actively recruit myeloid cells in the form of both peripheral blood monocytes and neighboring normal tissue resident macrophages by the production of chemokines (e.g. CCL2), growth factors (e.g. CSF-1), and other soluble factors (Noy & Pollard 2014). As discussed above, cancer is elegantly defined by several hallmarks described by Hanahan and Weinberg, which were updated in 2011 to include inflammation, immune evasion, and metabolic reprogramming. Table 1.1 summarizes the tumor promoting role of macrophages and provides examples of how each hallmark is actively enabled or promoted by tumor associated macrophages.

Table 1.1: Methods of macrophage enablement of the Hallmarks of Cancer

Hanahan & Weinberg Hallmark of Cancer	Method of macrophage enablement
Genomic instability	Release of reactive oxygen species
Invasion and metastasis	Secretion of proteases at tumor margin (i.e. metalloproteinases and cysteine cathepsin proteases); establishment of the pre-metastatic niche
Sustained proliferation	Production of growth factors (i.e. EGF)

Limited cell death	Activation of anti-apoptotic genes (i.e. survival factors)
Enhanced angiogenesis	Secretion or activation of angiogenic factors (i.e. VEGF)
Immune evasion	Release of immunosuppressive cytokines (i.e. secretion of IL-10, TGF-beta; Expression of immunosuppressive checkpoint ligands and receptors (i.e. PDL-1 and SIRP-alpha)
Chronic inflammation	Release of inflammatory mediators (IL1-alpha and IL1-beta), recruitment of inflammatory immune cells (via chemokine production i.e. CCL5, CCL22)

Outside of the tumor microenvironment, macrophages are key orchestrators and regulators of the innate immune system. Macrophages can be found in every tissue of the body, where they can adapt unique phenotypes and serve specified functions (Haldar & Murphy 2014). In the liver, macrophages adopt a Kupffer cell phenotype, upregulating phagocytic capacity in order to actively patrol the blood flow for pathogens, senescent erythrocytes, and apoptotic bodies (Nguyen-Lefebvre & Horuzsko 2015). In addition, Kupffer cells break down hemoglobin into bilirubin and play a key role in iron metabolism. In the spleen, splenic red zone macrophages are particularly well adapted at the phagocytosis of senescent red cells and iron recycling. In the brain, macrophages form microglial cells, capable of regulating neuronal synapse formation, axonal pruning, and many other functions (Saijo & Glass 2011). In the lung, macrophages form alveolar macrophages, particularly well adapted at the function of surfactant recycling and first

response to environmental pathogens, allergens, particulates, and toxins (Hussell & Bell 2014). Macrophages are particularly abundant in the submucosal lining of outward facing tissues, such as the respiratory system, the gastrointestinal system, and the skin – where they provide a key innate protective role in the form of phagocytosis and acute inflammatory response. Together, these cells types (and many other known and unknown macrophage subtypes) form the mononuclear phagocyte system, also known as the reticuloendothelial system.

Despite their known role in the promotion of tumor progression, inflammation, immunosuppression, invasion, and metastasis, macrophages also have anti-tumor potential – phagocytic destruction of tumor cells, T cell recruitment, degradation of fibrosis, reduction of angiogenesis, antigen presentation, and T cell stimulation. Macrophages can adopt a broad spectrum of activation states in response to environmental cues, cell-cell interactions, soluble factors, and metabolic factors. Though an oversimplified approach to the highly complex potential of macrophage activation states, the field has adopted the terms M1 (classically activated) and M2 (alternatively activated) to represent the polar opposite ends of the macrophage activation spectrum. M1 macrophages are associated with a pro-inflammatory, anti-tumor phenotype, in that they upregulate co-stimulatory ligands, antigen processing and presentation genes, MHC molecules, lymphocyte recruiting chemokines, and activating cytokines (e.g. interferons, TNF-alpha, IL-12, IL1-b, others). M2 macrophages, on the other hand, are anti-inflammatory, immunosuppressive, and pro-tumoral. M2 macrophages produce immunosuppressive factors such as IL-10 and TGF-beta, upregulate checkpoint ligands

such as PDL-1, and promote the invasion, metastasis, fibrosis, and angiogenesis of tumors. The terms M1 and M2 stem from the TH1 and TH2 type immune responses with which they associate.

In table 1.2 we summarize and show examples of macrophage stimuli and the resulting phenotype.

Table 1.2: Diverse inputs lead to variable macrophage activation states

Input	Receptor	Resulting Phenotype
Interferon-gamma (IFNγ)	IFNGR1	Classically activated / M1
Lipopolysaccharide (LPS)	TLR4 / CD14	Classically activated / M1
TNF-alpha (TNFα)	TNFR1	Classically activated / M1
Beta-glucan (β-glucan)	Dectin-1	Classically activated / M1
Interleukin-4 (IL-4)	IL4RA1	Alternatively activated / M2
Interleukin-13 (IL-13)	IL13RA1 / IL4RA1	Alternatively activated / M2
Interleukin-10 (IL-10)	IL10RA	Alternatively activated / M2
Apoptotic cell bodies	CD36, SRA, MARCO, SR-B1, CD68, MER, CD91, LRP1, JMJD6	Alternatively activated / M2

Human macrophage phenotype and activation state, though oft over-simplified and highly variable on epigenetic and transcriptomic levels, can be assessed by easily detectable and measurable surface proteins that are upregulated or downregulated depending on the stimuli to which the cell has been exposed. In table 1.3, we summarize

the common human macrophage surface markers used in flow cytometry and

immunohistochemistry:

Table 1.3: Common human macrophage markers and associated

function/phenotype

Marker	Function	Associated phenotype/marker purpose
CD11B (ITGAM)	Adhesion/migration	Myeloid identity
CD14	LPS co-receptor	Myeloid identity
CD68 (macrosialin)	Scavenger/lectin/selectin receptor	Myeloid identity
CD80 (B7-1)	Co-stimulatory ligand	Classical activation/M1 marker
CD86 (B7-2)	Co-stimulatory ligand	Classical activation/M1 marker
CD163	Scavenger receptor for hemoglobin/haptoglobin	Alternative activation/M2 marker
CD206 (MRC1)	C-type lectin/mannose receptor/PRR	Alternative activation/M2 marker
CD209 (DC-SIGN)	C-type lectin/PRR	Alternative activation/M2 marker

There is actively increasing interest in harnessing macrophage effector function for

cancer immunotherapy. Currently, most macrophage minded approaches can be split into

three categories: (i) depletion of immunosuppressive tumor associated macrophages, or

(ii) repolarization of suppressive macrophages to anti-tumor macrophages, or (iii)

enhanced tumor associated macrophage phagocytosis (Morrison 2016).

In the below table 1.4 we review some of the foundational current pre-clinical and clinical macrophage minded immunotherapeutic approaches for the treatment of cancer.

Table 1.4: Macrophage minded immuno-oncology approaches

Pharmacologic category	Mechanism of action	Reference
Anti-CD47 monoclonal antibody	Blockade of the anti-phagocytic CD47/SIRPa interaction leads to enhanced phagocytosis	(Weiskopf 2017; Weiskopf et al. 2016; Chao et al. 2010)
Anti-SIRPa monoclonal antibody	Blockade of the anti-phagocytic CD47/SIRPa interaction leads to enhanced phagocytosis	(Weiskopf et al. 2014; Liu et al. 2016)
Anti-CSF1/CSF1R monoclonal antibody	Reduction in the recruitment of monocytes and maintenance of tumor associated macrophages by blocking the activity of the macrophage colony stimulating factor (M-CSF, CSF-1) on the monocyte/macrophage CSF1 receptor	(Cannarile et al. 2017; Garcia et al. 2016; Ries et al. 2014; Holmgaard et al. 2016; Ryder et al. 2013)
CSF1R small molecule inhibitor	Reduction in the recruitment of monocytes and maintenance of tumor associated macrophages by blocking the activity of the macrophage colony stimulating factor (M-CSF, CSF-1) on the	(Butowski et al. 2016)

	monocyte/macrophage CSF1 receptor	
Anti-CD40 agonist antibody	Activates resting antigen presenting cells including macrophages and dendritic cells Induces the expression of MHC class I and MHC class II, as well as costimulatory molecules and adhesion molecules Increases antigen presenting cell derived cytokine production Reduction of tumor fibrosis	(Beatty et al. 2011; Beatty et al. 2017; Vonderheide & Glennie 2013; Long et al. 2016)
CCR2 antagonist	Reduction in the recruitment of monocytes to the tumor microenvironment by blocking the CCL2 chemokine from binding to the monocyte CCR2 receptor, subsequently resulting in fewer tumor associated macrophages	(Nywening et al. 2016; An et al. 2017; Schmall et al. 2015; Roblek et al. 2015)
CCL2 antagonist	Reduction in the recruitment of monocytes to the tumor microenvironment by blocking the CCL2 chemokine from binding to the monocyte CCR2 receptor, subsequently resulting in fewer tumor associated macrophages	(Qian, Li, Zhang, Kitamura, Zhang, Campion, E. a Kaiser, et al. 2011; Popivanova et al. 2009; Wang et al. 2018)
CXCR1/CXCR2 antagonist	Reduction in the recruitment of monocytes to the tumor microenvironment by blocking the monocyte CXCR1/CXCR2 chemokine receptors, subsequently resulting in fewer tumor associated macrophages	(Colin W. Steele et al. 2016; Colin W Steele et al. 2016)

JAK/STAT inhibitors	Reduced inflammatory and/or immunosuppressive gene expression in response to cytokines including IL4 (STAT6), IL13 (STAT6), IL10 (STAT3), IL6 (STAT3) Increased expression of M1 associated genes Enhanced responsiveness to chemotherapy and immunotherapy	(O'Shea et al. 2015; Li & Watowich 2014)
CXCL12/CXCR4 antagonist	Decrease in the recruitment of monocytes/macrophages to the tumor microenvironment Decreased macrophage-derived angiogenic support	(Tseng et al. 2011)
TIE2 antagonist	Inhibition of the Tie2 tyrosine kinase receptor (expressed in macrophage subsets and endothelial cells) reduces myeloid infiltration, angiogenesis, and decreases invasion/metastasis	(Forget et al. 2014; Harney et al. 2017)
TLR ligands	Induction of classically activated macrophage (M1) genes in TAMs Enhanced anti-tumor properties Enhanced antigen presenting properties Induction of type II interferon and TNF-alpha	(Whitmore et al. 2004; Chang et al. 2014; Lee et al. 2014)
Anti-IL4/IL4R antibody	Blockade of the cytokine IL4 from acting on the macrophage IL4 receptor, thus preventing or reducing M2 polarization	(Bankaitis & Fingleton 2015)

	Reduction in the macrophage proliferative signal derived from IL4 in the TME	
Anti-IL6/Anti-IL6R antibody	Reduced IL6 derived inflammatory signaling and JAK/STAT3 pathway activation Enhanced responsiveness to chemotherapy in pancreatic ductal adenocarcinoma Reduction of M2 TAMs and myeloid-derived suppressor cells	(Caetano et al. 2016; Long et al. 2017)
Trabectedin	Tetrahydroisoquinoline alkaloid developed as a DNA intercalating chemotherapeutic drug Monocyte/TAM depletion via activation of caspase-8 dependent apoptosis in these cells semi-selectively Inhibition of the expression of pro-inflammatory and pro-angiogenic genes such as IL-6, CCL2, CXCL8, ANG-2, and VEGF but not TNF-alpha	(Germano et al. 2013; D'Incalci et al. 2014)
Zoledronic acid	Direct depletion of TAMs by approximately 30-35% Decrease in MMP-9 (associated with invasion and metastasis) Enhancement of M1 associated genes in TAMs	(Green & Lipton 2010; Hiroshima et al. 2014)
Class IIA HDAC inhibitor	Epigenetic modulator leads to the repolarization of M2	(Guerriero et al. 2017)

	TAMs toward an anti-tumor M1 phenotype Induces the recruitment and differentiation of highly phagocytic and stimulatory macrophages within tumors (example: TMP195)	
PI3K-gamma inhibitor	Inhibition of PI3K-gamma reduces PDK1, AKT1, and TSC signaling and enhances pro-inflammatory NFkB mediated gene expression changes and macrophage activation	(Kaneda et al. 2016; Zheng & Pollard 2016)
Macrophage engaging bi-specific antibody	Crosslinking of tumor associated antigens and activating macrophage receptors, such as CD16, CD32, or CD64, leading to phagocytic clearance of targeted cells	(Wallace et al. 2001; Wallace et al. 2000)
Tumor targeted monoclonal antibody	Opsonization of tumor associated antigens and induction of antibody mediated cellular phagocytosis by activating macrophage Fc receptors The affinity for each class of IgG and the various Fc receptors varies and can be enhanced by altering the glycosylation pattern of the IgG heavy chain	(Braster et al. 2014; Weiskopf & Weissman 2015)

As of 2018, the most advanced approaches in this list (aside from traditional monoclonal antibodies like rituximab and trastuzumab, which have a myriad of functions aside from

macrophage activation) are inhibitors of CD47/SIRPa and CSF-1/CSF-1R. These approaches are currently in clinical trials, and their efficacy in sentinel phase III trials remains to be determined. Inhibitors of CD47/SIRPa are giving strong signals in the contest of rituximab refractory lymphoma, but the publicly disclosed efficacy in solid tumor trials is minimal. Notably, in the context of solid tumors, these pharmacological agents mechanistically rely on the function of already M2 polarized tumor associated macrophages, and the delivery of ex vivo activated and targeted cells is a logical next step in the development of anti-tumor macrophages.

Chimeric Antigen Receptor (CAR) T cells

Overview

Current approaches to immunotherapy include vaccines, monoclonal antibodies, inflammatory adjuvants, cytokines, oncolytic viruses, bispecific antibodies, and adoptive cell therapy. The first cell therapies in the context of cancer, dating back to the 1980s, consisted of either allogeneic lymphocyte transfers for leukemia or the infusion of tumor infiltrating lymphocytes (TILs). TIL therapy is based on the premise that if neoantigen reactive T cells were present in the cancer patient, they would likely exist within the tumor microenvironment. Metastatic melanoma patients have had profound curative responses to TIL therapy, though the majority of treated patients failed to respond to treatment (Hinrichs & Rosenberg 2014).

T cells, specifically alpha-beta T cells, naturally recognize short peptides in the context of MHC-restricted presentation via the heterodimeric and diverse T cell receptor (TCR), with self-reactive clones deleted through the processes of central and peripheral tolerance. B cells, on the other hand, recognize surface bound and soluble antigens in a non-MHC restricted fashion through the action of immunoglobulin receptors, which are also highly diverse through the process of VDJ recombination and somatic hypermutation. T cell specificity can be genetically manipulated through the exogenous overexpression of either engineered TCR-alpha and TCR-beta genes, as is the case with transgenic-TCR T cell therapy, or via the introduction of a chimeric antigen receptor (CAR). The CAR is a fully man-made construct, coupling the extracellular non-MHC restricted antigen specificity of the immunoglobulin or B-cell receptor, with the intracellular signaling capacity of the TCR and TCR co-stimulatory receptors.

Structure

CARs are generated by genetically fusing the variable antigen recognition domain of monoclonal antibodies – specifically the single chain variable fragment (scFv) – with a hinge domain, a transmembrane domain, and one or more intracellular signaling domains. The structural domains of the CAR, along with the function, tunable parameters, and examples are summarized in Table 1.5.

Table 1.5: CAR structural domains and function

Domain	Example(s)	Function	Parameters	Membrane orientation
Targeting domain	Monoclonal antibody derived single chain variable fragment (scFv) DARPin Centyrin Nature ligand	Antigen recognition	Affinity Dimerization	Extracellular
Hinge	CD8 Hinge IgG4 Hinge	Tethering and displaying the targeting domain	Length Flexibility Dimerization	Extracellular
Transmembrane (TM) domain	CD8 TM domain IgG TM domain	Connecting the extracellular portion to the intracellular portion	Dimerization Lipid raft association	Membrane spanning
Co-stimulatory domain	4-1BB CD28 OX40 ICOS	Providing signal 2 of the T cell activation cascade	Signaling pathway and downstream second messengers Intensity of activation Metabolic reprogramming	Intracellular

			Gene expression profile	
Stimulatory domain	CD3-zeta Fc-gamma	Providing signal 1 of the T cell activation cascade	Signaling pathway and downstream second messengers Signaling strength Induced effector functions/cytokines	Intracellular

While scFv's are the most common antigen binding domains used in CARs, alternative non-antibody-based antigen recognition domains such as DARPins, ankyrin based recognition motifs, have proven to also provide antigen specific T cell activation (Plückthun 2015). Furthermore, natural receptors or ligands have been used as the extracellular domain, allowing for natural affinity to the cognate ligand or receptor. The importance of the affinity for each target is determined in an empirical fashion, as the antigen density on tumor and normal tissue varies for each CAR target (Ellebrecht et al. 2016).

The hinge domain of the CAR serves a physical function to give length and flexibility to the scFv. Commonly used hinges include the CD8a hinge and the IgG4 hinge. The function and optimization of each scFv/hinge pair are determined empirically, and the rules are not fully understood. There is evidence that IgG based hinges are subject to reactivity with Fc receptors, leading to undesired effects (Hudecek et al. 2015). The hinge also serves the purpose of determining the length of the CAR. There have been studies demonstrating that there is an optimal length for the CAR/target cell interaction, and if

the combined length of the CAR/target is too short or too long, the efficacy of T cell activation is decreased (Kulemzin et al. 2017.).

The transmembrane domain provides the link between the extracellular and intracellular regions of the CAR. The transmembrane domain is the least studied structural CAR domain, and typically is acceptable as long as the CAR is expressed well on the cell surface. Some transmembrane domains lead to better levels of CAR expression than others, and the choice of transmembrane domain is determined empirically for every CAR with a unique extracellular and intracellular domain. The choice of the scFv, hinge, and transmembrane domain is also paramount to the inherent dimerization of the CAR molecule and therefore the level of background tonic signaling, which is unfavorable as it leads to the enhanced acquisition of an exhausted T cell phenotype (Long et al. 2015; Gomes-Silva et al. 2017).

The fundamentally key portion of the CAR is the intracellular signaling and co-stimulatory signaling domains. Currently, all clinically utilized CAR constructs encode the CD3-zeta primary CAR signaling domain. The co-stimulatory domain, on the other hand, derives from either the 4-1BB receptor in Novartis' Kymriah® or the CD28 receptor in Gilead's Yescarta®. Studies have shown that the presence of an immunoreceptor tyrosine-based activation motif (ITAM) is necessary for the activity of CARs. Specifically, the ITAM tyrosine's must be intact in order for downstream signaling as they are the targets of CAR phosphorylation and activation. Previous studies have shown that Fc-gamma based CARs are also effective in T cells (Eshhar et al. 1993; Hwu et al. 1995; Gross & Eshhar 1992).

The introduction of co-stimulatory domains from either 4-1BB or CD28 was the sentinel discovery that led to the clinical success of CARs in human leukemia and lymphoma patients. T cells require multiple signals for full and complete activation. The recognition of MHC-peptide ligand through the TCR alone is insufficient – T cells must receive a second signal through a co-stimulatory receptor/ligand pair in order to fully activate, produce cytokines and effector molecules, proliferate, and avoid anergy. All CARs that include co-stimulatory domains are referred to as second-generation CARs and have enhanced activation, cytokine secretion, proliferation, killing, and persistence as compared to first generation CARs. The choice of the co-stimulatory domain of the CAR leads to differential in vitro and in vivo activity. CD28 co-stimulated CAR constructs become activated more rapidly, have greater acute activity, upregulate exhaustion markers, have reduced long term activity, have an increased effector memory phenotype, and depend on glycolytic metabolism, as compared with 4-1BB co-stimulated CARs (Kawalekar et al. 2016). 4-1BB CARs, on the other hand, demonstrate increased persistence, decreased exhaustion, improved long term activity, an increase central memory phenotype, and depend on oxidative metabolism, as compared to CD28 CARs (Kawalekar et al. 2016). Direct head-to-head comparisons in the clinical setting of diverse CAR constructs have not been performed. There have been many studies of novel or diverse CAR co-stimulatory domains, such as OX40 and ICOS, and some have combined two co-stimulatory domains to produce "third-generation" CARs (Hombach et al. 2012; Guedan et al. 2014). The improvement in efficacy in third- versus second-generation CARs remains to be determined.

Mechanism of action

Upon the recognition of antigen and dimerization by CARs on a CAR-T cell, the CD3-zeta and co-stimulatory domains become phosphorylated and activated, leading to both immediate and delayed effects on the T cell. In the immediate phase, T cells secrete pre-formed granules containing lethal molecules, notably perforin and granzyme B. Upon release, perforin forms pores on the target cell's plasma membrane via calcium-dependent oligomerization. Perforin, as its name suggests, has the primary function of forming pores, which allow the dysregulation of ion flux and, more importantly, specifically allow the entry of pro-apoptotic granzyme proteins. Granzyme B is a protease that specifically cleaves and activates pro-apoptotic caspases 8, 10, 3 and 7. Furthermore, granzyme B can directly act on BID, Mcl-1, and potentially hundreds of other substrates via its protease activity (Chowdhury & Lieberman 2008). Ultimately, the combination of granzyme B and perforin leads to the rapid induction of target cell death.

Perforin and granzyme B are not the only methods by which CAR-T cells can induce target cell death. CAR-T cells upregulate Fas-L, the ligand for the extrinsic apoptosis receptor Fas, which is expressed by some but not all tumor cells. The interaction of Fas-L with Fas leads to the trimerization of the Fas receptor, recruitment of intracellular death domains and the formation of the death-inducing signaling complex, which ultimately activates caspase 8 and causes target cell apoptosis. CAR mediated T cell activation causes the induction of surface Fas ligand and is a direct mechanism for tumor killing. However, T cells themselves express Fas receptor, and the fratricidal interaction of CAR-T Fas-L with CAR-T Fas receptor is a mechanism of activation induced cell death

(AICD) (Tschumi et al. 2018). Furthermore, active CAR-T cells upregulate and produce TNFa, the ligand for the death receptor TRAIL, which is expressed on some but not all tumor cells. The binding of soluble or surface bound TNFa to TRAIL induces another form of extrinsic apoptosis, leading to again a caspase-8 mediated target cell death.

In addition to direct cytolytic killing of target cells, CAR-T cells produce a myriad of cytokines, each of which has its own myriad of receptors and downstream functions. Notably, CAR-T cells produce IL2, which serves to stimulate T cell proliferation and activation, and IFN-gamma, which also modulates the T cell gene activity and gene expression. CAR-T derived cytokines can directly impact the tumor cells and the tumor microenvironment, having both positive and negative effects.

Lastly and importantly, CAR activation leads to the proliferation of CAR-T cells. Upon seeing target, a proliferative signal leads to the rapid cell division of CAR-T cells, allowing for the expansion of the biological drug in a disease-related fashion. In other words, if there is a large tumor antigen burden, the number of CAR-T cells exponentially rises. As the tumor is cleared and antigen burden is reduced, the number of CAR-T cells dwindles – mimicking the reaction of natural T cells in an infectious response. As with natural immunity, CAR-T cells can serve to promote the prolonged response to tumor and prevention of relapse by inducing epitope spreading via lytic cell death and activation of antigen presenting cells, by augmenting the activity of endogenously reactive T cells via cytokines, and by the formation of long-lasting memory CAR-T cells, scavenging for relapsed cells (June & Sadelain 2018).

Efficacy in human clinical studies: Hematologic malignancy

CAR-T cells directed against CD19, a highly expressed B-cell restricted surface antigen, are by far the most studied and clinically developed CAR-T cells worldwide. CD19 is oft-said to be the perfect CAR target, as it is ubiquitously expressed in B cell malignancy, is restricted to B cells, and is brightly expressed on the cell surface. Tisagenlecleucel-T, also known as Kymriah®, was developed by Novartis and is currently indicated for patients up to 25 years of age with B-cell precursor acute lymphoblastic leukemia (ALL) that is refractory or in second or later relapse, and adult patients with relapsed or refractory (r/r) large B-cell lymphoma after two or more lines of systemic therapy including diffuse large B-cell lymphoma (DLBCL) not otherwise specified, high grade B-cell lymphoma and DLBCL arising from follicular lymphoma. Axicabtagene ciloleucel, also known as Yescarta®, was developed by Kite and Gilead and is currently indicated for the treatment of adult patients with relapsed or refractory large B-cell lymphoma after two or more lines of systemic therapy, including diffuse large B-cell lymphoma (DLBCL) not otherwise specified, primary mediastinal large B-cell lymphoma, high grade B-cell lymphoma, and DLBCL arising from follicular lymphoma. Neither of the cell products are approved for central nervous system lymphoma.

In the registration trial of Tisagenlecleucel-T in relapsed/refractory B-cell acute lymphoblastic leukemia in patients up to 25 years old, 68 patients were treated in a large multi-center single arm trial called the ELIANA trial. Out of 63 evaluable patients, 83% demonstrate a complete response (Maude et al. 2018; Mueller et al. 2018). This level of response in relapsed/refractory leukemia was unprecedented. In the registration trial of

Tisagenlecleucel-T in adult relapsed/refractory diffuse large B cell lymphoma, 68 patients were treated in the multi-center single arm JULIET trial. Of the 68 patients evaluated, 50% demonstrated an overall response, and 32% demonstrated a complete response. In the registration trial of Axicabtagene ciloleucel in relapsed/refractory large B cell lymphoma, 101 patients were treated in a multi-center single-arm study. Of the 101 patients evaluated, 72% demonstrated an objective response and 51% demonstrate a complete response (Neelapu et al. 2017). The median duration of response in this trial was 9.2 months.

Targets, toxicities and mechanisms of resistance

As with all cancer therapies, CD19 directed CAR-T cells, though effective in otherwise incurable patients, demonstrated significant expected and unexpected toxicity. The key issue in the immunotherapy of human cancer is that almost all tumor associated antigens are also expressed on normal tissues. In the below table 1.6, we summarize some of the many CAR targets that have been pre-clinically and clinically evaluated and provide the potential indications and the normal tissues on which each target is expressed.

Table 1.6: CAR targets, indications, and normal tissue expression

Target	Tumor category	Potential indications	Normal tissue expression	Reference
BCMA	Hematologic	Multiple myeloma	Plasmablasts Plasma cells	(Cho et al. 2018)
CD123	Hematologic	Acute myeloid leukemia	Hematopoietic stem cells	(Gill, Tasian, Ruella, Shestova, Li,

			Endothelial cells	Porter, Carroll, Danet-Desnoyers, et al. 2014)
			Myeloid precursors	
			Mature myeloid cells	
CD138	Hematologic	Multiple myeloma	Plasma cells	(Tian et al. 2017; Palaiologou et al. 2014)
			Epithelial cells	
			Hepatic/GI tissue	
CD171/L1CAM	Solid	Neuroblastoma	Cerebral grey matter	(Hong et al. 2014)
		Cervical carcinoma	Cerebellum	
		Ovarian carcinoma	Pituitary gland	
		Bladder cancer	Peripheral nerve	
		others	Kidney	
			Skin	
			Retina	
			Adrenal gland	
CD19	Hematologic	B-cell acute lymphoblastic leukemia	Pro-B cell	(Maude et al. 2015; Maude et al. 2018; Tasian & Gardner 2015)
		B-cell chronic lymphoblastic leukemia	Pre-B cell	
			Naïve B-cell	
		Diffuse large B cell lymphoma	Activated B-cell	
			Mature B-cell	
		Mantle cell lymphoma	Memory B-cell	
			Late plasmablast	

		Follicular lymphoma		
CD20	Hematologic	Non-Hodgkin lymphoma	Naïve B-cell Activated B-cell Mature B-cell Memory B-cell	(Till et al. 2012; Y. Wang et al. 2014)
CD22	Hematologic	B-cell acute lymphoblastic leukemia	Mature B-cell and other B-cell subsets	(Haso et al. 2013; Long et al. 2013)
CD30	Hematologic	Hodgkin's lymphoma	Activated T-cell Activated B-cell Activated NK-cell Subset of activated myeloid cells	(Ramos et al. 2017; Di Stasi et al. 2009; Horie & Watanabe 1998)
CD33	Hematologic	Acute myeloid leukemia	Hematopoietic stem cells Monocytes Macrophages Microglial cells Neutrophils Granulocytes Myeloid precursors	(Kenderian et al. 2015)
CD38	Hematologic	Acute myeloid leukemia	Hematopoietic stem cells	(Drent et al. 2016; Yoshida et al. 2016;

		T cell leukemia Multiple myeloma B-cell chronic lymphocytic leukemia	NK cells Monocytes Activated T-cells Activated B-cells	Hartman et al. 2010)
CD5	Hematologic	T cell leukemia	T-cells	(Mamonkin et al. 2015; Raikar et al. 2018; Chen et al. 2017)
CD70	Hematologic Solid	Diffuse large B cell lymphoma Follicular lymphoma Hodgkin lymphoma Waldenstrom macroglobulinemia Multiple myeloma Renal cell carcinoma glioblastoma Head and neck squamous cell carcinoma	Activated T-cell Activated B-cell Dendritic cells	(Park et al. 2018; Shaffer et al. 2011)
CEA	Solid	Colorectal carcinoma Breast cancer Liver cancer	Pulmonary epithelial cells (apical surface) Gastrointestinal epithelial	(Wang et al. 2016; Katz et al. 2015; Burga et al. 2015)

		Stomach cancer Pancreatic ductal adenocarcinoma Ovarian cancer Lung cancer	cells (apical surface) Embryonic tissue	
EGFR	Solid	Glioblastoma Non-small cell lung cancer Metastatic colorectal cancer Many other carcinomas	Keratinocytes Gastrointestinal tract Renal system	(Caruso et al. 2016; Liu et al. 2015)
EGFRvIII	Solid	Glioblastoma multiforme	None	(Johnson et al. 2015; Choi et al. 2017; O'Rourke et al. 2017)
EpCAM	Solid	Various carcinomas	All normal epithelial tissue except: epidermal keratinocytes gastric parietal cells myoepithelial cells thymic cortical epithelial cells	(Deng et al. 2015; Ang et al. 2017; Schmelzer & Reid 2008)

			hepatocytes	
EphA2	Solid	Glioma Non-small cell lung cancer Esophageal squamous cell carcinoma	Epithelial tissue GI tract Kidney Urinary system	(Li et al. 2018; Shi et al. 2018)
FAP	Solid	Mesothelioma Many carcinomas	Fibroblasts (activated)	(Lo et al. 2015; L.-C. S. Wang et al. 2014)
FR-alpha	Solid	Ovarian cancer Other carcinomas	bronchial epithelium renal tubules choroid plexus intestinal brush-border membranes type-1 and type-2 pneumocytes of the lung placental tissue	(Schutsky et al. 2015; Kandalaft et al. 2012; Song et al. 2016)
FR-beta	Hematologic	Acute myeloid leukemia	Normal myeloid lineage cells	(Lynn et al. 2015)
GD2	Solid	Neuroblastoma	Central nervous system Peripheral nerves Skin melanocytes	(Singh et al. 2014; Prapa et al. 2015; Louis et al. 2011; Heczey et al. 2014)

Glypican-3	Solid	Hepatocellular carcinoma Lung squamous cell carcinoma	Lung Liver Female reproductive tissues	(Baumhoer et al. 2008; Li et al. 2016; Gao et al. 2014)
HER2	Solid	Breast cancer Ovarian cancer Gastric cancer Glioblastoma Esophageal cancer Sarcoma Lung cancers	Pulmonary tissue Cardiac tissue	(Ahmed et al. 2015; Priceman, Tilakawardane, et al. 2018; Nellan et al. 2018; Feng et al. 2018; Lanitis et al. 2012)
IL13Ra2	Solid	Glioma	Testis Pituitary gland	(Brown et al. 2018; Kong et al. 2012; Brown et al. 2015)
Kappa Light Chain	Hematologic	Multiple myeloma Non-Hodgkin lymphoma Chronic lymphocytic leukemia	B cells Plasma cells	(Ramos et al. 2016)
Mesothelin	Solid	Mesothelioma Ovarian cancer Triple neg breast cancer Pancreatic cancer Lung cancer	Mesothelial cells	(Pastan & Hassan 2014; Adusumilli et al. 2014; Beatty et al. 2014; Zhao et al. 2010)

		Stomach cancer Bile duct cancers		
MUC1	Solid hematologic	Pancreatic cancer Leukemias	Glycosylation pattern dependent tumor specificity	(Posey, Clausen, et al. 2016; Posey, Schwab, et al. 2016; Maher et al. 2016; Steentoft et al. 2018)
PSCA	Solid	Prostate cancer bladder cancer renal cell carcinoma	Brain Stomach Placenta Kidney Pancreas Bladder	(Priceman, Gerdts, et al. 2018; Hillerdal et al. 2014; Abate-Daga et al. 2014)
PSMA	Solid	Prostate cancer	Kidney Proximal small intestine Salivary gland	(Ghosh & Heston 2004; Kloss et al. 2018; Junghans et al. 2016; Zuccolotto et al. 2014; Santoro et al. 2015)
ROR-1	Solid Hematologic	Breast cancer Non-small cell lung cancer Sarcomas Mantle cell lymphoma	B-cell precursors Adipocytes Pancreas Lung	(Hudecek et al. 2010; Hudecek et al. 2013; Berger et al. 2015)

		B-cell chronic lymphocytic leukemia		
VEGFR-II	Solid	Melanoma Renal cell carcinoma	Endothelial cells	(Chinnasamy et al. 2010)

In the case of CD19 directed CAR-T cells, the antigen is restricted to the B cell lineage. Expectedly, patients that received autologous anti-CD19 CAR-T therapy developed B cell aplasia and increased susceptibility to infection. B-cell aplasia is a tolerable side effect and can be overcome by providing patients with repeat infusion of pooled intravenous immunoglobulins from human donors. This is currently part of the standard treatment protocol. In addition to on-target off-tumor toxicity, CD19 CAR-T cells are associated with cytokine release syndrome (CRS), a serious side effect caused by the high level of pro-inflammatory cytokines produced by activated CAR-T cells at their peak proliferation and activation state. Cytokine release syndrome leads to flu-like symptoms, capillary leakage, hypoxia, and hypotension and requires intensive care management by trained physicians. Studies have shown that IL-6, and its activity on myeloid cells bearing IL-6 receptors, is a key mechanism of the syndrome and management with tocilizumab, an anti-IL6R antibody, significantly reduces the severity of CRS.

CAR-T cells may also lead to unexpected toxicities. In the case of CD19 CARs, neurotoxicity has been seen in a number of different centers, with diverse anti-CD19 trials and conditioning regimens. The mechanism of neurotoxicity is unclear and poorly understood, but the symptoms are largely reversible. Given that each CAR is unique in its

structure, unpredicted non-specific binding to proteins other than the target antigen is a safety concern. It is very difficult to measure and predict the binding of CARs to proteins other than the expected antigen in relevant pre-clinical models.

CAR-T cells in solid tumors: clinical efficacy and mechanisms of resistance

Despite the success of CD19 directed CAR-T cells in leukemia and lymphoma, the efficacy of CAR-T cells in the solid tumor setting is currently minimal. There is a single reported patient that received CAR-T cells targeted against the glioblastoma antigen IL13RA2 that demonstrated a significant tumor regression (Brown et al. 2016). Several trials of CAR-T cells against the well-established tumor antigen HER2 have been conducted. A single case report of a patient with colorectal cancer metastatic to the lung and liver treated with HER2 CAR-T cells described acute death (Morgan et al. 2010). This patient received a significantly higher cell dose than what is believed to be maximally tolerated, and numerous additional trials of HER2 CAR-T cells were conducted without any significant toxicity. These trials, however, failed to show any significant anti-tumor response. For example, a trial in which 19 patients with sarcoma were treated with autologous anti-HER2 CAR T cells led to stable disease in 4 patients – without any measurable tumor regression in any of the patients (Ahmed et al. 2015). Anti-EGFRvIII CAR-T cells failed to lead to significant tumor regression in a glioblastoma trial (Johnson et al. 2015). Overall, the response rate to CAR-T therapy in the solid tumor setting has been close to zero regardless of target, histology, or CAR design.

The exact mechanism by which solid tumors defend themselves against CAR-T mediated destruction remains unclear, and several distinct mechanisms are likely. First, the expression of solid tumor associated antigens is heterogenous throughout the primary and metastatic tumors, allowing for the rapid outgrowth of target dim or target negative cells via the action of evolutionary selection. Secondly, the tumor microenvironment of solid tumors is metabolically harsh and hypoxic and is unfavorable to the high metabolic needs of rapidly proliferating T cells. Thirdly, the tumor microenvironment is generally rich in immunosuppressive factors such as IL-10, TGF-beta, and high levels of immune checkpoint ligands such as PDL-1. Fourth, many solid tumors actively exclude T cell trafficking and penetration via the development of fibrosis and the recruitment of tumor associated macrophages which aid in restricting T cell entrance. In addition, tumors can rapidly downregulate surface antigens in response to T cell pressure, in line with the concept of immunoediting.

HER2 targeted therapy

In this thesis, we introduce and demonstrate the targeted anti-tumor potential of human CAR macrophages. In particular, we focus on CAR macrophages directed against the well-established tumor associated antigen HER2/neu. HER2 is encoded by the human ERBB2 gene, a member of the epidermal growth factor receptor family. HER2 is found to be amplified or over-expressed in approximately 30% of breast cancers and is associated with an aggressive phenotype. Aside from breast cancer, HER2 is found to be amplified on gastric cancers, sarcomas, lung cancers, pancreatic cancers, glioblastoma, esophageal cancers, and other solid tumor types.

Given the known role of HER2 in a myriad of solid tumors – particularly breast and gastric carcinomas – several HER2 targeted therapies have been developed and are currently FDA approved in the United States. Table 1.7 summarizes the currently available HER2 targeted therapies, their mechanism of action, their clinical efficacy, and their associated serious adverse events.

Table 1.7: FDA approved HER2 targeted therapies

Pharmacologic agent	Description	Mechanism of action	Efficacy	Serious adverse events
Trastuzumab (Herceptin®)	Humanized monoclonal antibody targeted to the extracellular domain (subdomain IV) of HER2	Interference with ligand dependent and independent HER2 signaling Induction of HER2 internalization or down-regulation Antibody dependent cellular cytotoxicity Antibody dependent cellular phagocytosis	Metastatic breast cancer: 7.2-month time to progression (trastuzumab + chemotherapy) vs. 4.5-month time to progression (chemotherapy alone) Metastatic gastric cancer: 13.5-month median overall survival (trastuzumab + chemotherapy) vs. 11.0-month median overall survival (chemotherapy alone)	Decreased left ventricular ejection fraction pulmonary toxicity infusion reactions febrile neutropenia

| Pertuzumab (Perjeta®) | Humanized monoclonal antibody specific for the extracellular domain (domain II) of HER2

The recognized epitope is distinct from trastuzumab

Used in combination with trastuzumab | Interference with ligand dependent and independent HER2 signaling

Induction of HER2 internalization or down-regulation

Antibody dependent cellular cytotoxicity

Antibody dependent cellular phagocytosis | Metastatic breast cancer:

56.5-month median overall survival (pertuzumab plus trastuzumab plus docetaxel) vs. 40.8-month median overall survival (trastuzumab plus docetaxel) | Decreased left ventricular ejection fraction

pulmonary toxicity

infusion reactions

febrile neutropenia

embryo-fetal toxicity |
|---|---|---|---|---|
| **Ado-trastuzumab emtansine (Kadcyla®)** | an antibody drug conjugate of trastuzumab with emtansine (also called cytotoxic DM1) | Targeted delivery of the microtubule inhibitor emtansine to HER2 positive cells via internalization of the antibody-drug conjugate complex

Microtubule disruption leads to cell cycle arrest and apoptosis | Metastatic breast cancer:

30.9-month median overall survival (ado-trastuzumab emtansine) vs. 25.1-month median overall survival (lapatinib plus capecitabine) | Pulmonary toxicity

Infusion reactions

Hemorrhage

Thrombocytopenia

Neurotoxicity |

		Ado-trastuzumab emtansine retains the other mechanisms of action of trastuzumab		
Neratinib (Nerlynx®)	Small molecule tyrosine kinase inhibitor	Small molecule kinase inhibitor of EGFR, HER2, and HER4 signaling Irreversible antagonist Reduces receptor autophosphorylation Reduces downstream MAPK and AKT signaling Leads to cell cycle arrest and apoptosis	Adjuvant treatment in breast cancer: 4.7% of patients having a disease recurrence (neratinib) vs. 7.5% of patients having a disease recurrence (placebo)	Diarrhea Hepatotoxicity Embryo-fetal toxicity
Lapatinib (Tykerb®)	Small molecule tyrosine kinase inhibitor	Small molecule kinase inhibitor of EGFR and HER2 signaling Reversible antagonist Reduces receptor autophosphorylation Reduces downstream MAPK and AKT signaling	Metastatic breast cancer: 75-week median overall survival (lapatinib plus capecitabine) vs. 65.9-week median overall survival (capecitabine)	Decreased left ventricular ejection fraction Hepatotoxicity Diarrhea Interstitial lung disease QT prolongation Cutaneous reactions

		Leads to cell cycle arrest and apoptosis		Embryo-fetal toxicity

References:

(Cameron et al. 2008; Chan et al. 2016; Perez et al. 2017; Shah et al. 2017; Verma et al. 2012; Swain et al. 2015; Tolaney et al. 2015; Swain et al. 2013)

Aside from being amplified on HER2 positive solid tumor cells, HER2 is expressed at lower levels on numerous normal tissues. In particular, HER2 is detected on cells of the cardiovascular and pulmonary systems, which explains why the serious adverse events associated with HER2 targeted therapies are cardiopulmonary in nature. Overall, the currently available HER2 targeted therapies are not curative in metastatic solid tumors and enhance overall survival by several months. HER2 is a strong candidate for adoptive cellular therapy, though care must be taken to monitor patients for signs of cardiopulmonary on-target off-tumor toxicity.

Macrophages in cell therapy

Activated monocyte derived macrophages were shown to have non-specific and low potency anti-tumor activity *in vitro* against cancer cell lines. Based on these results, researchers in the 1990s and early 2000s conducted numerous clinical trials in which cancer patients were treated with autologous monocyte derived macrophages. These cells were either infused as M0 non-activated macrophages or were pre-treated with M1-

inducing stimuli IFN-gamma and LPS. Patients with various solid tumors were treated with autologous macrophages injected either intraperitoneally, intravenously, intrapleurally, intra-hepatic arterially, and intra-vesicularly. In all routes of administration, autologous macrophages were safe but ineffective. Table 1.8 summarizes the previous clinical experience with adoptively transferred human macrophages in cancer.

Table 1.8: Previous experience with adoptively transferred macrophages in cancer patients

Cell type, activation method	Route & dose	Disease	Effect	PK/BD [1]	Reference
Leukapheresis and elutriation, cultured 7 days, 18 h in 1000 U/mL IFNγ	i.p., 3.5×10^7 cells/dose, weekly for 8 weeks	Colorectal cancer with peritoneal metastasis	N/A	In-111 label, signal stayed within the peritoneum for 5 days, blood peaked at 9% at 48 h, no transfer to other organs	(Stevenson et al. 1987)
Leukapheresis and elutriation, cultured 7 days, 18 h in 200 U/mL IFNγ	i.v. or i.p., $1–4 \times 10^8$ cells/dose, escalating every 2 weeks (i.v.) or weekly (i.p.)	Systemic metastasis (i.v.), Peritoneal metastasis (i.p.)	Only therapeutic effect: 2/7 disappearance of peritoneal ascites	N/A	(Andreesen et al. 1990)

MΦ Activated Killer (MAK) Leukapheresis and elutriation, cultured 6d in 500 U/mL GMCSF and 18 h in 166 U/mL IFNγ	i.v., 0.1–5 × 108 cells/dose, escalating weekly	Non-small-cell lung cancer	N/A	In-111 label, greatest signal in lungs at 24 h, migrating to liver and spleen at 72 h, decreasing thereafter	(Faradji, Bohbot, Schmitt-Goguel, et al. 1991)
MAK, Activated with mifamurtide	i.p., Escalating weekly dose from 107–109/dose	Peritoneal carcinomatosis (ovarian, pancreatic, gastric, appendiceal)	No therapeutic response. Increase of IL-1, IL-6 and TNFα in peritoneal cavity	In-111 label, signal stayed in abdominal cavity for up to 7 days, no signal in lungs, liver or spleen, 0.5% in blood	(Faradji, Bohbot, Frost, et al. 1991)
MAK, patients dosed with 50 μg/m2 IFNγ prior to cell collection	i.v. via hepatic artery, 1–10 × 108 cells/day, 3 sequential days, depending on cell recovery from patient	Colorectal or stomach cancer with liver metastasis	No therapeutic response	In-111, 1 h: 18% lung, 56% liver, 7 d: 12% lung, 43% liver	(Hennemann et al. 1995)
MAK	i.v., 1 × 109 cells/dose	Colorectal cancer	No therapeutic response. 11/14	N/A	(Eymard et al. 1996)

	weekly for 6 weeks		showed progression, 3/14 stabilized		
MAK, activated with 1 ng/mL LPS for 30 min. Patients dosed with 2–4 ng/kg LPS prior to cell collection	i.v., 3 × 106–4 ×108 cells/dose, escalating weekly for 7 weeks	Cancer (Colorectal, renal, pancreatic, melanoma or NSC lung)	Increase in TNFα and IL6 by 40×, 1/9 patients with stable disease (b25% growth), 8/9 showed progression	N/A	(B Henneman n et al. 1998)
MAK	i.p. 3x109/dose, 3 doses over 2 weeks	Metastatic renal carcinoma	Transitory stabilization (n=8) or partial regression (n=1) in 9 of 15 patients	In-111 label, at 72h, lung (6%), liver (24%), spleen (11%), blood (3%)	(Lesimple et al. n.d.)
MAK	i.v. or i.p., 1-2 × 109 in single dose	Metastatic ovarian carcinoma	N/A	In-111 or PET F18-FDG. i.v.: Accumulati on in lungs at 4 h (10%), at 24 h, liver (50%) and spleen (4%). Accumulati on in tumor in 4/10 patients i.p.: Accumulati on in tumor in 4/6 patients	(Ritchie et al. 2007)
MAK	Intravesica lly, 2 ×	Superficial Bladder Cancer	Recurrence occurred significantly	N/A	(Baron-Bodo et al. 2005;

	108/dose, weekly for 6 weeks		less frequent with standard treatment than with cells (12% vs. 38%; p b 0.001)		Burger et al. 2010)
Ixmyelocel-T – bone marrow aspirate enriched for regenerative macrophages and mesenchymal stromal cells by a proprietary process	Local injection to multiple sites in affected heart or limb, 30-300 × 106/dose	Dilated cardiomyopathy or critical limb ischemia	Reduced major adverse cardiovascular events (14% treated, 56% control), reduced time to first occurrence of treatment failure	N/A	(Henry et al. 2014; Powell et al. 2012)

- Table modified from: (Lee et al. 2016)

- i.p.=intraperitoneal; i.v.=intravenous

- MAK = macrophage activated killer cells

 [1] PK/BD=pharmacodynamics/biodistribution

Taken together, the results from the past experience with adoptive transfer of human

macrophages in cancer provided evidence that macrophages have the potential to traffic

into solid tumors and metastatic sites, are well tolerated, but fail to recognize and attack

the tumor. Retrospectively, without the provision of an opsonizing agent, the initiation of

the phagocytic program against tumor cells was unlikely to occur in these trials. These

studies set the precedent for genetically engineered macrophage cell therapy, and suggest

that if properly engineered, CAR macrophages have the potential to traffic to solid

tumors and productively engage tumor-associated antigens to debulk tumors via the

process of phagocytosis.

CHAPTER 2: Chimeric antigen receptors redirect human macrophage phagocytosis of cancer cells

Abstract

The non-MHC restricted redirection of T cell and natural killer (NK) cell activity via the introduction of chimeric antigen receptors leads to efficient targeted tumor recognition. Both T and NK cell effector function can be activated via CAR signaling. In this chapter, we hypothesize that macrophage phagocytosis of tumor cells can be redirected via the introduction of CD3-zeta and Fc-gamma intracellular domain-based CARs. Using in vitro microscopy based phagocytosis assays, we demonstrate the targeted and ITAM-dependent activity of CARs in the THP-1 human macrophage model. Macrophage phagocytosis was effective against all three antigens tested – CD19, mesothelin, and HER2. The activity of anti-CD19 CARs in THP-1 macrophages was augmented by pharmacologic and genetic ablation of the anti-phagocytic CD47/SIRPa interaction. The data presented in this chapter demonstrated the ability to genetically rewire phagocytosis and set the groundwork for translation of the CAR macrophage concept into primary human macrophages.

Introduction

Macrophages are sentinel cells of the immune system where they act as a crucial component of the immune system's first line of defense. The primary effector mechanism by which macrophages engage bacterial cells, fungal cells, apoptotic cells, and opsonized

cells is via the mechanism of phagocytosis. The phagocytic program requires the recognition of pro-phagocytic signals by a pro-phagocytic receptor, the absence of an anti-phagocytic signal acting on an anti-phagocytic-receptor, and the engagement of a complex signaling cascade that leads to the directional reorganization of the cellular cytoskeleton that allows the macrophage to engulf a large body. Macrophages naturally express a myriad of pro-phagocytic receptors that allow for the recognition and phagocytosis of infectious particles. For instance, the dectin-1 receptor recognizes beta-glucan on the surface of *Candida albicans*, a pathogenic yeast, and leads to the direct phagocytosis of these fungal cells. The lipopolysaccharide (LPS) receptor TLR4, with its co-receptor CD14, leads to the direct recognition and phagocytosis of gram-negative bacteria. Interestingly, recognition of LPS or beta-glucan not only triggers phagocytosis of the pathogen but induces a pro-inflammatory activated macrophage phenotype, which serves to trigger a first-responder alarm to the local tissue and immune system that an immune response should be initiated.

The pro-phagocytic receptors that recognize conserved patterns that are present and fundamental to the biology of pathogens (i.e. LPS, beta-glucan, flagellin) are broadly referred to as pattern recognition receptors. While not all pattern recognition receptors are phagocytic, all non-opsonic phagocytic receptors are pattern recognition receptors (PRR). The phagocytosis of live cells without PRR-mediated clearance is dependent on soluble intermediates, notably antibodies and complement. Antibody mediated cellular phagocytosis (ADCP) is the process by which antibody opsonized target cells are recognized by macrophage activating Fc receptors and subsequently phagocytosed.

Apoptotic cells, unlike live cells, are directly recognized by macrophage apoptotic/cell-corpse recognition receptors and internalized through the process of efferocytosis – a term describing the non-inflammatory clearance of apoptotic cells and cell corpses. The efferocytosis of apoptotic cells occurs via the recognition of conserved apoptotic features, such as extracellular exposure of phosphatidylserine, upregulation of extracellular calreticulin, or, in the case of old erythrocytes, reduced levels of the anti-phagocytic ligand CD47.

The interaction of human macrophage pro-phagocytic Fc receptors with the Fc domain of immunoglobulins leads to the phosphorylation of the intracellular domain of the Fc receptor or associated signaling molecules. Fc-gamma-RII, for instance, has an intracellular immunoreceptor tyrosine-based activating motif (ITAM) which allows the receptor to directly induce a phagocytic signaling program upon Fc recognition and receptor clusterization. Other Fc receptors require recruitment of the common Fc gamma chain, Fc-epsilon-RI, an intracellular adaptor and signaling protein, to provide the necessary ITAM in order to induce the phagocytic program. Antibody mediated phagocytosis can be augmented through the action of complement – a series of zymogens with pro-inflammatory properties, with activated forms of certain complement proteins capable of directly inducing phagocytosis by signaling through the complement receptors CR1, CR3, or CR4 (van Lookeren Campagne et al. 2007).

In the early development of CAR-T cells, Fc-espilon-R1, frequently referred to as "gamma-chain" or the "common Fc gamma chain", was the first CAR intracellular domain utilized. The common gamma chain does not naturally get expressed in T-cells, but was nevertheless capable of inducing T cell activation (Eshhar et al. 1993; Annenkov et al. 1998; Hwu et al. 1995).

Mechanistically, the likely mechanism by which the Fc gamma chain induces T cell activation is by mimicking the properties of CD247, the zeta chain of the CD3/TCR complex. FcERI and CD3-zeta are highly similar in both sequence and in structure, suggesting that though not identical, they have the potential to be replaceable in the context of a CAR. We hypothesized that CARs, which are capable of inducing the activation of T cells and NK cells in a non-MHC restricted fashion, may induce the targeted phagocytosis of target bearing cells. In particular, we hypothesized that CD3-zeta or Fc-gamma intracellular domain-based CARs can induce the phagocytosis of cognate-antigen expressing target tumor cells.

Significant research over the past two decades has proven that the ubiquitously expressed cell surface protein, CD47, serves as a "do-not-eat-me" signal to prevent phagocytosis of self-cells (Oldenborg et al. 2001; Oldenborg et al. 2000; Willingham et al. 2012). CD47 is downregulated on aging erythrocytes to enhance their uptake by macrophages and is upregulated on tumor cells to decrease their uptake by macrophages. CD47 exerts its inhibitory action on macrophage phagocytosis via a direct interaction with the SIRPa receptor. SIRPa is an inhibitory signal that bears an immunoreceptor tyrosine-based inhibitory motif (ITIM) that leads to the dephosphorylation of ITAM bearing activators

such as FcERI and Fc-gamma-RII. Multiple studies have shown that inhibition of the CD47/SIRPa interaction between macrophages and target tumor cells leads to the augmented phagocytosis of antibody-opsonized targets (Weiskopf 2017; Weiskopf et al. 2016; Weiskopf & Weissman 2015; Weiskopf et al. 2014; Alvey et al. 2017; Chao et al. 2010). Accordingly, we hypothesized that the blockade or genetic ablation of either CD47 or SIRPa may lead to the enhanced activity of CAR mediated phagocytosis.

In this chapter, we demonstrate the fundamental concept that CARs are active in human macrophages. Throughout this chapter we utilize the human myeloid cell line THP-1, a leukemic cell line commonly used as a model for human macrophage biology (Tsuchiya et al. 1980; Lund et al. 2016). We chose to test our hypothesis using the THP-1 model because primary human macrophages are difficult to transfect and transduce, and the identification of an effective gene delivery method in primary macrophages was the subject of the second aim and second chapter of this thesis. The data within this chapter demonstrates the concept that CD3-zeta and Fc-gamma chain-based CARs can induce the phagocytosis of cognate antigen expressing tumor cells, without any phagocytosis of target negative cells. This process requires an active intracellular ITAM bearing signaling motif, and mimics the complex signaling that occurs during antibody dependent cellular phagocytosis (ADCP). We show that THP-1 CAR macrophage phagocytosis is augmented with the blockade of the CD47/SIRPa axis, and provide a groundwork for the translation of this concept into primary human cells.

Results

To model the potential for CAR-mediated redirection of macrophage phagocytosis, we first used an anti-CD19 CAR in the human macrophage THP-1 cell line. We used a first-generation CAR encoding the CD3ζ intracellular domain (CAR19ζ), which has significant sequence and structural homology to the Fc common γ-chain, FcεRI-γ, a canonical signaling molecule for ADCP in macrophages. We measured the phagocytic potential of macrophages expressing an intact (CAR19ζ) or a truncated CAR (CAR19Δζ), lacking the CD3ζ intracellular domain (**Figure 2.1**). CAR19ζ but neither CAR19Δζ nor control untransduced (UTD) macrophages phagocytosed antigen-bearing tumor cells in vitro (**Figure 2.2A**). Furthermore, CAR19ζ macrophages selectively phagocytosed CD19+ but not CD19- tumor cells (**Figure 2.2B**), demonstrating that CAR – antigen binding is integral to drive redirected macrophage phagocytosis. CAR macrophage phagocytosis was an active process requiring Syk, non-muscle myosin IIA, and actin polymerization, similarly to Fc receptor mediated ADCP, as demonstrated by the inhibition of CAR activity upon pre-treatment with R406, blebbistatin, or cytochalasin D, respectively (**Figure 2.2C**). The phagocytic activity of anti-CD19 CARs against CD19+ targets was equivalent in macrophages expressing CD3ζ and Fcγ based CARs (**Figure 2.3A**), and the signaling of both gamma and zeta CARs was dependent on Syk, as demonstrated by inhibition of CAR-mediated phagocytosis with the Syk inhibitor R406 **(Figure 2.3B)**. Furthermore, the specific lysis of CD19+ target cells at an effector to target ratio of ten to one, after 48 hours of co-culture, was equivalent between gamma

and zeta-based CAR constructs **(Figure 2.3C)**. All subsequent experiments were therefore performed using CD3ζ as the primary CAR intracellular domain. CAR-mediated macrophage phagocytosis was confirmed via live cell video microscopy against antigen bearing and control tumor cells and by imaging flow cytometry (**Figure 2.4A**). The behavior of a single CAR macrophage was tracked over time and key steps of the phagocytic process are demonstrated (**Figure 2.4B)**. CAR macrophages were capable of polyphagocytosis, defined as the ability to engulf two or more target cells at once (representative images, **Figure 2.4C**). Having shown that anti-CD19 CARs can redirect macrophage phagocytosis, we sought to demonstrate that CAR macrophages can also be targeted toward solid tumor associated antigens. We therefore introduced CARs against mesothelin and HER2, utilizing singe chain variable fragments (scFvs) derived from antibody clones SS1 and 4D5, respectively, and demonstrated phagocytic activity against target cells expressing the appropriate cognate antigens (**Figure 2.4D**). Together these data demonstrated that CD3ζ-based CARs can direct the phagocytic activity of human THP-1 macrophages and provided support for subsequent efforts to translate this platform to primary human macrophages.

Furthermore, to test whether CAR mediated phagocytosis is regulated by the same mechanisms as Fc receptor mediated ADCP, we sought to test whether the CD47/SIRPa interaction has an inhibitory effect on CAR19-zeta mediated phagocytosis. There was an anti-CD47 and anti-SIRPa dose-dependent increase in the phagocytic activity of CAR19, but not UTD, macrophages against target bearing tumor cells (**Figure 2.5**). This data suggested that blocking either the ligand or the receptor is sufficient for antagonizing the

inhibitory CD47/SIRPa axis, and that CARs are also potentially subject to SIRPa mediated regulation. To test whether the additive phagocytic activity in the presence of CD47 / SIRPa blockade is due to additional non-specific opsonization or is genuinely a result of a lack of SIRPa activity, we compared the activity of a CD47 binding and blocking clone (B6H12) to the activity of a CD47 binding but non-blocking clone (2D3). The anti-CD47 2D3 monoclonal antibody binds to an epitope on the extracellular domain of CD47 that does not interfere with SIRPa, unlike the blocking B6H12 clone. The additive phagocytic activity was only seen with B6H12 and SIRPa blocking clone SE5A5, but not with 2D3 **(Figure 2.6)**.

To further validate the impact of antibody mediated blockade of CD47/SIRPa on CAR-mediated phagocytosis, we genetically ablated SIRPa on THP-1 macrophages using the CRISPR/Cas9 system. We designed and in vitro transcribed three anti-SIRPa guide RNA constructs and tested their ability to knock out SIRPa. Only one guide of the three – Guide 2 – was capable of inducing measurable SIRPa knockout one-week post electroporation of the Cas9-gRNA ribonuclear protein complex **(Figure 2.7A)**. The SIRPa negative cells were sorted for purity and used as effector cells in phagocytosis assays. To validate the impact of the knockout, CAR19z or SIRPaKO-CAR19z THP1 macrophages were used as effectors in phagocytosis assays in the absence or presence of anti-SIRPa blocking antibody. SIRPa KO led to the same level of phagocytic enhancement as anti-SIRPa blocking antibody, and the addition of anti-SIRPa antibody to SIRPa KO cells did not further enhance phagocytosis, suggesting that both the antibody and knockout were specific **(Figure 2.7B)**.

Discussion

In conclusion, we show in this chapter the following fundamental concept: CARs are active in macrophages. More importantly, we show that phagocytosis is rewireable. In addition to the evolutionarily-obtained methods of phagocytosis via antibody receptors, complement receptors, pattern recognition receptors, and efferocytosis receptors, we show that the coupling of single chain variable fragment derived antigen recognition domains to ITAM-bearing intracellular domains allows for the genetic manipulation of the phagocytic process.

Furthermore, the data within this chapter demonstrates that CAR mediated activity in a human macrophage model requires active CAR mediated signaling. The signaling of both CD3-zeta and Fc-gamma based CARs led to targeted phagocytosis, sparing target negative cells. Inhibitors of three distinct stages of the phagocytosis program – actin polymerization, non-muscle myosin IIa mediated force generation, and Syk phosphorylation – led to the ablation of CAR activity, suggesting that CARs activate the internal machinery of ADCP signaling. We show that the concept of CAR mediated phagocytosis is modifiable – as CARs against CD19, mesothelin, and HER2 were all active against cells displaying the appropriate cognate antigens.

Given that CD47/SIRPa inhibits the activity of Fc receptor mediated phagocytosis, we tested the impact of this regulatory axis on CAR activity. The pharmacologic and genetic inhibition of CD47/SIRPa led to increased phagocytic activity by CAR19-zeta THP1 macrophages, suggesting that there is potential synergy in combining CAR macrophages

with CD47 or SIRPa inhibitors. However, the importance of CD47/SIRPa in THP-1 cells, which are not primary cells, may or may not be equally relevant in primary human monocyte derived macrophages. Furthermore, given the known importance of the distance between macrophage and target for phagocytosis (Bakalar et al. 2018), whether or not this synergy will hold true for all CARs and all targets remains to be determined. One can envision a scenario in which a long target or very short target could physically preclude CD47 from binding to SIRPa and regulating phagocytosis.

Lastly, the success of CAR-T cells was largely due to the discovery and development of co-stimulatory domains that augmented anti-tumor activity, cytokine release, proliferation, phenotype, persistence, and other T cell characteristics. The CARs utilized in this chapter and thesis are all "1st-generation" CARs – meaning there is no co-stimulatory domain included. The incorporation of co-stimulatory domains, alternative signaling domains, and multiplexed signaling domains is the subject of future research.

Materials and Methods

Cell lines.

The THP-1, SKOV3, K562, MDA-468, CRL-2351, HTB-20, HTB-85, CRL-5803, CRL-5822, CRL-1555, HTB-131, HTB-20, and CRL-1902 cell lines were purchased from American Type Culture Collection (ATCC). Cells were culture in RPMI media with 10% fetal bovine serum, penicillin, streptomycin, 1x Glutamax, and 1x HEPES unless otherwise recommended by ATCC. All cell lines were transduced with a lentiviral vector

co-encoding click beetle green (CBG) luciferase and green florescent protein (GFP) under an EF1α promoter, separated by a P2A sequence. Transduced target cell lines were FACS sorted for 100% GFP positivity prior to use as targets in vitro and in vivo. THP-1 cells were lentivirally transduced, FACS sorted, and maintained in liquid culture. CAR expression and purity was routinely validated.

Plasmid construction and virus.

For lentivirus production, CAR constructs were cloned into the third generation pTRPE lentiviral backbone using standard molecular biology techniques. All CAR constructs utilized a CD8 leader sequence, (GGGGS)3 linker, CD8 hinge, and CD8 transmembrane domain and were expressed under the control of an EF1α promoter. Lentivirus was packaged in HEK293 cells and purified/concentrated as described previously(Gill, Tasian, Ruella, Shestova, Li, Porter, Carroll, Danet-desnoyers, et al. 2014). In indicated experiments, Vpx was incorporated into lentivirus at the packaging stage as previously described(Bobadilla et al. 2013). Cell lines were transduced with lentivirus MOI 3-5 unless otherwise noted. For replication deficient adenovirus production, anti-HER2 CAR was cloned into the pShuttle transfer plasmid using Xba-I and Sal-I, and subsequently cloned into pAd5f35 using I-Ceu I and PI-Sce I. All cloning steps were validated by restriction enzyme digest and sequencing. pAd5f35 is first generation E1/E3 deleted adenoviral backbone. Ad5f35-CAR-HER2-ζ was generated, expanded, concentrated, and purified using standard techniques in 293 cells by the Baylor Vector Development

Laboratory. All adenoviral batches were verified negative for replication competent adenovirus and passed sterility and endotoxin analysis. Adenoviral titer was determined using Adeno-X Rapid Titer Kit (Clontech, USA) and validated by functional transgene expression in human macrophages. An MOI of 1000 PFU/cell was used unless otherwise stated.

Microscopy.

Microscopy based phagocytosis assay:

Control or CAR-expressing monomeric red fluorescent protein positive (mRFP+) THP1 cells were plated at 7.5×10^4 per well in 48 well plates and differentiated with 1ng/mL phorbol 12-myristate 13-acetate (PMA) in RPMI with 10% FBS for 48 hours. Following differentiation, PMA was washed out with media and 7.5×10^4 control or target GFP+ K562 tumor cells were added and co-cultured for 4 hours at 37°C. After 4 hours, tumor cells (non-adherent) were washed out and the plate was imaged for mRFP and GFP fluorescence. The average number of phagocytic events in three random fields of view per well were averaged, in triplicate wells, on a 10x field of view. Cells were imaged using an EVOS FL Auto 2 Imaging System (ThermoFisher Scientific, AMAFD2000). Data represent the mean +/- standard error of triplicate wells. Statistical significance was calculated via t-test.

Live video imaging microscopy:

3.0x105 CAR or control mRFP+ THP-1 cells were differentiated as above in 6 well

plates and co-cultured with 3.0x105 control or target GFP+ K562 cells for 16-24 hours in

an incubated 37°C live imaging chamber and imaged ever 30-120 seconds for mRFP and

GFP using the EVOS FL Auto 2 Live Imaging System (ThermoFisher, USA) using the

10x lens.

Image cytometry.

Control or CAR mRFP+ THP-1s were differentiated and co-cultured with CD19+GFP+

K562 target cells as described above. After 4-hour co-culture, cells were washed and

harvested with trypsin-EDTA and stained with L/D aqua for viability. Imaging cytometry

was performed on Amnis ImageStreamX (EMD Millipore, Germany). Cells were gated

for mRFP+GFP+ double-positive events and the phagocytosis-identification algorithm

(Amnis ImageStreamX) was applied, which identifies GFP signal within an mRFP

positive event.

CD47/SIRPa inhibition and knockout experiments.

Control or CAR-expressing monomeric red fluorescent protein positive (mRFP+) THP1

cells were plated at 7.5x104 per well in 48 well plates and differentiated with 1ng/mL

phorbol 12-myristate 13-acetate (PMA) in RPMI with 10% FBS for 48 hours. Following

differentiation, PMA was washed out with media and the blocking CD47 antibody clone

B6H12, the non-blocking anti-CD47 clone 2D3, or the anti-SIRPa clone SE5A5 were

added in RPMI 10% FBS media for 30 minutes prior to the addition of 7.5x104 control or

target GFP+ K562 tumor cells were added and co-cultured for 4 hours at 37°C. After 4

hours, tumor cells (non-adherent) were washed out and the plate was imaged for mRFP and GFP fluorescence. The average number of phagocytic events in three random fields of view per well were averaged, in triplicate wells, on a 10x field of view. Cells were imaged using an EVOS FL Auto 2 Imaging System (ThermoFisher Scientific, AMAFD2000). Data represent the mean +/- standard error of triplicate wells. Statistical significance was calculated via t-test.

In vitro transcribed guide RNA's, designed with the Benchling tool, were cloned, transcribed, and purified following the manufacturer's protocol of the GeneArt Precision gRNA Synthesis Kit (ThermoFisher Scientific, A29377). In vitro transcribed guide RNA was pre-incubated with S.p.Cas9 protein in vitro to form the Cas9:gRNA ribonuclear protein complex, which was subsequently electroporated into THP-1 cells using a BTX ECM 830 square wave electroporation system (BTX). Knockout efficiency was assessed 5-7 days post electroporation using surface SIRPa analysis with FACS. SIRPa negative THP-1 cells were serially FACS sorted for purity and were used for functional assays.

Statistics.

Statistical analysis was performed in Prism 6.0 (GraphPad, Inc). Each figure legend denotes the statistical test used. Error bars indicate standard error of the mean unless otherwise indicated. ANOVA multiple comparison p-values were generated using Tukey's multiple comparisons test. All t-tests were two-sided. * indicates $p<0.05$, ** indicates $p<0.01$, *** indicates $p<0.001$, and **** indicates $p<0.0001$.

Figures

Figure 2.1: CAR19 constructs used in THP-1 macrophages
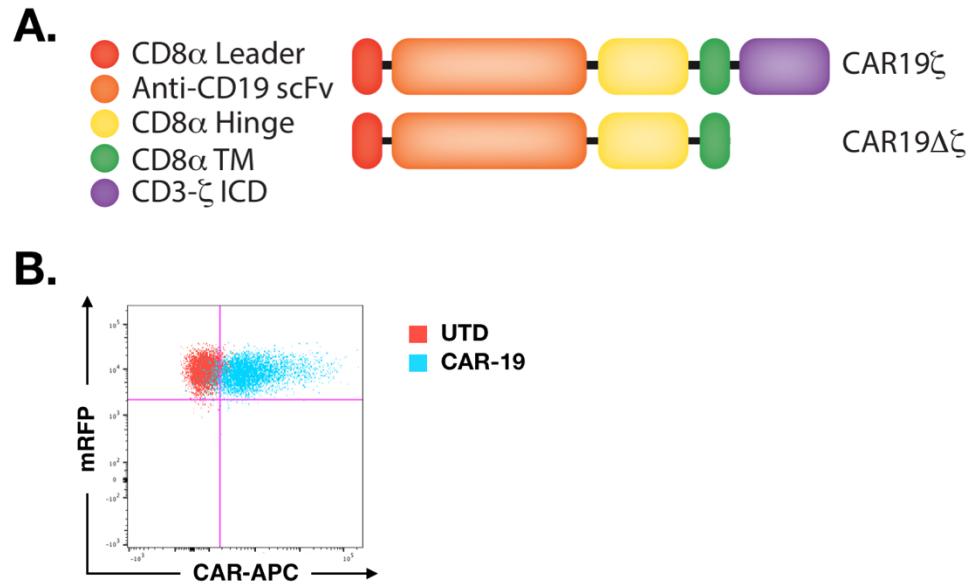
Figure 2.1:

(A.) Constructs utilized in lentiviral vectors to express CAR-19 variants in THP-1 cells (left). Both constructs were expressed downstream of an EF1A promoter.

(B.) Representative FACS plot of CAR19 expression (post-sort) in mRFP+ THP-1 cells (right). The red population represents the control untransduced (UTD) THP-1 macrophages and the blue population represents the CAR-19 THP-1 macrophages post sort.

Figure 2.2: CAR19 THP-1 macrophage phagocytosis of CD19+ targets
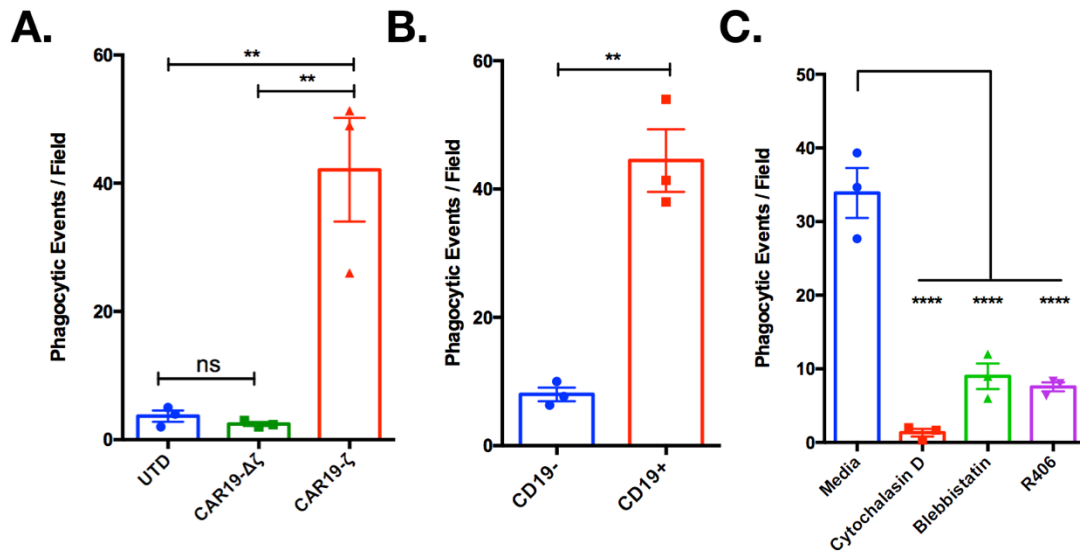
Figure 2.2:

(A): In vitro microscopy based phagocytosis assays by indicated THP-1 macrophages against CD19+ K562 target cells. Data represent the mean +/- standard error (SEM) of triplicate wells. Statistical significance was calculated via one-way ANOVA with multiple comparisons (1b) or two-sided t-test (1c) , **$p<0.01$.

(B): In vitro microscopy based phagocytosis of CD19+ or control CD19- K562 target cells by CAR19ζ+ THP-1 macrophages. Data represent the mean +/- standard error (SEM) of triplicate wells. Statistical significance was calculated via one-way ANOVA with multiple comparisons (1b) or two-sided t-test (1c) , **$p<0.01$.

(C): CAR19ζ+ THP-1 macrophages were pre-treated with media, cytochalasin-D (actin polymerization inhibitor), blebbistatin (non-muscle myosin IIa inhibitor), or R406 (Syk inhibitor) prior to the phagocytosis assay. Data represent the mean +/- SEM of triplicate wells. Statistical significance was calculated via ANOVA with multiple comparisons, ****p<0.0001.

Figure 2.3: Comparison of CD3-zeta and Fc-gamma chain CARs
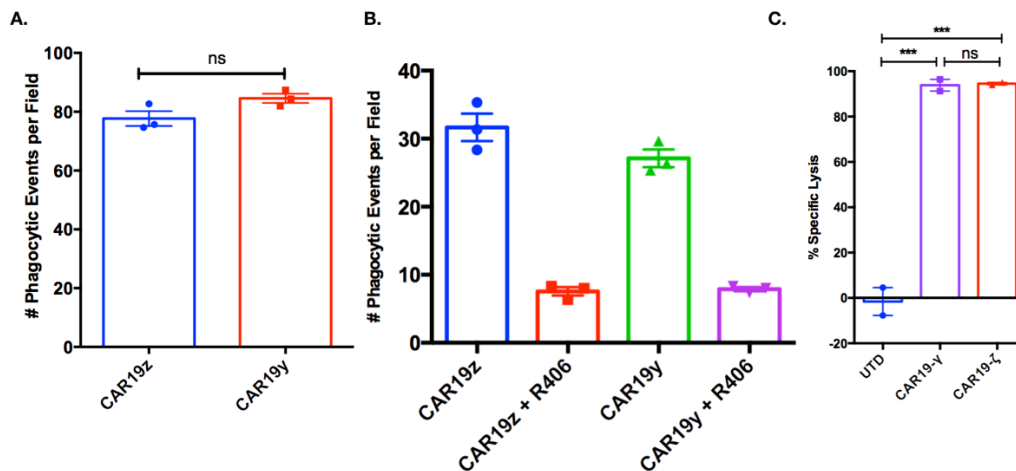
Figure 2.3:

(A): In vitro microscopy based phagocytosis assays by CAR19-zeta or CAR19-gamma expressing THP-1 macrophages against CD19+ K562 target cells. Data represent the mean +/- standard error (SEM) of triplicate wells. Statistical significance was calculated via two-sided t-test **p<0.01.

(B): In vitro microscopy based phagocytosis assays by CAR19-zeta or CAR19-gamma expressing THP-1 macrophages against CD19+ K562 target cells that were pre-treated with R406 (Syk inhibitor).

(C): Luciferase-based killing assay of CD19+K562 cells by UTD, CAR-19γ, or CAR-19ζ THP-1 macrophages (E:T=10:1;48hrs). Data represent the mean +/- SEM of triplicate wells. Statistical significance was calculated via ANOVA with multiple comparisons, ***p<0.001; ns=non-significant.

Figure 2.4: Visualization of phagocytosis and validation of solid tumor targets
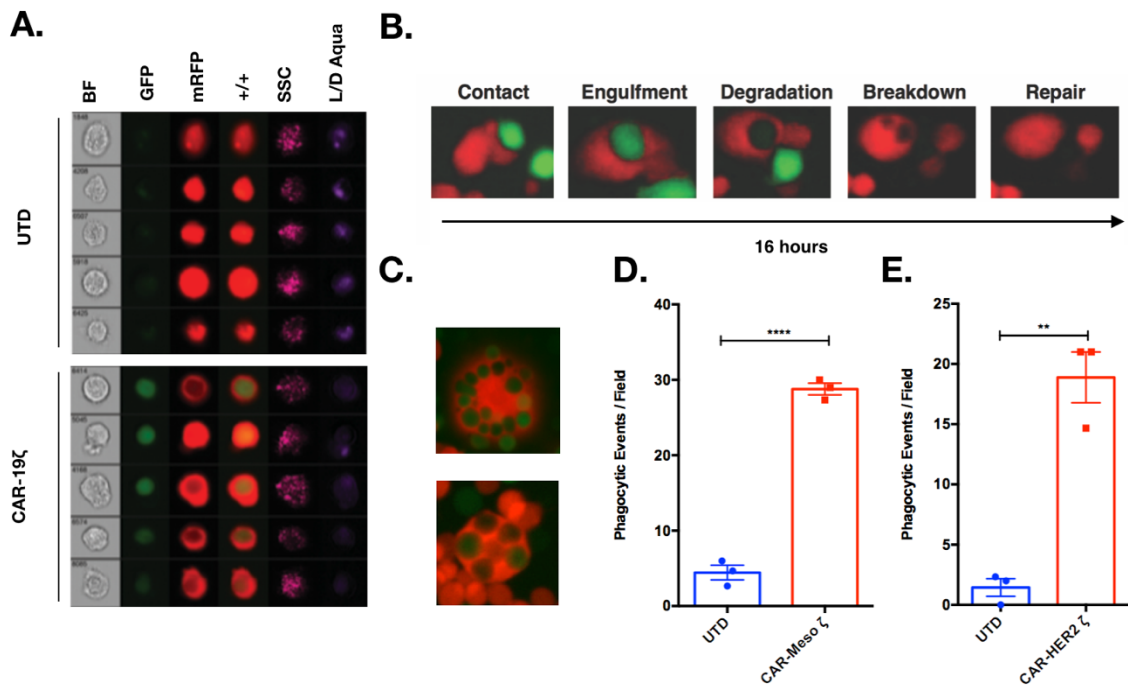
Figure 2.4:

(A): Imaging cytometry of UTD or CAR19ζ mRFP+ THP-1 macrophages after co-culture with GFP+ CD19+ K562 target cells.

(B): Key steps of the CAR-19ζ THP-1 macrophage phagocytosis during a 24-hour live cell fluorescent microscopy analysis.

(C): Representative image of poly-phagocytic CAR19ζ THP-1 macrophages from 4-hour co-culture at a 1:1 effector to target ratio.

(D): In vitro microscopy based phagocytosis of UTD or CAR-meso-ζ THP-1 macrophages of mesothelin+ K562 cells. Data is represented as mean +/- SEM. Statistical significance was calculated via t-test. ****p<0.0001; **p<0.01.

(E): In vitro microscopy based phagocytosis of UTD or CAR-HER2-ζ of HER2+ K562 cells. Data is represented as mean +/- SEM. Statistical significance was calculated via t-test. ****p<0.0001; **p<0.01.

Figure 2.5: CD47/SIRPa inhibition augments CAR19 phagocytosis
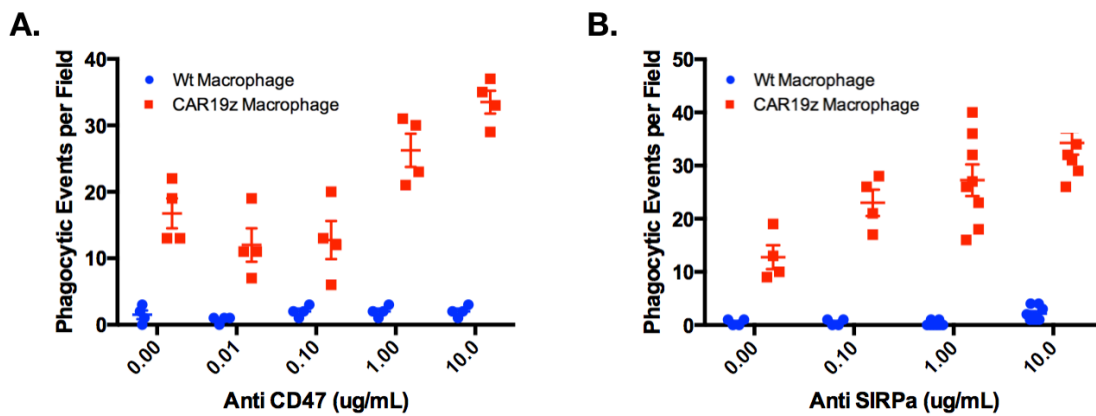
Figure 2.5:

(A): In vitro microscopy based phagocytosis of CD19+ K562 target cells by control (Wt) or CAR19-zeta THP-1 macrophages in the presence of increasing quantities of a CD47 blocking monoclonal antibody.

(B): In vitro microscopy based phagocytosis of CD19+ K562 target cells by control (Wt) or CAR19-zeta THP-1 macrophages in the presence of increasing quantities of a SIRPa blocking monoclonal antibody.

Figure 2.6: CD47/SIRPa inhibition only enhances CAR-mediated phagocytosis of target-bearing cells
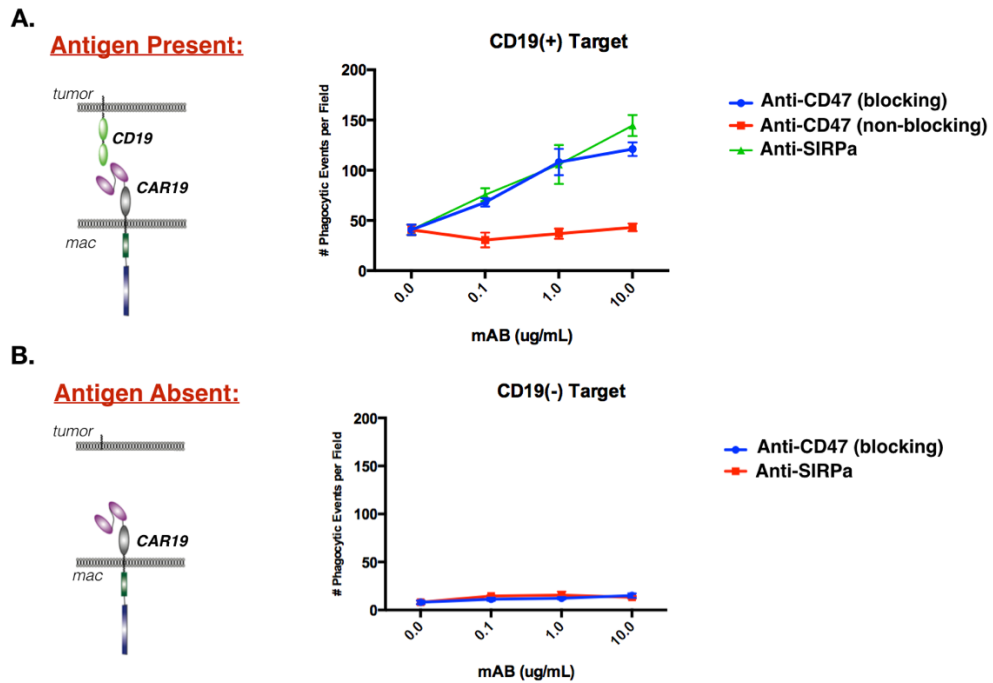
Figure 2.6:

(A): In vitro microscopy based phagocytosis of CD19+ K562 target cells by CAR19-zeta THP-1 macrophages in the presence of increasing quantities of a CD47 blocking monoclonal antibody, a control non-blocking CD47 monoclonal antibody, or a SIRPa blocking antibody.

(B): In vitro microscopy based phagocytosis of control CD19(-) K562 target cells by CAR19-zeta THP-1 macrophages in the presence of increasing quantities of a CD47 blocking monoclonal antibody or a SIRPa blocking antibody.

Figure 2.7: SIRPa KO CAR19 THP-1 macrophages display enhances phagocytosis
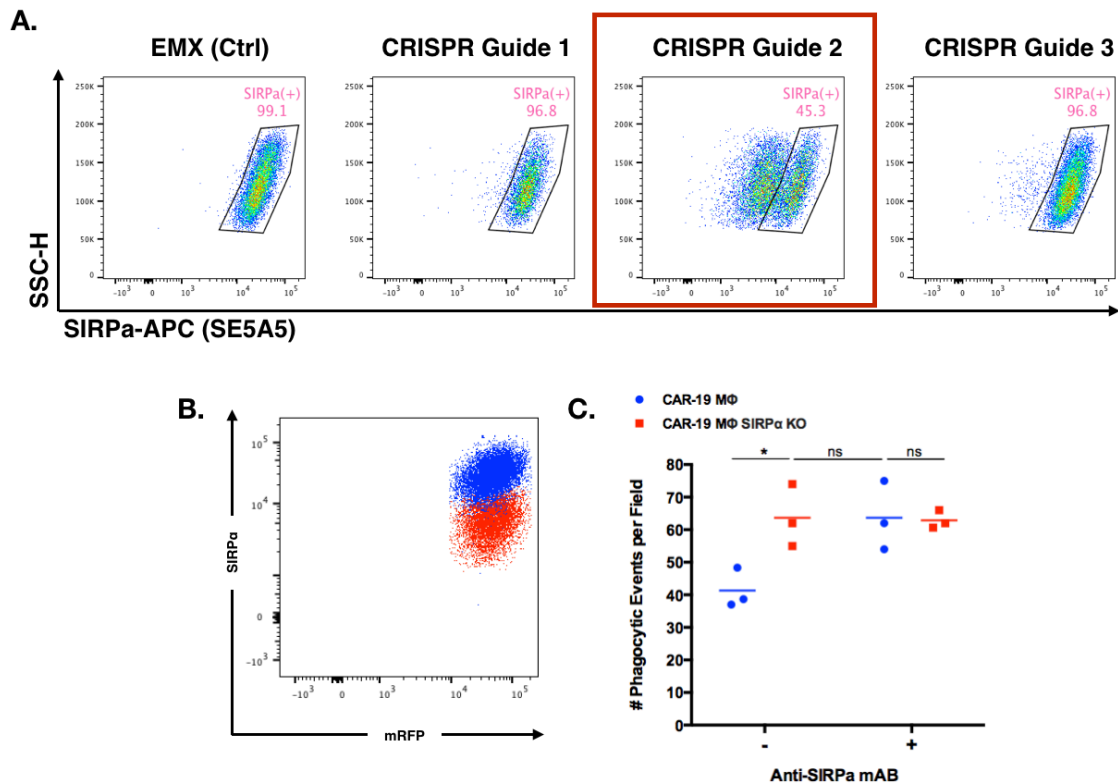
Figure 2.7:

(A): Evaluation of three anti-SIRPa CRISPR guide RNAs or a negative control EMX target guide RNA by FACS analysis of surface SIRPa expression.

(B): Post-sort expression and purity of CAR19(+) THP-1 macrophages that are control (blue) or SIRPa KO using CRISPR Guide 2 (red).

(C): In vitro microscopy based phagocytosis of CD19(+) K562 tumor cells by CAR-19 or CAR19 SIRPa KO THP-1 macrophages in the absence or presence of 10ug/mL anti-SIRPa monoclonal antibody.

CHAPTER 3: Primary human macrophages are efficiently transduced to express CAR using Ad5f35 and demonstrate targeted anti-tumor activity

Abstract

The genetic manipulation of primary human monocytes, macrophages, and dendritic cells is a known challenge in the field. In this chapter, we assess physical and viral methods of the genetic manipulation of primary human monocyte derived macrophages and show that the chimeric fiber adenoviral vector Ad5f35 is efficient in the transduction of primary human macrophages. Furthermore, we utilize this vector to engineer primary human macrophages with CD3-zeta based anti-HER2 CARs and test their phagocytic and tumor killing specificity and potency. The activity of anti-HER2 CAR macrophages required a moderate-to-high level of target HER2 surface expression to trigger activity. Finally, we test the activity of primary human HER2 CAR macrophages in mouse xenograft models of human HER2 positive ovarian cancer and demonstrate that with both intraperitoneal and intravenous administration a single dose of human anti-HER2 CAR macrophages prolongs overall survival.

Introduction

In chapter 2, we show the potential for CAR mediated phagocytosis using the THP-1 cell line model of human macrophages. In order to validate the potential of the CAR macrophage approach, we sought to genetically engineer primary human macrophages with CAR. This brought upon us the fundamental issue of genetically engineering

primary human macrophages. Previous studies have shown that macrophages are difficult to engineer with retroviral and lentiviral vectors. In addition, chemical and physical approaches to macrophage transfection are either largely inefficient, transient kinetically, or induce high-level toxicity to the macrophage population. In this chapter we assess multiple methods of genetic alteration of human macrophages. In particular, we focus on monocyte derived macrophages which are the ex vivo differentiated progeny of circulating CD14 cells. Specifically, the cells used in this chapter are classical monocytes, as non-classical CD16+ CD14- monocytes are lost in the selection process. We chose to use peripheral blood CD14+ monocytes because this is the largest potential source of human macrophages. Alternatively, tissue macrophages, peritoneal macrophages, or CD34+ hematopoietic stem cell derived cells would need to be used.

We further evaluate the potential role of primary human anti-HER2 CAR macrophages as a therapeutic approach to the cell therapy of solid tumors. Chimeric antigen receptor T cells have failed to show significant efficacy in several clinical trials targeting HER2 in sarcoma and other solid tumors. There has famously been a single case of HER2 CAR-T cell mediated fatal toxicity, though this patient likely received a toxic dose, as several dozen patients treated in follow on studies did not experience marked toxicity. We chose HER2 as the target of choice for proof-of-concept because of the known normal tissue expression, the prevalence of this tumor associate antigen in many solid tumors where there is a medical need, and the known ability of macrophages to phagocytose HER2+ cells via the action of anti-HER2 monoclonal antibodies.

Previous studies of adoptively transferred autologous monocyte-derived macrophages in solid tumors failed to demonstrate efficacy, though were well tolerated and did not induce any notable adverse reactions. Without the introduction of a CAR, these cells were likely unable to recognize tumor antigens and thus unable to initiate a phagocytic program. In this chapter we test the potential for primary human anti-HER2 CAR macrophages to phagocytose target bearing tumor cells, to kill various tumor targets, we assess the dependence of CAR activity on antigen density and test the outcome of treating mice xenografted with human tumors with human CAR macrophages.

Results

We generated primary human macrophages by differentiating human CD14+ monocytes derived from the peripheral blood of normal donors using recombinant human GM-CSF for 7 days (**Figure 3.1A**) (B. Hennemann et al. 1998; Hennemann et al. 1997). Normal human donor apheresis product was subject to elutriation to deplete platelets, erythrocytes, and lymphocytes. The relative abundance of lymphocytes, granulocytes, and monocytes in Elutra fractions 3, 4, and 5 were measured by FACS and quantified using a Beckman Coulter Counter. The monocyte rich fractions were subject to CD14+ selection using Miltenyi MACS CD14+ isolation beads. The selection purity was measured by FACS and is showing in **Figure 3.2B**. Following selection, monocytes were seeded into GMP cell differentiation bags (Miltenyi) in RPMI with 10% FBS, Glutamax, and antibiotics with recombinant human GM-CSF to induce the monocyte-to-macrophage differentiation program. Cells were grown for seven days then harvested and

used for assays or cryopreserved. The day-seven macrophage purity was >95%, with the most significant contaminant immune cell being the neutrophil **(Figure 3.2C)**.

Since transduction of primary human monocytes and macrophages is challenging (unlike with the THP-1 cell line), we first tested the potential for macrophages to express CAR via direct electroporation of in vitro transcribed anti-HER2 CAR. Both primary human monocytes (undifferentiated CD14+ cells) and seven-day differentiation monocyte-derived-macrophages (with GM-CSF) were efficiently transected with an optimized RNA electroporation program. The monocytes and macrophages expressed >70% CAR on their surface **(Figure 3.2A and Figure 3.2B)**. Given the transient nature of mRNA, we tested the persistence of expression of RNA-CAR and found that RNA-CAR persists for only approximately 5 days after electroporation, despite the lack of proliferation of the terminally differentiated myeloid cells **(Figure 3.2C)**. Given the short-term transfection with in vitro transcribed CAR mRNA, we then tested a broad array of integrating and non-integrating viral vectors including lentivirus, Vpx-modified lentivirus (Bobadilla et al. 2013), a panel of AAV serotypes, and the modified chimeric fiber adenoviral vector Ad5f35 (Nilsson et al. 2004). Vpx is an HIV-2/SIV derived protein that binds to SAMHD1 and targets it for E3-ubiquitin mediated degradation (Romani & Cohen 2012). SAMHD1 is an enzyme that actively depleted dNTPs, which serves to inhibit retroviral infection as dNTPs are required for the key step of the retroviral infection process – reverse transcription (Ballana & Esté 2015). Previous studies have shown that incorporation of Vpx into HIV-1 based lentiviral vectors enhance the transduction

efficiency of human myeloid cells (Bobadilla et al. 2013; Moyes et al. 2017). We selected Ad5f35 in the panel of viral vectors because of the differential expression on human macrophages of the Ad5 and Ad5f35 docking receptors, CXADR and CD46, respectively (**Figure 3.3**). Our data showed minimal transduction with a broad panel of AAV serotypes, ineffective transduction with VSV-G pseudotyped lentivirus, and improved yet still relatively low-level transduction with Vpx-LV. Given the low transduction efficiency of standard third generation lentiviral and AAV vectors (data not shown), and the high multiplicity-of-infection (MOI) and viral volumes required for Vpx-lentivirus, we chose to pursue Ad5f35 further (**Figure 3.4**). We engineered a CD3ζ-based anti-HER2 CAR into an Ad5f35 backbone, and demonstrated the production of CAR-encoding vector, capable of transducing human macrophages at a high rate of efficiency (Figure 3.5). We proceeded to validate the efficacy of this transduction method utilizing Ad5f35 on macrophages derived from ten human donors and demonstrated reproducibility across all ten donors with an ~70% CAR transduction efficiency (**Figure 3.6**). The resultant primary human anti-HER2 CAR macrophages demonstrated antigen-specific phagocytosis (**Figure 3.7A**). Furthermore, anti-HER2 CAR macrophages achieved dose-dependent killing of several HER2^{high} cancer cell lines *in vitro* (**Figure 3.7B**). The level of CAR expression directly correlated with the MOI of Ad5f35 used during transduction (**Figure 3.8A**). In order to demonstrate the requirement of CAR for phagocytic activity, we sought to demonstrate a correlation between CAR expression and phagocytosis. We found that there was a direct correlation between phagocytosis of HER2+ SKOV3 cells and the percentage of CAR positive macrophages (**Figure 3.8B**). In

order to validate that the 4-hour phagocytic readout via FACS was a meaningful assay, we correlated the level of phagocytosis as readout by FCS with a non-biased specific lysis luciferase-based killing assay and saw a strong correlation, suggesting that phagocytosis was leading to tumor death (**Figure 3.8C**).

We sought to demonstrate a dose-response association between antigen density and phagocytic activity by electroporating a HER2^{negative} cell line with increasing amounts of *in vitro* transcribed HER2 mRNA and measuring phagocytic activity (**Figure 3.9A**). We confirmed this using a panel of human cancer cell lines with graded expression of HER2 and demonstrated a clear correlation between antigen density and phagocytic activity (**Figure 3.9B**), with minimal activity against antigen dim targets.

A major advantage to the adoptive transfer of macrophages is their potential for accumulation in solid tumors. Previous studies have demonstrated that autologous monocyte derived macrophages, upon intravenous infusion, localize at sites of primary and metastatic disease (Faradji, Bohbot, Frost, et al. 1991; Lesimple et al. n.d.). A variety of chemoattractant molecules are involved in myeloid cell trafficking, and studies have shown that the chemokine CCL2 and its receptor CCR2 is of particular importance (Qian, Li, Zhang, Kitamura, Zhang, Campion, E. A. Kaiser, et al. 2011). In order to test the ability of human macrophages to traffic to SKOV3 tumors, we established an imaging based biodistribution assay by engrafting GFP/luciferase labeled SKOV3 into NOD *scid* $_{yc}^{-/-}$ hIL3-hGMCSF-hSCF (NSGS) mice via subcutaneous injection and systemically injecting macrophages pre-labeled with an intracellular dye with an infrared spectrum. Tumors were grown until large, palpable, and visible for 3-4 weeks and macrophages

were injected either IV or intra-tumorally. Five days post administration, mice were subject to live whole-body imaging, followed by euthanasia, organ harvest and imaging. Macrophages trafficked to subcutaneous tumor after systemic administration **(Figure 3.10A).** Terminal organ harvest and fluorescent imaging revealed the presence of macrophages in lung, spleen, liver, and tumor. Importantly, aside from the tumor, the liver seemed to be the major organ in which macrophages accumulated **(Figure 3.10B and Figure 3.10C)**. The presence of anti-HER2 CAR did not have any significant impact on the trafficking pattern of macrophages in NSGS mice. A fundamental shortfall of this model is that the non-SKOV3 derived tumor stroma secreted chemokines, the tumor microenvironment, and the pattern of normal tissue HER2 expression in NSGS mice is not reflective of human patients.

We next tested the *in vivo* anti-tumor activity of CAR macrophages using two distinct models and routes of administration. The immunodeficient triple transgenic mouse strain NOD *scid* $_{yc}^{-/-}$ hIL3-hGMCSF-hSCF (NSGS) was used for all *in vivo* xenograft experiments(Wunderlich et al. 2010). In the first model, NSGS mice were injected intraperitoneally (IP) with luciferase-expressing SKOV3, a HER2^{high} human ovarian cancer cell line, and treated 2-4 hours later with a single IP injection of phosphate buffered saline (PBS), UTD macrophages as a control for non-specific anti-tumor effects, or anti-HER2 CAR macrophages (CAR) (**Figure 3.11A**). CAR, but not UTD macrophages, led to marked tumor regression in the majority of treated mice as demonstrated by serial bioluminescent imaging over 100 days (**Figure 3.11B**). The treatment was not associated with significant toxicity as demonstrated by body weights

(**Figure 3.11C**) and led to significantly improved overall survival in the CAR treatment

group (median survival 96 (CAR) vs. 38 days (UTD), p<0.0001)(**Figure 3.11D**). In the

second approach, we modeled metastatic disease by injecting SKOV3 intravenously (IV)

and allowing 7 days for engraftment. Mice then received a single IV injection of PBS,

macrophages transduced with empty Ad5f35 vector (Empty), or anti-HER2 CAR

macrophages (**Figure 3.12A**). CAR-treated mice demonstrated a marked reduction in

tumor burden (**Figure 3.12B and Figure 3.11C**). Though all mice eventually progressed,

a single infusion of CAR macrophages led to a prolongation of overall survival (median

survival 88.5 (CAR) vs. 63 days (Empty), p=0.0047) (**Figure 3.12D**). Collectively, these

results demonstrate that CAR macrophages can be efficiently generated from human

peripheral blood derived monocytes to affect targeted anti-tumor activity *in vitro* and in

murine xenograft models.

Discussion

In this chapter, we extend our findings from Chapter 2 into primary human macrophages.

These findings represent a significant advance on the concept as the ability to efficiently

transduce primary human macrophages served as a barrier to advancement in the field of

genetically engineered macrophage cell therapy. We identify the chimeric fiber

adenoviral vector, Ad5f35, which has tropism toward CD46, as a highly effective gene

transfer approach for primary human macrophages. Logically, human macrophages from

all donors tested expressed CD46 on their cell surface. We show that Ad5f35 is superior

in potency and level of gene expression to a myriad of adeno-associated virus serotypes,

VSV-G pseudotyped HIV-1 based lentiviral vectors, and lentiviral vectors encapsulated the Vpx protein to aid in transduction efficiency. Furthermore, though physical electroporation of in vitro CAR mRNA was highly efficient, the persistence of RNA-CAR was transient. In ten human donors tested, the transduction efficiency of an anti-HER2 CAR with Ad5f35 was approximately 70%.

Peripheral blood monocyte derived macrophages are terminally differentiated cells, so the choice of a high titer and high quantity vector is necessary to achieve translational potential with these cells. The average human apheresis product contains approximately 3×10^9 monocytes. Unlike with CAR-T cells, where a relatively small number of cells ($\sim 1 \times 10^8$) is transduced and then expanded, all $\sim 3 \times 10^9$ monocyte derived macrophages need to be transduced in bulk. Ad5f35 is a high titer virus ($\sim 2 \times 10^{11}$ PFU/mL) and can be scaled up to large viral production volumes and is thus a uniquely appropriate viral vector for the generation of primary human monocyte derived CAR macrophages. In addition, the viral vector has key impact on macrophage activation status and phenotype, which will be described in Chapter 3.

We show that CD3-zeta CARs are effective in inducing the phagocytic program in primary human macrophages, and that the results in the THP-1 model are representative of primary human macrophages. Anti-HER2 CAR macrophages phagocytosed HER2+ SKOV3 tumor cells but not HER2 negative control cells. In this chapter, we chose to focus on HER2 as the target antigen of choice to demonstrate proof-of-concept primary CAR macrophage activity. HER2 is a well validated target with multiple targeted therapeutics available on the market with proven efficacy in metastatic breast and gastric

cancer. Overall, the impact of HER2 targeted therapy on overall survival in metastatic solid tumors is marginal. Importantly, given the history of HER2 as a biomarker of aggressive breast cancer and a target for commonly prescribed therapeutics like trastuzumab, the normal tissue expression of HER2 is well studied and understood. Unlike with other novel solid tumor associated surface antigens, the expected toxicity with HER2 directed therapy is understood, with cardiac and pulmonary risks being the most significant concerns. In order to address the potential risk of anti-HER2 trastuzumab scFv based CAR macrophages to HER2 positive but dim cells, we performed HER2 titration assays and determined phagocytic activity. We show that when HER2 dim cancer cell lines or HER2 negative cells with low levels of induced HER2 are used as targets for phagocytosis assays, they are not eaten. These results suggest that there is a threshold minimum for triggering of CAR signaling in macrophages and serve as a potential positive sign for the safety profile of this approach. However, these in vitro models are merely reductionist models and the potential for on-target off-tumor toxicity must be carefully monitored and studied in clinical trials.

We show in this chapter that anti-HER2 primary human CAR macrophages, but not untransduced negative control macrophages, are capable of killing target bearing tumor cells in vitro in a dose-dependent manner. Furthermore, we provided proof-of-concept in a murine xenograft model of human ovarian cancer, demonstrating the anti-tumor efficacy of anti-HER2 CAR macrophages in a relevant disease model. In these experiments, mice were treated with a single dose of the CAR engineered macrophages. The persistence of human macrophages in mice and specifically in these experiments is

79

unclear. Repeat dosing may lead to deeper and/or more persistent responses. Importantly, the animal model in which efficacy was tested is the NSGS mouse – a genetically engineered immunodeficient strain. Therefore, any efficacy seen in these experiments stemmed directly from CAR macrophage mediated phagocytosis and killing of tumor. The absence of the adaptive immune system in these mice did not offer the opportunity for macrophage mediated antigen presentation and T cell stimulation, which would potentially induce deeper response through the process of epitope spreading. Identification of the appropriate models in which to test this hypothesis is the subject of future research.

Materials and Methods

Cell lines.

The THP-1, SKOV3, K562, MDA-468, CRL-2351, HTB-20, HTB-85, CRL-5803, CRL-5822, CRL-1555, HTB-131, HTB-20, and CRL-1902 cell lines were purchased from American Type Culture Collection (ATCC). Cells were culture in RPMI media with 10% fetal bovine serum, penicillin, streptomycin, 1x Glutamax, and 1x HEPES unless otherwise recommended by ATCC. All cell lines were transduced with a lentiviral vector co-encoding click beetle green (CBG) luciferase and green florescent protein (GFP) under an EF1α promoter, separated by a P2A sequence. Transduced target cell lines were FACS sorted for 100% GFP positivity prior to use as targets in vitro and in vivo. THP-1 cells were lentivirally transduced, FACS sorted, and maintained in liquid culture. CAR expression and purity was routinely validated.

<u>Plasmid construction and virus.</u>

For lentivirus production, CAR constructs were cloned into the third generation pTRPE lentiviral backbone using standard molecular biology techniques. All CAR constructs utilized a CD8 leader sequence, (GGGGS)3 linker, CD8 hinge, and CD8 transmembrane domain and were expressed under the control of an EF1α promoter. Lentivirus was packaged in HEK293 cells and purified/concentrated as described previously(Gill, Tasian, Ruella, Shestova, Li, Porter, Carroll, Danet-desnoyers, et al. 2014). In indicated experiments, Vpx was incorporated into lentivirus at the packaging stage as previously described(Bobadilla et al. 2013). Cell lines were transduced with lentivirus MOI 3-5 unless otherwise noted. For replication deficient adenovirus production, anti-HER2 CAR was cloned into the pShuttle transfer plasmid using Xba-I and Sal-I, and subsequently cloned into pAd5f35 using I-Ceu I and PI-Sce I. All cloning steps were validated by restriction enzyme digest and sequencing. pAd5f35 is first generation E1/E3 deleted adenoviral backbone. Ad5f35-CAR-HER2-ζ was generated, expanded, concentrated, and purified using standard techniques in 293 cells by the Baylor Vector Development Laboratory. All adenoviral batches were verified negative for replication competent adenovirus and passed sterility and endotoxin analysis. Adenoviral titer was determined using Adeno-X Rapid Titer Kit (Clontech, USA) and validated by functional transgene expression in human macrophages. A MOI of 1000 PFU/cell was used unless otherwise stated.

<u>Animal studies.</u>

All mouse studies were conducted in accordance with national guidelines for the humane treatment of animals and were approved by the Institutional Animal Care and Use Committee (IACUC) at the University of Pennsylvania. Schemas of the utilized xenograft models are shown in detail in the first panel of each relevant figure. NOD/SCID Il2rg-/-hIL3-hGMCSF-hSF (NSG-SM3 or NSGS) mice originally obtained from Jackson Laboratories were purchased and bred by the Stem Cell and Xenograft Core at the University of Pennsylvania. Cells (SKOV3 tumor cells, human macrophages, or human T-cells) were injected in 200-300uL PBS for both IP and IV tail vein injections. IV injections of human macrophages were split into consecutive injections to attain the target dose. Bioluminescent imaging was performed at least weekly using an IVIS Spectrum (Perkin Elmer, USA) and analysis as performed using LivingImage v4.3.1 (Caliper LifeSciences). Mice were weighed weekly and were subject to routine veterinary assessment for signs of overt illness. Animals were euthanized at experimental termination or when predetermined IACUC rodent health endpoints were reached.

<u>Flow cytometry.</u>

Primary human macrophages were tested for CAR-HER2 expression using a two-step staining protocol: human HER2/ ERBB2 Protein-His tag (Sino Biological Inc, 10004-H08H-100) primary stain followed by Human TruStain FcX (Biolegend, 422302) and Anti-His Tag APC (R&D Systems, IC050A) secondary stain. TruStain FcX (Biolegend, 422302) was always used for FACS staining of monocytes, macrophages, or monocytic

cell lines expressing Fc receptors. Macrophage purity was tested using the following panel: Anti-CD11b PE (Biolegend, 301306), Anti-CD14 BV711 (Biolegend, 301838), Anti-CD3 FITC (eBioscience, 11-0038-42), Anti-CD19 PE-CY7 (eBioscience, 25-0198-42), Anti-CD66b PerCP-CY5.5 (Biolegend, 305108), Anti-CD56 BV605 (Biolegend, 318334), and Live/Dead Fixable Aqua (L/D aqua) Dead Cell Stain Kit (ThermoFisher, L34957). The same panel was used for testing the monocyte purity post CD14 MACS selection, prior to seeding for differentiation. M1/M2 markers on primary human macrophages were detected with the following panel: Anti-CD11B PE (Biolegend, 301306), Anti-CD80 BV605 (Biolegend, 305225), Anti-CD86 BV711 (Biolegend, 305440), Anti CD206 BV421 (Biolegend, 321126), Anti CD163 APC-CY7 (Biolegend, 333622), anti HLA-DR BV785 (Biolegend, 307642), Anti-HLA ABC PE/CY7 (Biolegend, 311430) and Live/Dead Fixable Aqua Dead Cell Stain Kit. CD46 expression was detected with Anti-CD46 APC (Biolegend, 352405) and CXADR was detected with Anti-CAR PE (EMD Millipore, FCMAB418PE-I). Appropriate fluorescence matched isotype controls were acquired from Biolegend. Surface HER2 was detected using Anti-Human CD340/HER2 APC (Biolegend, 324408). Flow cytometry data were acquired on a BD Fortessa with HTS (BD Biosciences, USA), and analyzed with FlowJo X10 (FlowJo, LLC).

FACS based phagocytosis assay.

1x105 UTD or CAR-HER2-ζ human monocyte derived macrophages (48 hours post transduction) were co-cultured with media (Mac Alone), 1x105 GFP+ MDA-468 cells (HER2-) or 1x105 GFP+ SKOV3 (HER2+) target cells for 3-4 hours at 37°C in triplicate.

Following co-culture, cells were harvested with Accutase (Innovate Cell Technologies, Inc., USA), stained with Anti-CD11b APC-CY7 (Biolegend, 301342) and analyzed via FACS using a BD Fortessa (Beckton Dickinson, New Jersey). The percent of GFP+ events within the CD11b+ population was plotted as percentage phagocytosis. Data are represented as mean +/- standard error of triplicate wells. Statistical significance between CAR-HER2-ζ and UTD was calculated using ANOVA with multiple comparisons; ****$p<0.0001$, ns = non-significant.

Primary human macrophages and T-cells.

Normal donor apheresis was either performed at the hematology unit at the Hospital of the University of Pennsylvania under an IRB approved protocol through the Human Immunology Core of the University of Pennsylvania or were acquired and shipped fresh from HemaCare (HemaCare Corporation, CA, USA). Apheresis derived leukopacs were subject to elutriation using an Elutra Cell Separation System (Terumo BCT) to reduce erythrocytes, platelets, lymphocytes, and granulocytes. Monocyte enriched fractions were pooled and subjected to MACS CD14 positive selection (Miltenyi) per manufacturer's instruction. The pre-selection and post-selection (positive and negative fraction) purity was tested using flow cytometry. Selected CD14 monocytes were seeded in Cell Differentiation Bags (Miltenyi) in RPMI with 10% FBS, penicillin, streptomycin, 1x glutamax, 1x HEPES, and 10ng/mL recombinant human GM-CSF (Peprotech, 300-03) for 7 days. Differentiation was monitored by light microscopy. Adenovirus was added on

day 5 at an MOI of 1x103 based on plaque-forming unit (PFU) titer. Differentiated macrophages were harvested at day 7 and tested for CAR expression, differentiation, and macrophage purity by FACS. For smaller scale experiments macrophages were plated directly in tissue-culture treated well-plates or flasks and transduced at an MOI of 1000 PFU directly in well plates or flasks. CD3 selected T-cells were provided by the University of Pennsylvania Human Immunology Core and were expanded/transduced as previously described.

<u>In vitro cytotoxicity assay.</u>

CBG/GFP double positive SKOV3, HTB-20, and CRL-2351 tumor cells were used as targets in luciferase based killing assays by control (UTD) or CAR-HER2-ζ (CAR) macrophages. The effector to target (E:T) ratio was serially titrated from 10:1 down to 1:30 for both effector groups. Bioluminescence was measured using an IVIS Spectrum (Perkin Elmer, USA). Percent specific lysis was calculated based on luciferase signal (total flux) relative to tumor alone, using the following formula.

% Specific Lysis = [(Sample signal – Tumor alone signal)/(Background signal – Tumor alone signal)] x 100

Data is shown as mean +/- SEM, with each condition in triplicate. Negative specific lysis values indicate more signal than in the tumor alone wells. Statistical significance was calculated using ANOVA with multiple comparisons; ****$p<0.0001$; ***$p<0.001$; **$p<0.01$; *$p<0.05$; ns=non-significant.

In vitro transcription and RNA electroporation.

In vitro transcription (IVT) was performed using the mMessage mMachine T7 Ultra Kit (ThermoFisher, AM1345). Briefly, the cDNA for human HER2 was cloned into the pDA vector downstream of a T7 promoter, linearized with PacI, and IVT was performed per manufacturer's instruction. For RNA electroporation, MDA-468 cells were washed twice in PBS and resuspended in Opti-MEM (ThermoFisher, 31985062). Increasing amounts of IVT HER2 mRNA were added (from 0 to 20ug) prior to electroporation using the BTX ECM 830 Square Wave Electroporation System (Harvard Apparatus) using a single pulse of 300V and 0.7msec. Cells were incubated at 37C overnight and HER2 MFI was determined via FACS prior to use.

Statistics.

Statistical analysis was performed in Prism 6.0 (GraphPad, Inc). Each figure legend denotes the statistical test used. Error bars indicate standard error of the mean unless otherwise indicated. ANOVA multiple comparison p-values were generated using Tukey's multiple comparisons test. All t-tests were two-sided. * indicates $p<0.05$, ** indicates $p<0.01$, *** indicates $p<0.001$, and **** indicates $p<0.0001$.

Figures

Figure 3.1: Primary human monocyte derived macrophage process overview and cell purity throughout the process
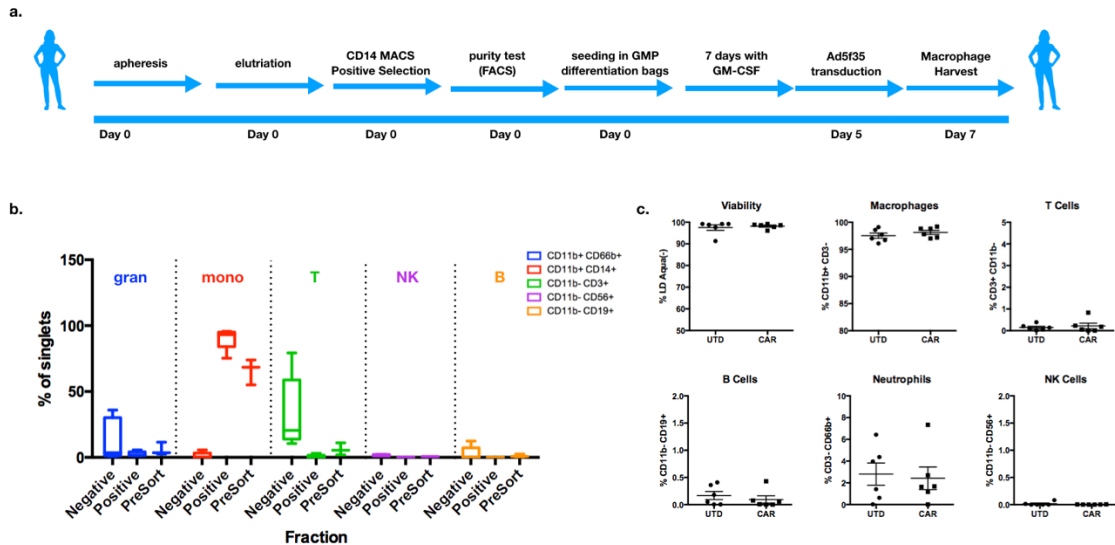
Figure 3.1:

(A): Overview of the CAR macrophage 7-day manufacturing process and timeline.

(B): Relative abundance of granulocytes, monocytes, T cells, NK cells, and B cells in the pre-selection or post-selection positive/negative fractions, as determined by FACS analysis. The post-selection positive fraction was used for macrophage differentiation.

(C): The inter-donor variability in viability and leukocyte purity (macrophages, T cells, B cells, neutrophils, and NK cells) at the time of harvest from 6 normal donors for both control (UTD) and CAR macrophages.

Figure 3.2: RNA electroporation of CAR mRNA is efficient but transient

A.

B.

C.
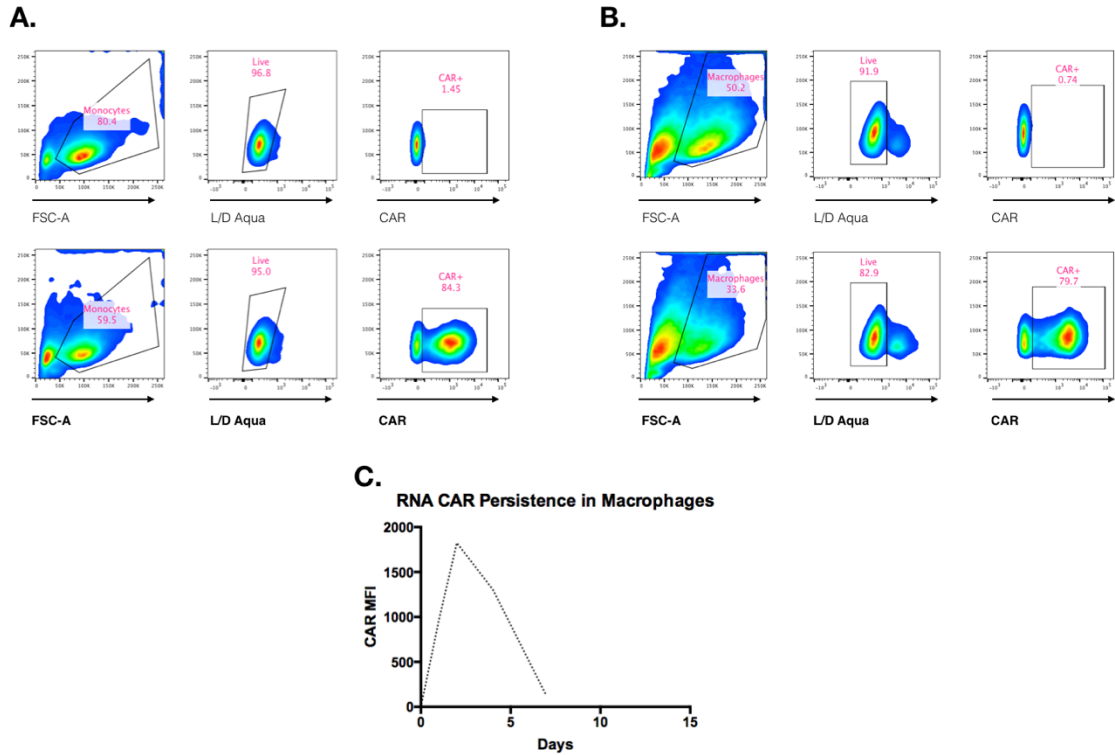
Figure 3.2:

(A): Electroporation of in vitro transcribed and capped anti-HER2 CAR mRNA of primary human monocytes. CAR expression and viability are shown from mock electroporated cells (top row) or CAR electroporated (bottom row) primary human monocytes, 24 hours post electroporation.

(B): Electroporation of in vitro transcribed and capped anti-HER2 CAR mRNA of primary human macrophages. CAR expression and viability are shown from mock electroporated cells (top row) or CAR electroporated (bottom row) primary human macrophages, 24 hours post electroporation.

(C): Persistence of expression of the CAR protein on the surface of RNA electroporated macrophage over the course of seven days, as measured by FACS.

Figure 3.3: Human macrophages express CD46 but not CXADR
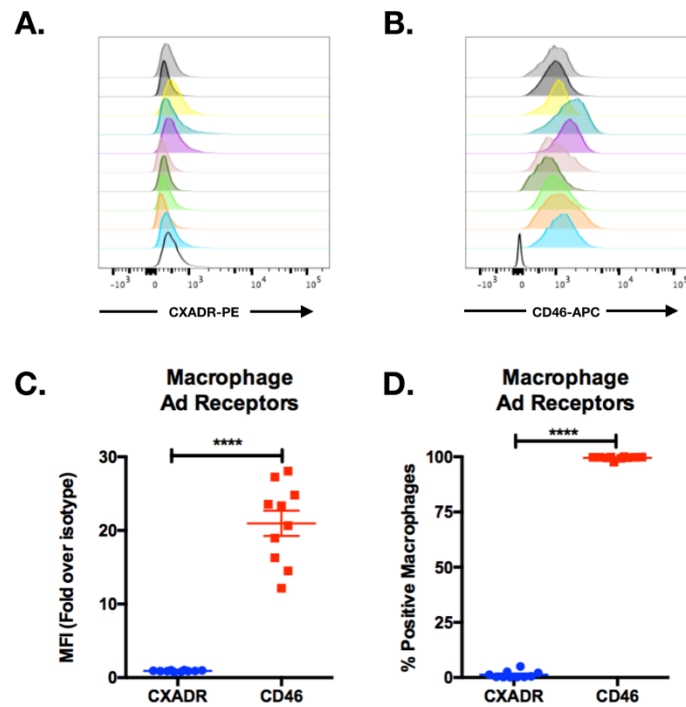
Figure 3.3:

(A): Expression of Ad5-docking protein Coxackie-adenovirus receptor (CXADR) relative to isotype control antibody (unfilled histogram) on primary human macrophages by FACS.

(B): Expression of Ad5f35-docking protein CD46 relative to isotype control (unfilled histogram) on primary human macrophages by FACS.

(C/D): MFI and percent positivity for CXADR and CD46 from 10 donors. Data represents mean +/- SEM. Statistical significance was determined using t-test; ****p<0.0001.

Figure 3.4: Ad5f35 is highly efficient in macrophage transduction
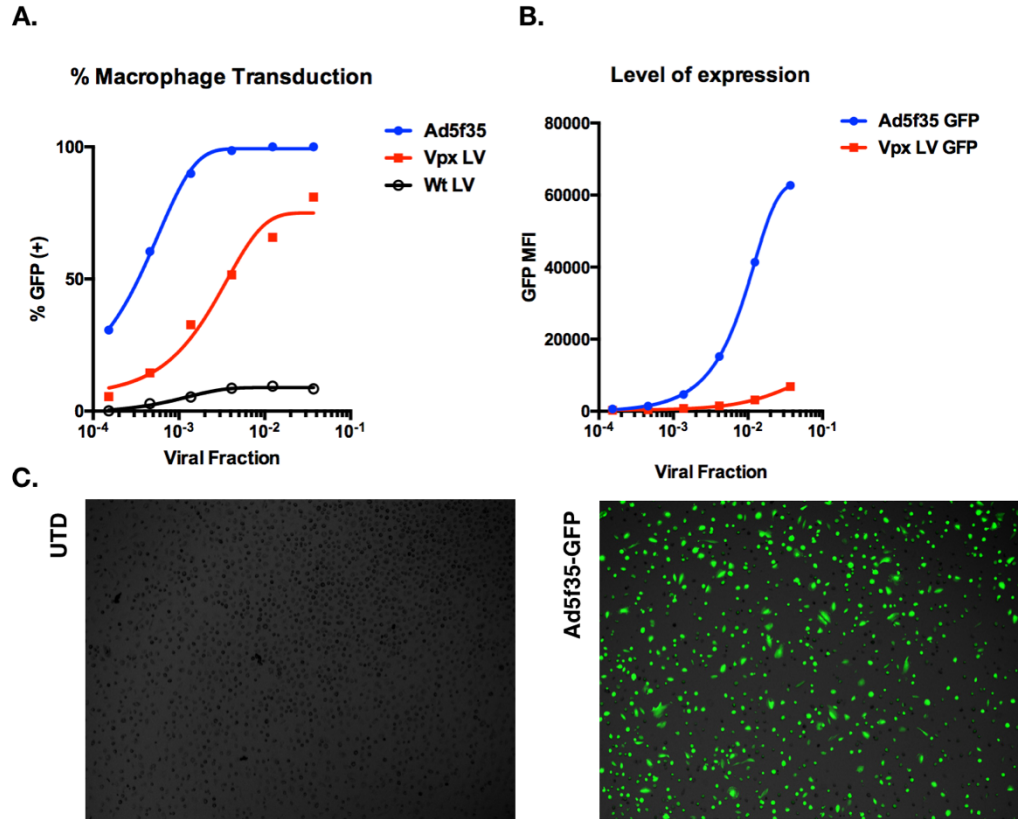
Figure 3.4:

(A/B): Primary human macrophages were transduced with GFP encoding viruses at decreasing dilution factors. Ad5f35, standard 3rd generation VSV-G pseudotyped lentivirus (Wt LV), or Vpx-packaged lentivirus were compared for transduction efficiency (A) and expression intensity (B). Viral fraction is calculated as the level of viral dilution in a serial titration.

(C): Representative image of UTD or Ad5f35-GFP transduced macrophages 48-hours post transduction.

Figure 3.5: Representative gating strategy and expression of anti-HER2 CAR on Ad5f35-transduced macrophages
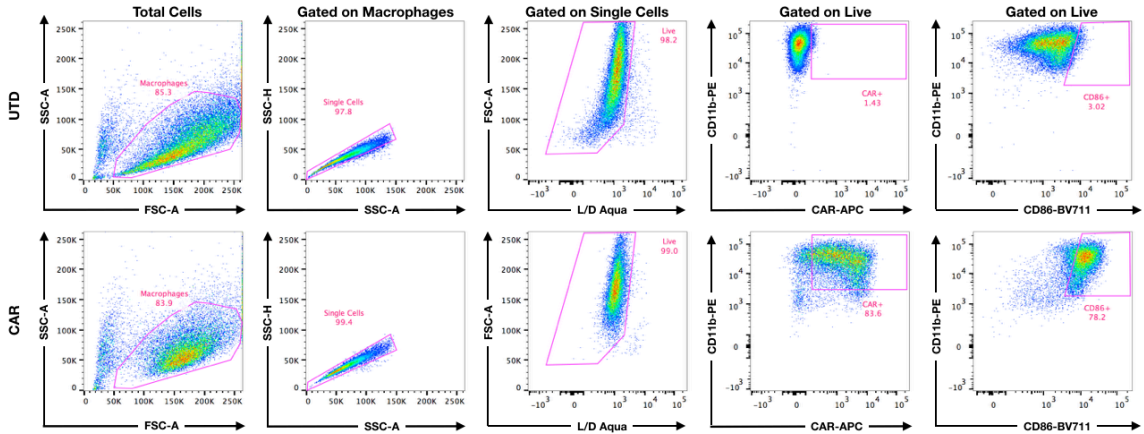
Figure 3.5:

Representative FACS gating strategy for anti-HER2 CAR and CD86 in UTD (top-row) and CAR (bottom-row) primary human macrophages.

Figure 3.6: Induction of CD86 by Ad5f35 on macrophages from 10 human donors
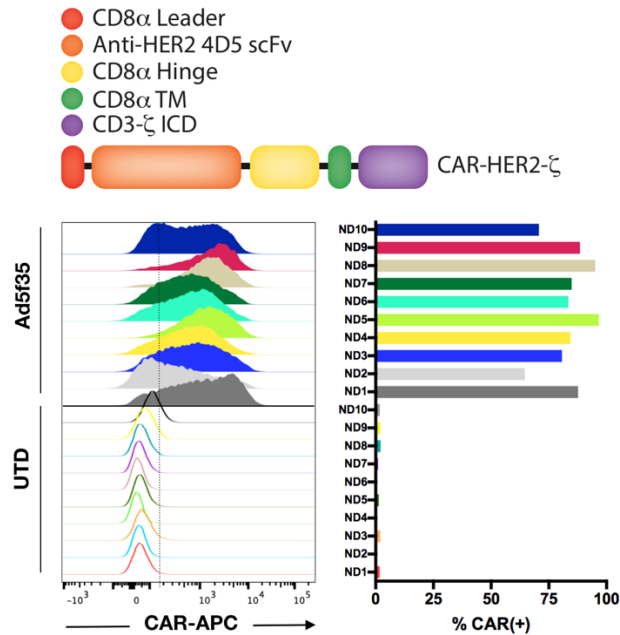
Figure 3.6:

Anti-HER2 CAR construct (top). CAR expression in 10 human donors at an MOI of

$1x10^3$ PFU, 48-hours post-transduction, as measured by FACS surface CAR staining

(bottom).

Figure 3.7: Primary human anti-HER2 CAR macrophage phagocytosis and tumor killing *in vitro*
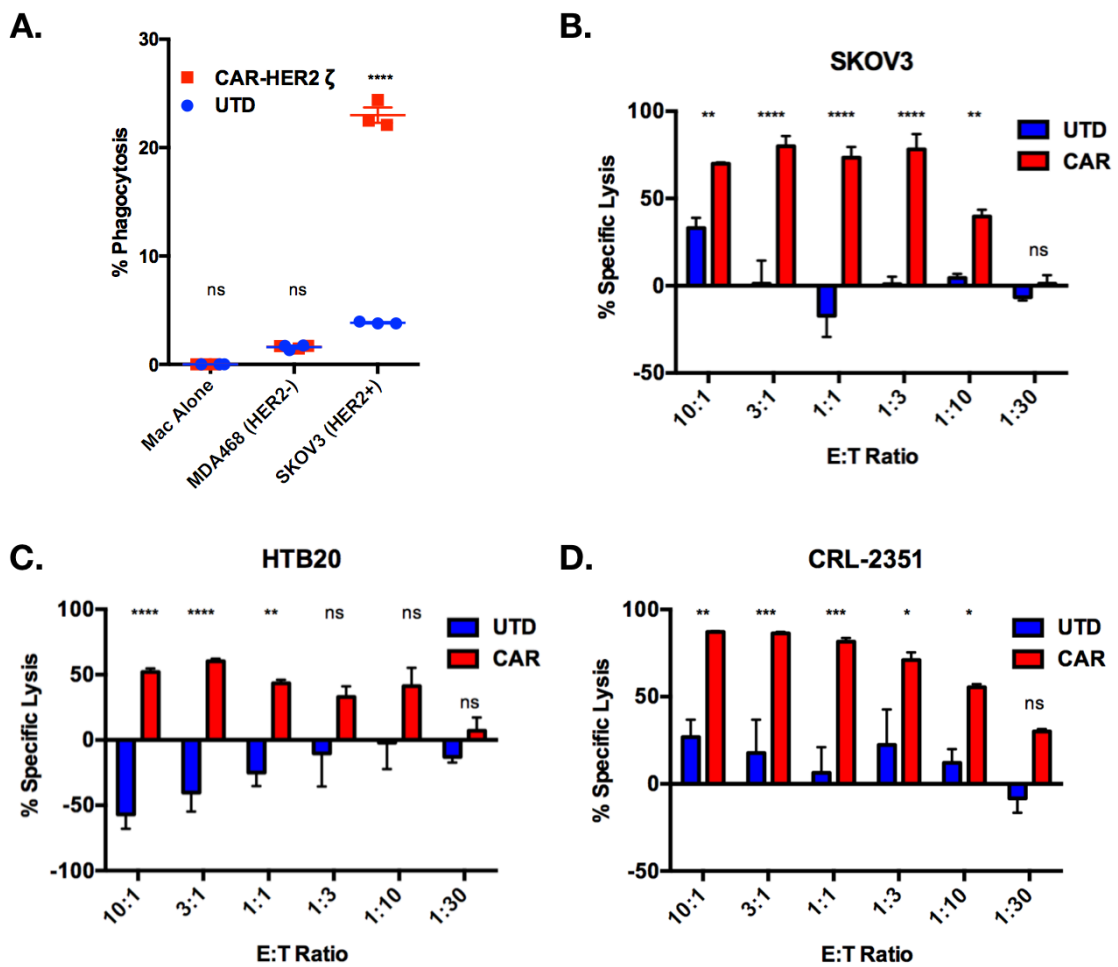
Figure 3.7:

(A): Quantification of phagocytosis by primary human control (UTD) or anti-HER2 CAR-macrophages of MDA-468 (HER2-) or SKOV3 (HER2+). Data is represented as mean +/- standard error. Statistical significant between CAR-HER2-ζ and UTD was calculated using ANOVA with multiple comparisons; ****$p < 0.0001$, ns = non-significant.

(B-D): Luciferase+ SKOV3, HTB-20, or CRL-2351 were used as targets in in vitro cytotoxicity assays with control (UTD) or CAR-HER2-ζ (CAR) macrophages at different E:T ratios. Data is shown as mean +/- SEM for triplicate wells. Statistical significance was calculated using ANOVA with multiple comparisons; ****$p < 0.0001$; ***$p < 0.001$; **$p < 0.01$; *$p < 0.05$; ns=non-significant.

Figure 3.8: Correlation of CAR expression with phagocytosis and specific lysis
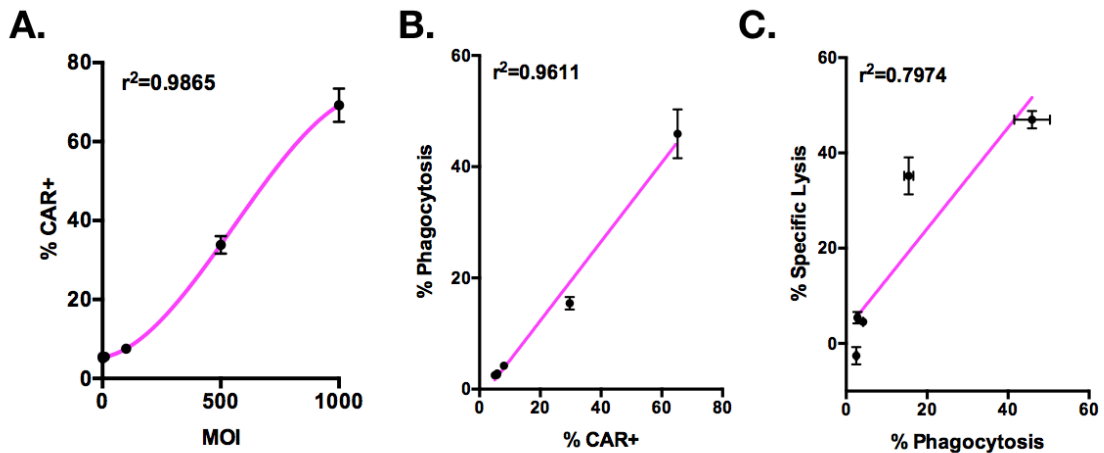
Figure 3.8:

(A): Human macrophages were transduced with CAR-HER2-ζ Ad5f35 at MOIs of 0, 100, 500, or 1000 PFU. CAR expression correlated with MOI. Data are represented as mean +/- SEM. Correlation was determined via linear regression and Pearson correlation.

(B): Human macrophages were transduced with CAR-HER2-ζ Ad5f35 at MOIs of 0, 100, 500, or 1000 PFU. In vitro phagocytosis of SKOV3 correlated with CAR expression. Data are represented as mean +/- SEM. Correlation was determined via linear regression and Pearson correlation.

(C): Human macrophages were transduced with CAR-HER2-ζ Ad5f35 at MOIs of 0, 100, 500, or 1000 PFU. Luciferase-based specific lysis of SKOV3 at 48-hours correlated with in vitro phagocytosis of SKOV3 at 4-hours. Data are represented as mean +/- SEM. Correlation was determined via linear regression and Pearson correlation.

Figure 3.9: Antigen density regulates anti-HER2 CAR macrophage activity with a threshold/switch-like pattern
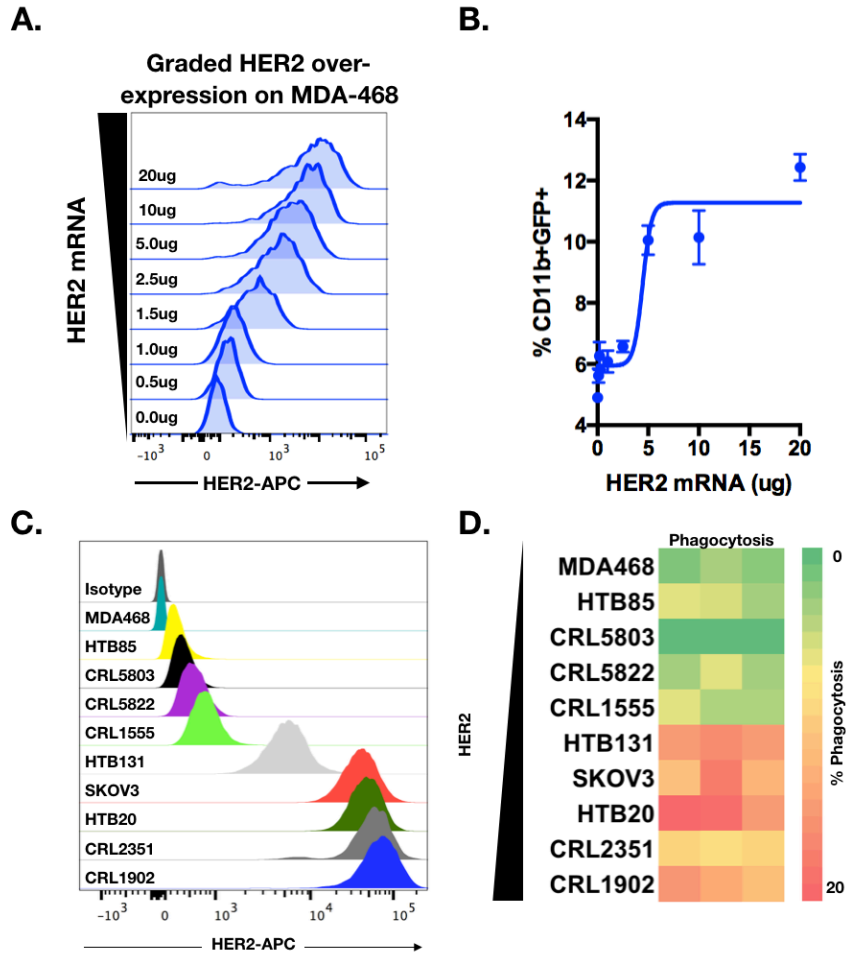
Figure 3.9:

(A-B): Increasing amounts of *in vitro* transcribed HER2 mRNA were electroporated into GFP+ MDA-468 (HER2-) target cells to generate titrated antigen expression and was validated by surface anti-HER2 FACS staining. These cells were used as phagocytic targets for CAR-HER2 macrophages. Data is shown as mean +/- standard error.

(C-D): A panel of 10 human cancer cell lines were tested for surface HER2 expression (isotype and MDA-468 are negative controls). These cell lines were exposed to CAR-HER2-ζ macrophages. Percent phagocytosis is shown as a heatmap, with each column representing a different donor. Cell lines are ordered by HER2-MFI from low-to-high.

Figure 3.10: Macrophage trafficking and biodistribution in vivo assessed via imaging
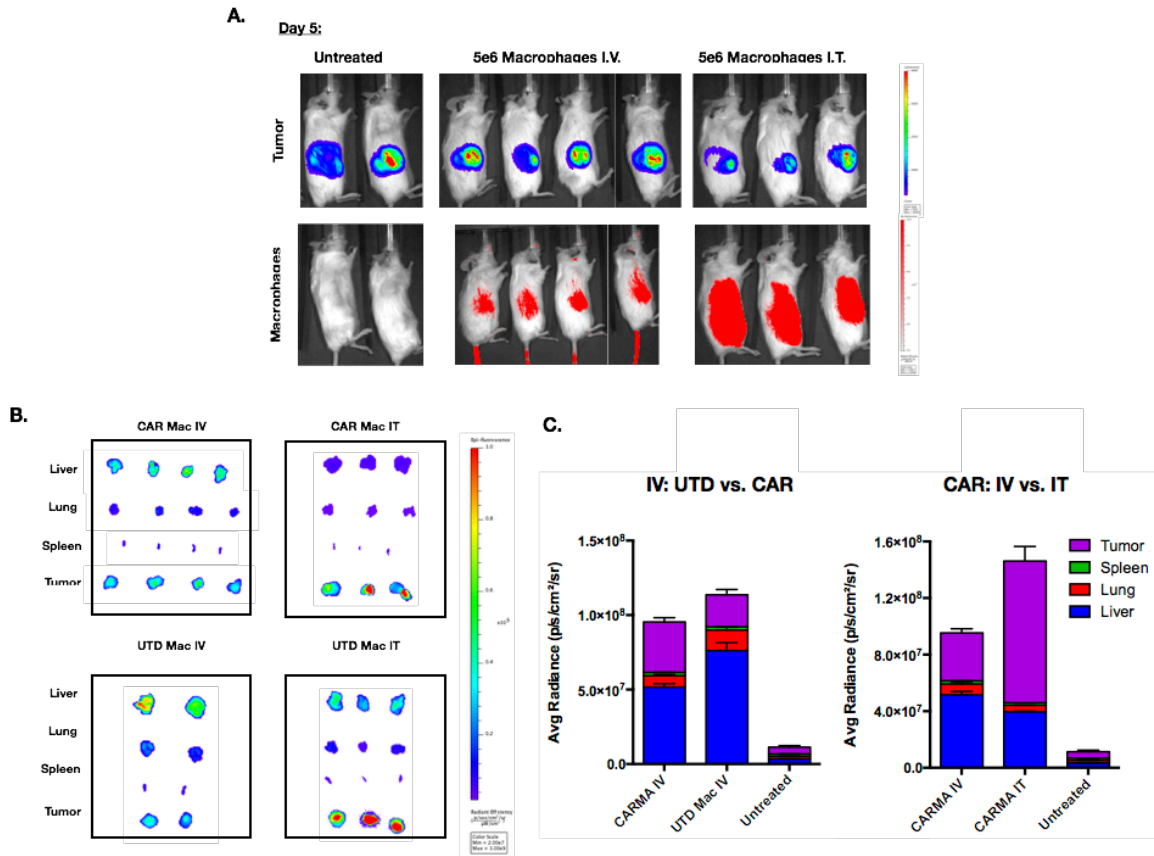
Figure 3.10:

(A): NSGS mice were engrafted with subcutaneous SKOV3 CBG/GFP tumors for 3-4 weeks until large. Mice were injected either intravenously (IV) or intratumorally (IT) with 5e6 VivoTrack680 labeled human macrophages. Mice were imaged 5 days post macrophage administration for tumor (luciferase; top row) and macrophages (VivoTrack680; bottom row). Red represents macrophages.

(B): Biodistribution of adoptively transferred macrophages via terminal organ harvest and imaging of VivoTrack680 signal in liver, lung, spleen, and tumor.

(C): Quantification of the relative VivoTrack680 signal in tumor, spleen, lung, and liver after terminal organ harvest and fluorescent imaging.

Figure 3.11: In vivo anti-tumor activity of anti-HER2 CAR macrophages in a peritoneal carcinomatosis model
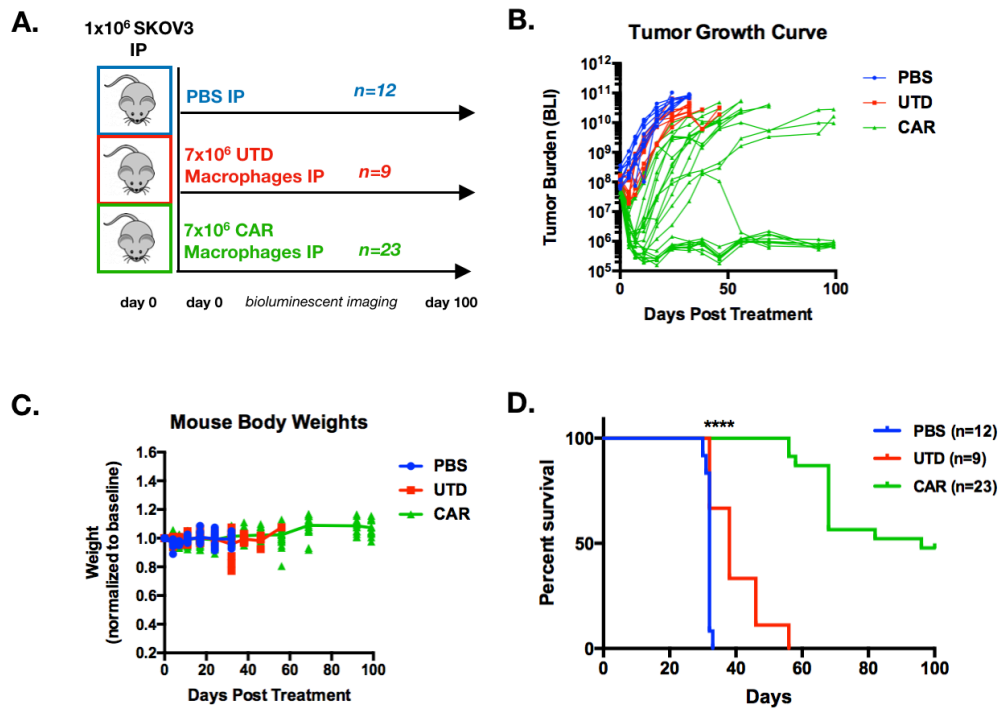
Figure 3.11:

(A): NSGS mice were injected with SKOV3 IP 2-4 hours prior to receiving injections of either PBS, control (UTD) or CAR-HER2 human macrophages IP as shown.

(B-C): Tumor burden, measured by bioluminescence (total flux), and body weight over 100 days.

(D): Kaplan-Meier survival curve over 100 days. Statistical significance was calculated using Log-Rank Mantel Cox test; ****p<0.0001.

Figure 3.12: In vivo anti-tumor activity of anti-HER2 CAR macrophages in a lung metastasis model
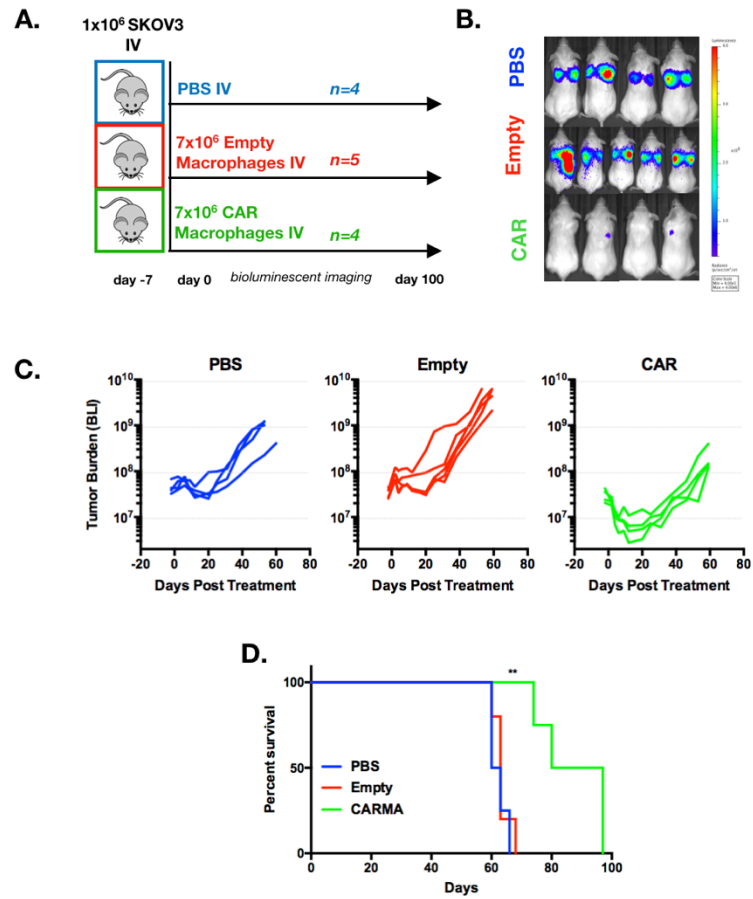
Figure 3.12:

(A): Female NSGS mice were intravenously injected with SKOV3 and treated with IV macrophages 7 days later as shown.

(B-C): Representative image of tumor burden 31-days post treatment and tumor burden (total flux) over time.

(D): Kaplan-Meier survival curve. Statistical significance was calculated using Log-Rank Mantel Cox text; **$p<0.01$.

CHAPTER 4: Adenoviral infection polarizes human macrophages toward a pro-inflammatory phenotype and renders resistance to immunosuppressive cytokines

Abstract

Macrophages constitutively express receptors that allow them to respond to a wide range of environmental cues, and intracellular signaling mediators and transcription factors that modify the gene expression profile appropriately in response to each cue. Notably, macrophages possess a thorough viral recognition program that allows them to respond to viral pathogen associated molecular patterns with the release of pro-inflammatory factors. We hypothesized that the Ad5f35 viral vector passively triggers a pro-inflammatory, anti-tumor phenotype during the CAR engineering process. In this chapter, we show that the exposure of macrophages to adenoviral vectors leads to the induction of a strong macrophage interferon signature, the induction of M1 programs, and the enhancement of the antigen processing and presentation machinery. Furthermore, the response of adenovirally transduced macrophages to immunosuppressive cytokines was significantly blunted. Taken together, the results in this chapter demonstrate that Ad5f35 transduced CAR macrophages are polarized to an irreversible anti-tumor phenotype and demonstrate augmented T cell priming potential.

Introduction

Macrophages have the capacity to transform their identity, phenotype, activation state, and function based on tissue and environmental cues (Lavin et al. 2015). Adult bone marrow derived peripheral blood monocytes traffic into inflamed or damaged tissues

where they differentiate into macrophages, potentially adopting the local phenotype and proliferative capacity of tissue resident macrophages (Varol et al. 2015). Within tissues, macrophages become activated in response to environmental cues. The activation status of macrophages lies on a spectrum, often defined by its opposing ends: M1 and M2. M1 macrophages are pro-inflammatory - they recruit T cells, upregulate antigen processing machinery and co-stimulatory ligands, and secrete activating cytokines (IL12, TNF, IFNy, etc) are therefore thought to exhibit anti-tumor function. M2 macrophages, on the other hand, are pro-tumoral and immunosuppressive - they upregulate checkpoint ligands, inhibit T cell function, promote angiogenesis, and secrete inhibitory cytokines (Mosser & Edwards 2008).

Macrophages are abundant in the tumor microenvironment (TME) of most cancers where they generally adopt an M2 phenotype and exert pro-tumoral functions such as invasion and angiogenesis, priming the pre-metastatic niche, facilitating metastasis and immunosuppression (Noy & Pollard 2014). In the context of an adoptively transferred macrophage-based cell therapy for cancer, macrophages of the M1 phenotype are likely to be far more beneficial than M0 or M2 macrophages. In fact, care must be taken to ensure that the adoptively transferred macrophages are not M2-polarized, as the addition of M2 immunosuppressive macrophages can potentially worsen the prognosis by accelerating tumor growth, invasion, and metastasis.

In this chapter, we assess the phenotype and activation state of Ad5f35 transduced CAR macrophages. Furthermore, we assess the impact of M2 inducing immunosuppressive cytokines on Ad5f35 transduced CAR macrophages. Macrophages, which are first

responders of the immune cells, lining the submucosal region of environmental barriers such as those of the gastrointestinal and respiratory lumens, constitutively expressed pattern recognition receptors capable of recognizing bacterial, fungal, and viral pathogen associated molecular patterns. Macrophages express several receptors capable of reacting to viral patterns – TLR3, TLR7, TLR9, RLR's, NLR's, cGAS/STING, and others. We hypothesized that Ad5f35, a double stranded DNA virus, has the potential to induce an M1 phenotype by triggering an antiviral response. The induction of an antiviral macrophage response would enhance the expression of lymphocyte recruiting chemokines, antigen processing and presentation genes, co-stimulatory ligands, major histocompatibility complex proteins, and pro-inflammatory cytokines. In this chapter we explore the impact of Ad5f35 on macrophage phenotype and test the further responsiveness of these cells to secondary M2 subversion in response to classic immunosuppressive cytokines IL4 and IL13.

Results

Macrophage phenotype is plastic and can change in response to cytokines, pathogen-associated molecular patterns, metabolic cues, cell-cell interactions, and tissue-specific signals (Mosser & Edwards 2008). We hypothesized that exposure to Ad5f35, a double stranded DNA virus, may induce a pro-inflammatory (M1) phenotype. Using non-biased hierarchical clustering of macrophage transcriptomes from four human donors, transduced macrophages clustered distinctly from untransduced macrophages, demonstrating a broad phenotypic shift (**Figure 4.1A**). Furthermore, when UTD, Ad5f35-

CAR transduced, empty-vector Ad5f35 transduced (Empty), IFNγ/LPS stimulated (classically activated, M1), or IL4 stimulated (alternatively-activated, M2) macrophage transcriptomes from multiple human donors were subject to non-biased principal component analysis, adenovirally transduced macrophages clustered toward the classically-activated and away from the alternatively-activated macrophages, regardless of CAR expression (**Figure 4.1B**). Transduction led to the induction of many interferon-associated genes, consistent with a classically-activated M1 phenotype (**Figure 4.2**; IFI, interferon induced; ISG, interferon stimulated gene). Unbiased pathway analysis demonstrated the induction of M1-associated pathways, such as interferon, pattern recognition receptor, Th1, RLR, JAK1/JAK2, and iNOS signaling (**Figure 4.2**). Furthermore, key components of the antigen-presentation machinery such as co-stimulatory ligand, antigen processing/presentation, and MHC-Class I/II genes were induced upon transduction (**Figure 4.3).** We validated the induction of a pro-inflammatory M1 phenotype by RT-qPCR and flow cytometry, demonstrating an MOI-dependent response (**Figure 4.4**). The induction and repression of these markers was equivalent between CAR and empty vector Ad5f35, validating that the phenotype is induced by the vector and not related to expression of CAR in macrophages (**Figure 4.5**). Ad5f35 mediated M1-induction was validated on macrophages from 10 human donors (**Figure 4.6**).

Given the upregulation of co-stimulatory ligand and antigen processing/presentation genes, and the established role of macrophages as professional antigen presenting cells (APCs), we sought to test the capacity for CAR macrophages to co-stimulate and present

antigens to T-cells. CD8+ T-cells stimulated with phytohemagglutinin (PHA) *in vitro*, a non-specific mitogen, proliferated significantly more in the presence of transduced versus untransduced macrophages (**Figure 4.7A**). To test the capacity for Ad5f35-transduced macrophages to process and present antigen, we transduced macrophages with the tumor-associated antigen NY-ESO1 and the HLA-A2*01 molecule. Macrophages were then transduced with Ad5f35, or not (UTD), and co-cultured with transgenic anti-NY-ESO-1 (1G4) TCR+ autologous T-cells. Ad5f35-transduced NY-ESO1-expressing macrophages induced significantly more proliferation of 1G4+ CD8+ T-cells than NY-ESO1-expressing control macrophages or Ad5f35 transduced macrophages lacking NY-ESO1 (**Figure 4.7B**). In order to test the potential of CAR macrophages to stimulate T-cells *in vivo*, NSGS mice were engrafted with metastatic SKOV3 and treated with CAR macrophages, CAR macrophages plus donor-derived polyclonal T-cells (CAR+T), T-cells alone, or left untreated. Mice treated with CAR macrophages plus donor-derived T-cells had deeper anti-tumor responses (**Figure 4.8A**) and generated more xenogeneic graft-versus host disease (data not shown) than the control conditions, suggesting that Ad5f35-transduced macrophages stimulated autologous T-cells *in vivo* (**Figure 4.8B**). In addition, given the enhanced physiological relevance of this semi-immune reconstituted mouse model, we measured peripheral blood chemistries to track any over toxicity, and saw no impact on red blood cell count, hemoglobin, hematocrit, platelet count, alanine aminotransferase, aspartate aminotransferase, and creatinine (**Figure 4.9).**

To address the potential concern that adoptively transferred macrophages may respond to M2-inducing cytokines, we sought to test phenotype plasticity by challenging control or

Ad5f35-transduced human macrophages with two canonical M2-inducing cytokines, IL4 or IL13. Upon stimulation with IL4, IL13, or SKOV3-conditioned media, only UTD macrophages upregulated the canonical M2 marker CD206 (**Figure 4.10A**). Furthermore, upon stimulation with IL4 only UTD macrophages increased their basal oxygen consumption rate, an expected characteristic of IL4-induced M2 macrophages (**Figure 4.10B**) (Kelly & O'Neill 2015). Transcriptome analysis revealed significantly fewer genes were induced by IL4 or IL13 in CAR versus UTD macrophages, including the CD206 encoding M2-associated gene MRC1 (**Figure 4.11**). Collectively, these results demonstrate that Ad5f35 induces a potent pro-inflammatory M1 macrophage phenotype during the transduction process, promotes the ability of macrophages to stimulate adaptive immunity, and reduces the responsiveness of macrophages to M2-inducing cytokines.

Discussion

In Chapter 4, we explore the phenotype of Ad5f35-transduced primary human CAR macrophages. Macrophages are highly plastic cells with a wide spectrum of activation states. We hypothesized that the transduction of macrophages with an adenoviral vector, regardless of the payload transgene (in this case CAR), may induce an M1 phenotype by triggering viral recognition receptors and leading to an interferon response. We show that transduction with Ad5f35 leads to a broad gene expression change as determined by RNA sequencing. Upon analyzing the transcriptome of transduced macrophages and comparing them to classically or alternatively activating macrophages, we show that Ad5f35 transduced macrophages cluster in the direction of classically activated cells.

Further validating the M1 phenotype of Car macrophages, we show that Ad5f35 transduction leads to the upregulation of co-stimulatory ligands, activating cytokines, numerous chemokines, and a myriad of genes of the antigen processing and presentation machinery. Nonbiased analysis of the transcriptome shows that there is a strong interferon signature in Ad5f35 transduced macrophages. Given that macrophages are antigen presenting cells, we hypothesized that activated M1 Ad5f35 transduced CAR macrophages may have augmented T cell priming activity. In several T cell activation assays, Ad5f35 transduced macrophages led to enhanced T cell proliferation, suggesting that the viral priming and phenotypic reprogramming augments their APC activity and enhances the likelihood of CAR macrophages leading to epitope spreading in an immunotherapeutic setting.

Interestingly, and perhaps surprisingly, the response to two classic M2 inducing immunosuppressive cytokines, IL4 and IL13, was strongly blunted or even absent in Ad5f35 transduced macrophages. We confirmed these findings on a transcriptomic, metabolic, and M2 surface phenotypic marker level. The specific mechanism by which Ad5f35 transduced macrophages were resistant to IL4 and IL13 remains to be determined, but likely involves epigenetic reprogramming at a chromatin level that renders the response to these cytokines ineffective in inducing M2 gene expression changes.

While the data show that the CAR macrophages generated in this thesis are M1 polarized and resistant to IL4 and IL13, the importance of the phenotype in more physiologically relevant animal models with intact immune systems and tumor microenvironments

remains to be determined. Furthermore, while we show in vitro resistance to several immunosuppressive cytokines, the tumor microenvironment has a myriad of potentially suppressive factors that we are unable to model in vivo. The persistence of the M1 phenotype of CAR macrophages within the tumor will be the subject of correlative studies in a future clinical trial.

Materials and Methods

Primary human macrophages and T-cells.

Normal donor apheresis was either performed at the hematology unit at the Hospital of the University of Pennsylvania under an IRB approved protocol through the Human Immunology Core of the University of Pennsylvania or were acquired and shipped fresh from HemaCare (HemaCare Corporation, CA, USA). Apheresis derived leukopacs were subject to elutriation using an Elutra Cell Separation System (Terumo BCT) to reduce erythrocytes, platelets, lymphocytes, and granulocytes. Monocyte enriched fractions were pooled and subjected to MACS CD14 positive selection (Miltenyi) per manufacturer's instruction. The pre-selection and post-selection (positive and negative fraction) purity was tested using flow cytometry. Selected CD14 monocytes were seeded in Cell Differentiation Bags (Miltenyi) in RPMI with 10% FBS, penicillin, streptomycin, 1x glutamax, 1x HEPES, and 10ng/mL recombinant human GM-CSF (Peprotech, 300-03) for 7 days. Differentiation was monitored by light microscopy. Adenovirus was added on day 5 at an MOI of $1x10^3$ based on plaque-forming unit (PFU) titer. Differentiated

macrophages were harvested at day 7 and tested for CAR expression, differentiation, and

macrophage purity by FACS. For smaller scale experiments macrophages were plated

directly in tissue-culture treated well-plates or flasks and transduced at an MOI of 1000

PFU directly in well plates or flasks. CD3 selected T-cells were provided by the

University of Pennsylvania Human Immunology Core and were expanded/transduced as

previously described.

Macrophage polarization.

For M1 or classically-activated macrophage polarization, human monocyte derived

macrophages were exposed to 20ng/mL recombinant interferon-γ (Peprotech, 300-02)

and 100ng/mL lipopolysaccharide (LPS-EK, Invivogen, tlrl-eklps) in RPMI with 10%

FBS for 24 hours. For M2 or alternatively activated macrophage polarization, human

monocyte derived macrophages were exposed to 20ng/mL recombinant human IL4

(Peprotech, 200-04) or IL13 (Peprotech, 200-13). In some experiments, 48-hour

conditioned media from SKOV3 was used (50% diluted in RPMI with 10% FBS) to

polarize macrophages toward M2 for 24 hours. In experiments where control or CAR

macrophages were challenged with M2 inducing cytokines, cells were treated with

cytokine for 24 hours, 48 hours post-viral transduction.

RNA-sequencing of human macrophages.

RNA was isolated from human macrophages from matched donors, treated as described

in each figure and polarized/challenged as above using Ambion RiboPure RNA

purification kit (Thermo Fisher Scientific, AM1924). RNA-seq libraries were generated

using TruSeq RNA Library Prep Kit (Illumina, RS-122-2001/2) and validated via BioA

by the University of Pennsylvania Next Generation Sequencing Core facility prior to

sequencing. The libraries were sequenced on 75bp single-end reads using a NextSeq

sequencer (Illumina). Low quality reads were trimmed using Trimmomatic (v0.36) and

mapped to human genome (hg38) using STAR (v2.6.0c) with default parameters. Gene

count was calculated using featureCounts (v1.6.1)(Liao et al. 2014). Non-expressed genes

with read count < 1 in all samples were removed prior to differential expression analysis.

DESeq2 with log fold change of 1 and adjusted P-value of 0.05 was used to identify

differentially expressed genes.

For genome browser tracks, bam files were first converted into bed files using bedtools

(v2.27.1). Normalized bedgraph tracks were generated using makeUCSCfile with

10,000,000 normalization factor (Homer v2) and converted into bigwig format for

integrative genomics viewer (IGV; Broad Institute) usage. Reads were mapped to the

human genome (hg38) using RUM prior to using DegSeq and EdgeR for differential

analysis. Group auto-scale was applied to all conditions for y-axis equalization in IGV.

Ingenuity Pathway Analysis (Qiagen Bioinformatics) was used to map differentially

expressed genes to canonical pathways.

Real-time PCR.

RNA was isolated using Ambion RiboPure RNA purification kit (Thermo Fisher

Scientific, AM1924) and reverse transcribed using iScript RT Supermix for RT-qPCR

(Bio-Rad, 1708841). For q-PCR, template cDNA, primers, Taqman Gene Expression

primer/probe, and Taqman Gene Expression Master Mix (Applied Biosystems, 4369016)

were used per manufacturer's instructions. The following human primer/probes from

Applied Biosystems were used: TNF (Hs00174128_m1), IL12A (Hs01073447_m1),

GAPDH (Hs02786624_G1), TAP1 (Hs00388675_m1), CD206 (Hs00267207_m1), CD80

(Hs01045161_m1), and IFNβ (Hs01077958_s1).

T-cell stimulation assays.

Phytohemagglutinin T cell proliferation assay :

Human T-cells were labeled with CellTrace CFSE Cell Proliferation Kit (ThermoFisher,

C34554) per manufacturer's protocol. CFSE labeled T-cells were cultured alone or at a

1:1 E:T ratio for 5 days with control UTD or transduced CAR-HER2-ζ autologous

macrophages in the presence or absence of 0.5% phytohemagglutinin (PHA-L, Sigma-

Aldrich, 11249738001). Proliferation of CD8 T-cells was determined by FACS by

measuring the % loss of CFSE (CFSE dilution).

NY-ESO-1 antigen processing and presentation assay:

Primary human macrophages were transduced with HLA-A201-P2A-NY-ESO1 Vpx lentivirus or not (Ag and No Ag, respectively). 1G4 NY-ESO-1 TCR T-cells were generated as previously described and stained with CellTrace Violet (CTV) Cell Proliferation Kit (ThermoFisher, C34557) per manufacturer's instruction(Rapoport et al. 2015). 48 hours post lentiviral transduction, macrophages were transduced with Ad5f35-CAR-HER2-ζ for polarization, or not, for an additional 48 hours prior to the addition of CTV labeled 1G4 anti-NY-ESO1 TCR autologous T-cells for 5 days. Proliferation of anti-NYESO1 TCR+ CD8+ T-cells was determined by FACS by measuring dilution of CTV.

Mitochondrial respiratory analysis in human macrophages.

Mitochondrial function was assessed using an extracellular flux analyzer (Agilent/Seahorse Bioscience). Primary human control or CAR macrophages (48-hours post-transduction), with or without 24-hour exposure to 20ng/mL recombinant human IL-4 (Peprotech, 200-04) were seeded at 1x105 cells/well onto XF96 cell culture microplates. To assay mitochondrial function, the medium was replaced with XF assay base medium supplemented with 5.5mM glucose, 2mM L-glutamine and 1mM sodium pyruvate. Prior to use, XF96 assay cartridges were calibrated in accordance with the manufacturer's instructions. During instrument calibration (60min) the cells were switched to a CO_2-free, 37 °C, incubator. Cellular oxygen consumption rates (OCR) and

extracellular acidification (ECAR) levels were measured under basal conditions and

following treatment with 1.5 µM oligomycin, 1.5 µM fluoro-carbonyl cyanide

phenylhydrazone (FCCP) and 40nM rotenone, with 1µM antimycin A.

Figures

Figure 4.1: Ad5f35 transduced macrophages undergo a broad gene expression change and cluster toward the M1 phenotype
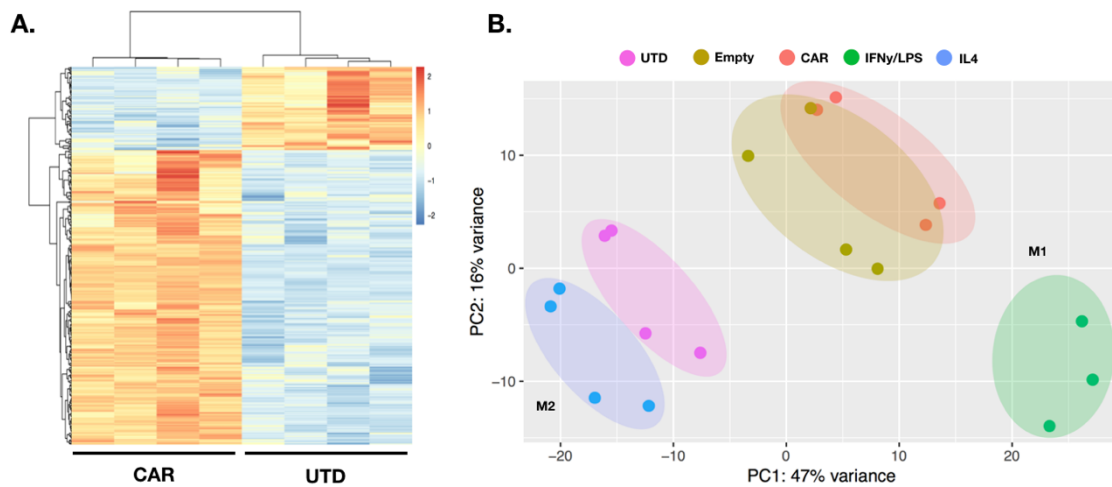
Figure 4.1:

(A): Hierarchical clustering of differentially expressed genes from UTD or Ad5f35-CAR-HER2-ζ transduced human macrophages from 4 matched donors, 48 hours post transduction. The heatmap shows $\log_2$ fold-change in gene expression relative to UTD.

(B): Transcriptome-derived principal component analysis clustering from UTD, Ad5f35-empty vector transduced, Ad5f35-CAR-HER2-ζ transduced, classically-activated M1 or alternatively-activated M2 human macrophages. Replicates represent distinct human donors.

Figure 4.2: Ad5f35 transduction of macrophages leads to M1 and interferon associated pathway induction
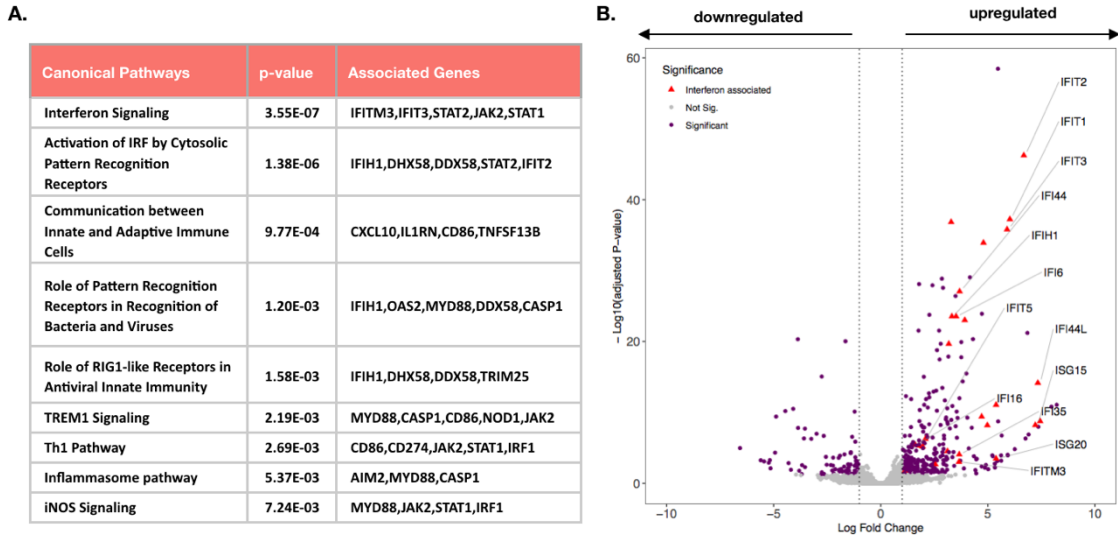
Figure 4.2:

(A): Table of Ad5f35 induced canonical pathways in human macrophages.

(B): Volcano-plot of UTD vs. Ad5f35-CAR-HER2-ζ macrophage differentially expressed genes. Purple indicates p-adj <0.05 and $\log_2$ fold change >1 or <-1. Red triangles indicate upregulated interferon-associated genes.

Figure 4.3: Ad5f35 transduction induces upregulation of co-stimulatory ligands, antigen presentation genes, and MHC Class I/II molecules
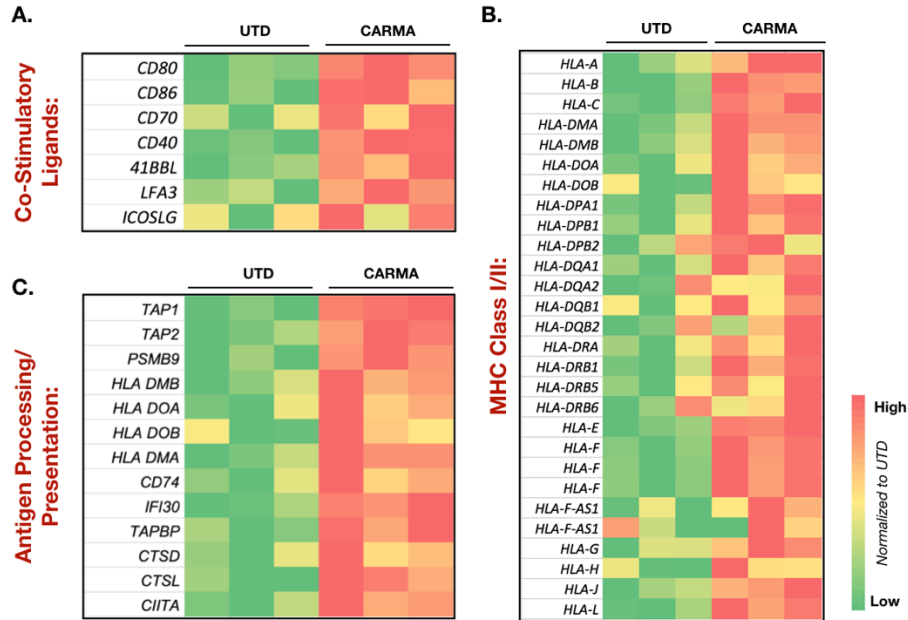
Figure 4.3:

(A-C): Gene expression heatmaps of represented co-stimulatory ligands, antigen processing/presentation, and MHC class I/II genes from 3 normal donors as determined by RNA sequencing of control UTD or Ad5f35 transduced CAR macrophages. Expression is normalized to UTD for each gene.

Figure 4.4: The M1 induction by Ad5f35 is MOI-dependent and CAR-independent
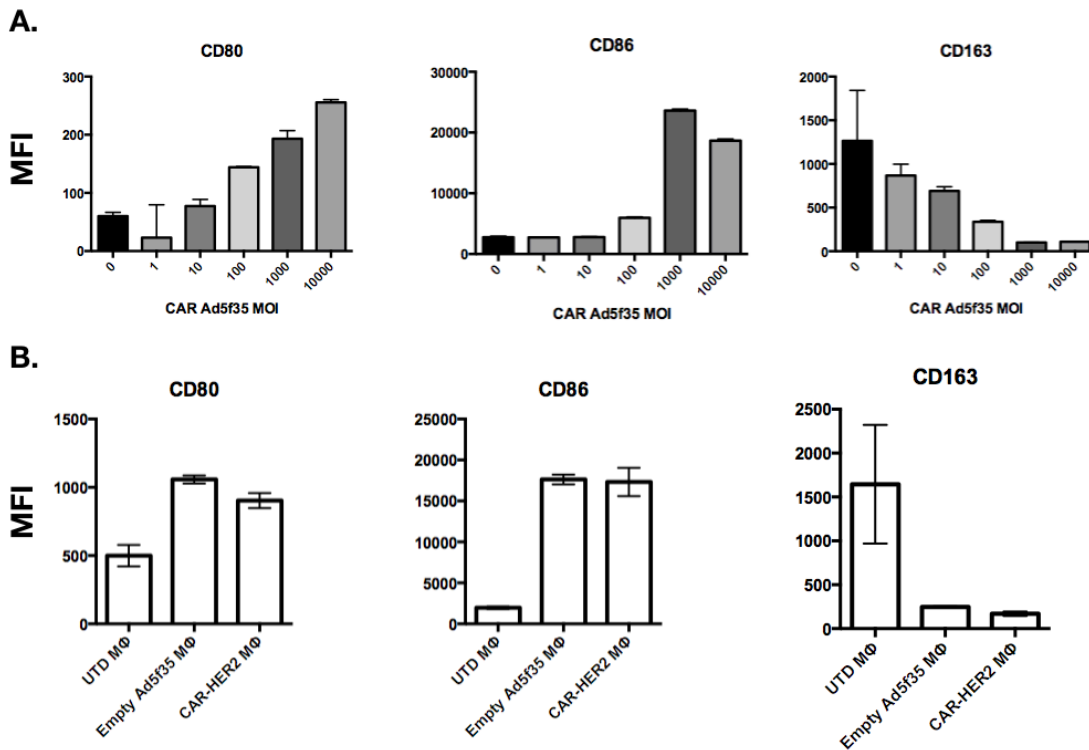
Figure 4.4:

(A): Surface expression of select human M1 markers (CD80 and CD86) and M2 marker CD163 in response to transduction with increasing MOIs of Ad5f35-CAR by FACS. Data is represented as mean +/- SEM of the mean fluorescent intensity (MFI) of each marker for duplicate wells.

(B): Surface expression of human M1 markers (CD80 and CD86) and M2 marker CD163 after transduction with equivalent MOIs of control empty-vector Ad5f35 or Ad5f35-CAR. Data is represented as mean +/- SEM of the MFI of each marker for duplicate wells.

Figure 4.5: Reverse transcription real time PCR confirmation of RNA sequencing results
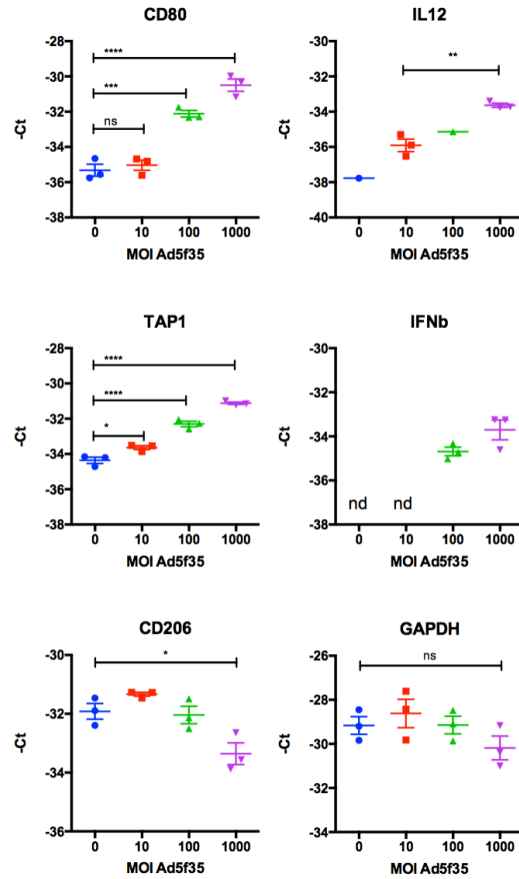
Figure 4.5:

Confirmation of select M1 genes by RTqPCR from human macrophages transduced with increasing MOIs of Ad5f35-CAR. GAPDH was used as a housekeeping control gene. Data is represented as mean +/- SEM. Statistical significance was calculated using ANOVA with multiple comparisons; ****$p<0.0001$; ***$p<0.001$; **$p<0.01$; *$p<0.05$; ns=non-significant.

Figure 4.6: Induction of the M1 marker CD86 on macrophages from 10 human donors
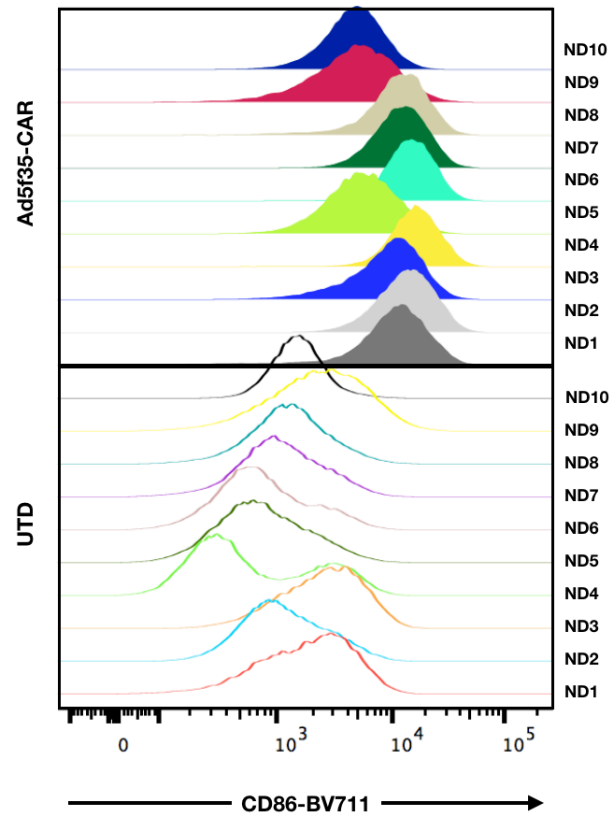
Figure 4.6:

Surface expression of M1 marker CD86 on control UTD or Ad5f35-CAR transduced

macrophages from 10 human matched-donors.

Figure 4.7: Ad5f35-transduced CAR macrophages demonstrate augmented T cell stimulation in vitro
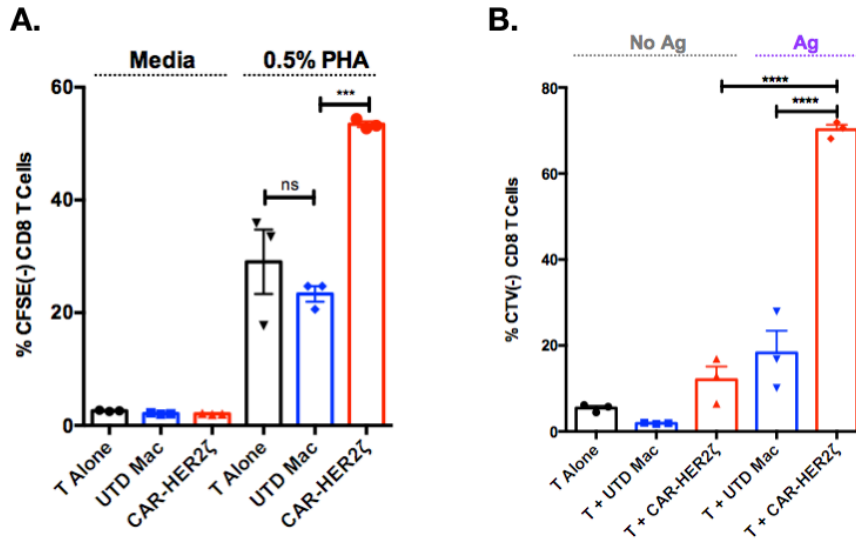
Figure 4.7:

(A): CFSE labeled T cells were cultured alone or at a 1:1 E:T ratio for 5 days with UTD

or autologous CAR macrophages in the presence or absence of PHA. Proliferation of

CD8 T cells is shown as percent of CFSE(-)CD8(+) T cells, mean +/- SEM. (***p<0.001;

ns=non-significant.)

(B): Control or NY-ESO-1 expressing macrophages (No Ag and Ag, respectively), with

or without Ad5f35-CAR were co-cultured with CTV-labeled anti-NY-ESO-1 T cells.

Proliferation of anti-NY-ESO-1 TCR+ CD8+ T cells is shown as mean +/- SEM.

Statistical significance was determined using ANOVA with multiple comparisons.

****p<0.0001.

Figure 4.8: In vivo anti-tumor response in a semi-immune reconstituted model
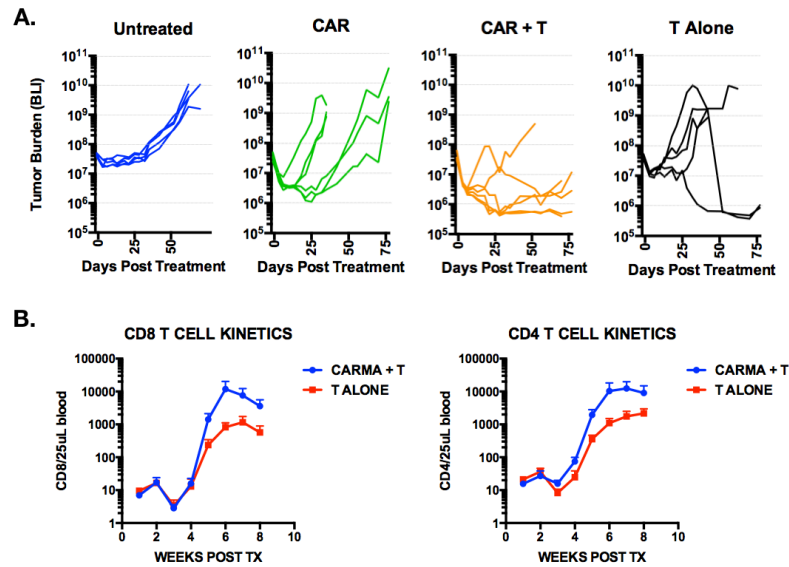
Figure 4.8:

(A): NSGS mice were IV injected with SKOV3 as shown in Figure 2m. 7 days later mice were treated with either IV PBS, CAR macrophages ($8x10^6$) +/- autologous T cells ($3x10^6$), or T cells alone. Tumor burden over time is shown for each mouse.

(B): Peripheral blood CD8+ human T-cell counts over the course of 8 weeks post treatment in mice that received T cells are T cells and CAR macrophages, as quantified by FACS per 25uL blood.

(C): Peripheral blood CD4+ human T-cell counts over the course of 8 weeks post treatment in mice that received T cells are T cells and CAR macrophages, as quantified by FACS per 25uL blood.

Figure 4.9: CAR macrophages have a promising in vivo blood chemistry safety profile
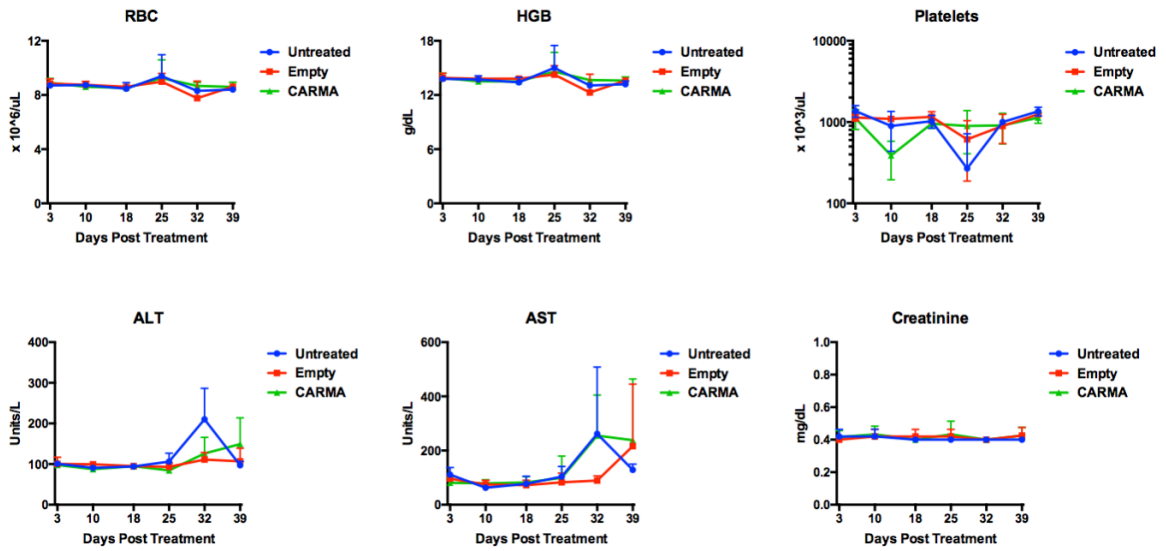
Figure 4.9:

Peripheral blood derived toxicity measures including red blood cell count (RBC), hemoglobin level (HGB), platelet count, alanine aminotransferase (ALT), aspartate aminotransferase (AST), and creatinine from SKOV3 tumor bearing NSGS mice treated with nothing (untreated), empty Ad5f35 vector transduced, or anti-HER2 CAR macrophages intravenously.

Figure 4.10: Ad5f35-transduced CAR macrophages are resistant to immunosuppressive cytokines
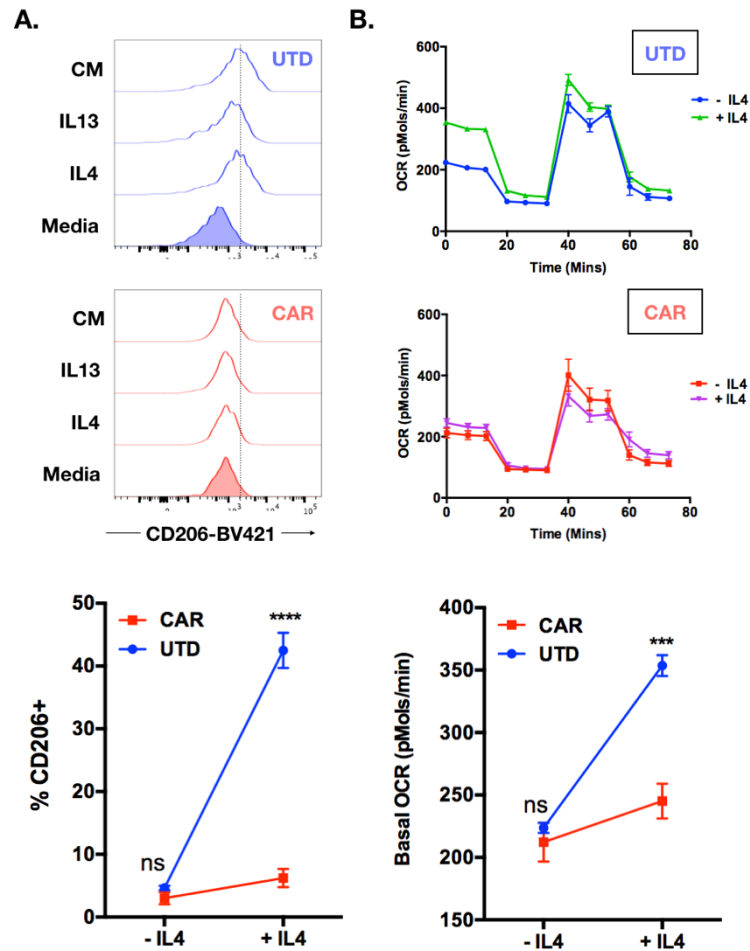
Figure 4.10:

(A): Upregulation of CD206 in response to M2-challenge in UTD or CAR macrophages (representative histograms; top panel, %CD206(+) in response to IL-4; bottom panel). Data is shown as mean +/- SEM from triplicate conditions. Statistical significance was calculated with t-test (****p<0.0001; CAR vs. UTD).

(B): The change in oxygen consumption rate (OCR) upon treatment with IL-4 in UTD or CAR macrophages (representative OCR diagrams, top panel; mean basal OCR; bottom panel). Data is shown as mean +/- SEM from triplicate conditions. Statistical significance was calculated with t-test (***$p<0.001$; CAR vs. UTD).

Figure 4.11: CAR macrophages have a blunted response to IL4 and IL13 on a transcriptome wide level
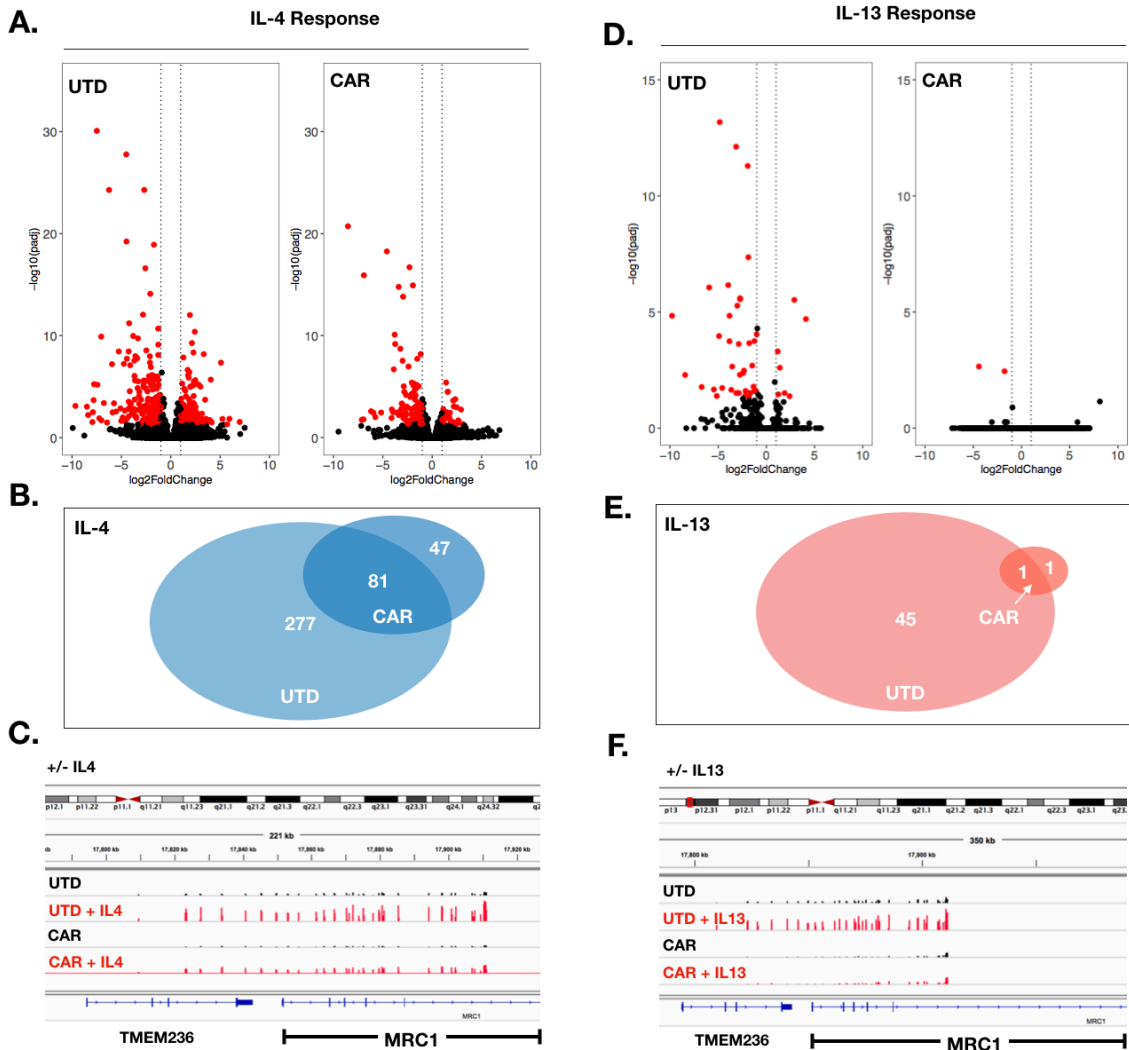
Figure 4.11:

(A): Volcano plot of IL4 response genes in UTD or CAR macrophages from RNA

sequencing. Genes on the left represent IL4-downregulated genes, while genes on the

right represent IL4-upregulated genes. Red indicates p-adj <0.05 and $\log_2$ fold change >1 or <-1.

(B): Venn diagram shows the number of IL4 M2-cytokine induced genes in UTD, CAR, or both macrophage types.

(C): Mapping of the RNA-sequencing results to the known M2 gene MRC1 (CD206) demonstrate a lack of response to IL4 in the CAR but not UTD condition.

(D): Volcano plot of IL13 response genes in UTD or CAR macrophages from RNA sequencing. Genes on the left represent IL13-downregulated genes, while genes on the right represent IL13-upregulated genes. Red indicates p-adj <0.05 and $\log_2$ fold change >1 or <-1.

(B): Venn diagram shows the number of IL13 M2-cytokine induced genes in UTD, CAR, or both macrophage types.

(C): Mapping of the RNA-sequencing results to the known M2 gene MRC1 (CD206) demonstrate a lack of response to IL13 in the CAR but not UTD condition.

Chapter 5: Conclusion, discussion and future directions

Current macrophage minded approaches to cancer immunotherapy aim to deplete the tumor-promoting mechanisms of TAMs or to engage their phagocytic activity. In this thesis, we hypothesized that genetically engineering macrophages with CAR may rewire phagocytic activity and lead to targeted anti-tumor activity. In this thesis, we introduce the concept of CAR macrophages, demonstrate for the first time the activity of CAR on human macrophages, realize the concept toward an immediately translatable primary human cell format, and provide data and rationale for the use of CAR macrophages as a platform for the cellular immunotherapy of human cancer.

In chapter 2, we show that the introduction of CD3-zeta and Fc-gamma based CARs into THP-1 macrophages allow for the phagocytic activity of cognate-antigen bearing human tumor cells. Importantly, the phagocytic activity of Car macrophages is demonstrated in the absence of any additional opsonizing agents such as monoclonal antibodies or complement, and in the absence of blockade of the inhibitory CD47/SIRPa axis. To our knowledge, this is the first study demonstrating that the addition of a single gene can redirect the phagocytic activity of tumor cells by human macrophages. The foundational proof-of-concept data using the THP-1 model was performed using anti-CD19 CARs, a well-studied model antigen in our lab. We chose this antigen as a model of CAR mediated activity, rather than as a potential clinical target, as anti-CD19 CAR-T cells are inducing deep remissions in several CD19 positive malignancies.

The functionality of CD3-zeta, a molecule which naturally is not expressed in macrophages, as the intracellular signaling domain of the macrophage CAR is perhaps surprising. CD3-zeta is naturally a component of the T-cell receptor complex and is a T-cell specific gene. In this study, we did not assess the specific signaling mechanisms or second messenger systems by which CD3-zeta activates phagocytosis. However, given the dependence on Syk, actin polymerization, and non-muscle myosin IIA activity, our data suggests that CD3-zeta is achieving phagocytosis via activation of the Fc-gamma program. In support of this concept, CD3-zeta and FcERI are highly similar in both sequence and structure, with CD3-zeta being the evolutionary result of FcERI duplication and mutation.

Upon deletion of the intracellular domain of anti-CD19 CARs in the THP-1 macrophage system, phagocytosis of CD19 positive cells was lost. This result suggests that there is a requirement for an ITAM-bearing intracellular signaling motif. In addition, we mutated the tyrosine residues of the CD3-zeta ITAMs to phenylalanines, which cannot be phosphorylated, and saw the loss of phagocytic activity, suggesting that CAR ITAM phosphorylation is required for activity in macrophages, just as in CAR T and CAR NK cells. Whether the specific choice of ITAM-bearing intracellular domain holds potential to impact the phagocytic activity remains to be determined. Interestingly, though phagocytosis was abrogated in the CD3-zeta null (delta-zeta) CAR, killing of target bearing tumor cells was strongly reduced but not completely lost. This result suggests that there may be killing mechanisms other than phagocytosis, and that the binding of an

scFv on the surface of a macrophage to an antigen on the surface of a tumor cell may lead to a low level of anti-tumor activity. The exact mechanism of killing by delta-zeta CARs, and the secondary non-phagocytic mechanisms by which CAR macrophages exert anti-tumor activity, are the subject of future research. In this thesis, we compared CD3-zeta and Fc-gamma based CARs against CD19 in terms of both phagocytosis, Syk dependence, and *in vitro* tumor killing, and were unable to detect any statistically significant differences. It is worth noting, however, that while the THP-1 model is representative of human macrophage phagocytosis, it is possible that the intracellular domains of CARs will behave differently in primary human macrophages. Future work will closely assess and compare the functionality of various intracellular domains in primary human macrophages.

The design of the CAR structures used in this thesis are based on CARs that have been optimized for T cells. We used a CD8a leader sequence, an scFv-based antigen recognition domain, a CD8a hinge, a CD8a transmembrane domain, and a CD3-zeta based intracellular domain. The biophysical interaction of macrophages with targets is distinct from that of T cells with targets, and thus it is likely that, while functional, the T-cell based CAR may not be optimal for macrophage effector activity. Future work will aim to optimize the extracellular and intracellular domains of macrophage CARs. The impact of CAR length, dimerization, tonic signaling, stimulation, and co-stimulation on phagocytosis and other macrophage effector activity remains to be determined. Notably, in this thesis we exclusively utilized "first-generation" CARs, lacking a secondary co-

stimulatory intracellular domain. The addition of a rationally-designed macrophage co-stimulatory, pro-phagocytic, or activating co-stimulatory domain is the subject of future research. Of particular interest are co-stimulatory domains derived from phagocytosis pathways distinct from and synergistic to the Fc receptor family pathways. Accordingly, a promising group of receptors that may augment CD3-zeta CAR based phagocytosis are the complement receptors. Complement has been shown to augment phagocytosis of antibody opsonized target cells independently of Fc receptors. The complement pathway is a complex cascade comprised of a series of zymogens that directly or indirectly (via antibody-antigen complexes) opsonize the surface of targets and leads to the activation of pro-inflammatory mediators, chemokines, and phagocytic signals, and is thus is a key component of innate immunity. Complement derived phagocytic signals, such as C3b, iC3b, and C4b can activate phagocytic complement receptors such as CR1 (CD35), CR3 (CD11b/CD18), and/or CR4 (CD11c/CD18) on monocytes and macrophages (Bakema & van Egmond 2014; Stasiłojć et al. 2016). The signaling pathways downstream of CR1, CR3, and CR4 activation are distinct from Fc receptor mediated pathways, and thus the intracellular domains of these receptors may potentially be effective co-stimulatory domains in macrophage CARs. Overall, the incorporation of co-stimulatory domains is the subject of future research.

In Chapter 3, we establish the CAR macrophage concept in primary human macrophages and provide proof-of-concept *in vitro* and *in vivo* efficacy data against a clinically relevant solid tumor associated antigen – HER2. Genetic manipulation of human

monocytes and macrophages has been a long-standing challenge in the field. Retroviral transduction with either gamma-retrovirus or HIV-1 based lentivirus requires high multiplicities of infection, which for integrating viruses, pose risks for insertional mutagenesis. In addition, given that human monocytes and macrophages do not expand *ex vivo,* the use of high MOI retroviral vectors to transduce ~3x109 cells per donor would not be technically feasible. Even at high multiplicities of infection, retroviral vectors demonstrate low levels of macrophage transduction. The addition of Vpx, a SAMHD1 degrading HIV-2 protein, into HIV-1 based LV vectors enhances the transduction efficiency but still required high MOIs to achieve high transduction rates. Adeno-associated virus vectors of various serotypes failed to transduce human macrophages ex vivo. Chemical approaches such as lipofection and others generally show inefficient macrophage transfection with high rates of cell toxicity. We show that the electroporation of in vitro transcribed CAR mRNA is highly efficient but leads to toxicity and is transient in expression, lasting less than 5 days on the cell surface.

Ad5, the most commonly used adenoviral serotype in gene therapy, binds to the Coxackie-adeno receptor on the surface of target cells in order to facilitate entry. Human macrophages do not express the Coxackie-adeno receptor. Ad35, however, binds to the CD46 protein for entry, and human monocytes and macrophages ubiquitously express this protein on their surface. We thus hypothesized that Ad5f35, a chimeric adenoviral vector with the fiber of Ad35 cloned in place of the Ad5 on an Ad5 vector plasmid, may lead to high levels of primary human macrophage transduction. We show that Ad5f35

leads to the mean CAR transduction rate of ~70% of macrophages at an MOI of 1000

PFU per cell.

The use of Ad5f35 to deliver CAR enabled our studies of the activity of primary human

monocyte derived anti-HER2 CAR macrophages. We demonstrate that like with THP-

1's, primary human macrophages can trigger phagocytosis and tumor clearance with the

introduction of CD3-zeta based CARs in the absence of additional opsonization. The

activity of primary human macrophages directly correlated with CAR density and HER2

negative cells were not phagocytosed by anti-HER2 CAR macrophages. Furthermore, we

correlated CAR activity with antigen density, and HER2 positive but dim cells

demonstrated resistance to CAR mediated phagocytosis.

Using NSGS mouse models, we grew SKOV3 xenografts and treated mice either

intravenously or intraperitoneally with a single injection of anti-HER2 CAR

macrophages. In mice that received CAR, but not control UTD, macrophages the overall

survival was significantly improved, and tumor burden regressed. In these models, mice

were treated with a single dose of CAR macrophages. A key question to the in vivo

activity of CAR macrophages is their overall and function persistence. Based on the

kinetics of the anti-tumor response, our data suggest that CAR macrophages persist on

the order of weeks but not months. This suggests that there may potentially be a need for

multiple doses of CAR macrophages to sustain response, unless epitope spreading via

antigen presentation leads to the adaptive rejection of tumor. The appropriate dosing

schedule of CAR macrophages will be empirically optimized in future studies and will likely vary by target and model. Whether the persistence and activity of human macrophages in NSGS mice is predictive of activity in humans, with intact immune systems, remains to be determined in clinical trials. There are pros and cons to the NSGS immunocompetent xenograft model – the activity seen is directly mediated by the adoptively transferred CAR macrophages, as there is no adaptive immunity for the cells to present antigen to. This suggests that in the setting of immunocompetency CAR macrophages may lead to deeper and more prolonged anti-tumor responses. On the other hand, by definition the tumor microenvironment in immunocompromised animals is missing or deficient, and as such lacks several of the barriers which reduce responses to therapy. In order to test synergistic action between CAR macrophages and the adaptive immune system, we co-injected NSGS mice with CAR macrophages and donor-derived non-engineered T cells and showed an increased tumor regression, suggesting that there is cross-talk between CAR macrophages and T cells occurring. Future work will assess the role of CAR macrophages in syngeneic or humanized mouse models.

A potential concern of the use of autologous primary human monocyte derived macrophages is a limited supply of cells. On average, an apheresis yields approximately $3x10^9$ peripheral blood monocytes. Given the lack of expansion of monocytes ex vivo, the maximum CAR macrophage yield with a single apheresis round is indeed $3x10^9$. Whether or not $3x10^9$ is an effective dose remains to be determined in clinical trials, as pharmacokinetic modeling of cell therapies in mice cannot be allometrically scaled. In

addition, if patients require multiple infusions of $3x10^9$ cells, there is a limit in the feasibility and clinical appropriates of repeat apheresis. Future work will examine the induction of expansion of human monocytes and macrophages ex vivo. Studies have shown the deletion of c-Maf and Maf-B in murine macrophages lead to non-neoplastic ex vivo expansion (Aziz et al. 2009). Other studies have shown that the deletion of Hoxb8 in murine macrophages couples with the expression of a constitutively active GM-CSF receptor leads to proliferation (Lee et al. 2017). The large-scale expansion of human monocytes and macrophages ex vivo remains enigmatic. Alternatively, studies have shown that the administration of mobilizing agents, such as GM-CSF, G-CSF, or plerixafor, studied for their mobilization of CD34 positive hematopoietic stem cells, increase the number of circulating monocytes by several fold. The pre-treatment of patients prior to monocyte collection serves as an approach to increase the maximal dose per manufacturing cycle.

Furthermore, given that macrophages do not express T cell receptors and are not capable of inducing graft versus host immunity, the use of allogeneic or universal donor CAR macrophages holds promise. The use of universal donor TCR deleted CD19 CAR-T cells, still expressing variable MHC which rendered the CAR-T cells susceptible to rejection, were effective in the treatment of leukemia with pre-conditioning therapy (Qasim et al. 2017). The utility of allogeneic macrophages is conceptually safe in that graft versus host disease would be highly unlikely. The rejection of the grafted macrophages may be an issue, but with pre-conditioning the macrophages may persist long enough to cause tumor

regression. In addition, further genetic modifications of CAR macrophages to decrease the potential for allogeneic rejection using gene editing techniques are possible and are the subject of future investigation.

Past clinical trials with autologous monocyte derived macrophages and the in vivo murine studies presented in this thesis demonstrate trafficking of macrophages to sites of tumor. Despite these data, the thorough understanding of macrophage biodistribution throughout the system will have important safety and efficacy implications. Macrophages are likely to distribute to all major organs, subject to blood flow and route of administration. We anticipate that the lungs will be a major initial location of macrophage accumulation, with the liver being the subsequent and perhaps final location in which systemically infused macrophages will accumulate. Our data in NSGS mice does not demonstrate any difference in the biodistribution or trafficking of CAR macrophages as compared to untransduced macrophages, but these mouse models do not accurately reflect the human condition as there are several issues of absent cross-reactivity (chemokines, stromal interactions, target antigen, and normal tissue antigen expression). In terms of efficacy, it is likely that efficacy will correlate with the accumulation of CAR macrophages at sites of disease, and macrophage loss to normal tissues will reduce the effective dose at the appropriate site. It is possible that patients with lung and liver metastases may be the patients to potentially benefit most from this therapy, as macrophages naturally distribute to lungs and liver. Whether adoptively transferred macrophages can cross the blood-brain-barrier and traffic to the central nervous system remains to be determined.

The persistence of CAR-T cells correlates with depth and persistence of response (van der Stegen et al. 2015; Maus & June 2016; Song et al. 2011; Priceman, Gerdts, et al. 2018). The persistence of macrophages is highly variable, depends on source, and is the subject of current research in the field. Bone marrow monocyte-derived inflammatory macrophages are generally short or intermediate in their lifespan (days to months), while embryonically derived tissue resident macrophages (microglial cells, Kupffer cells, alveolar macrophages, etc) can persist for many years and potentially a lifetime (Parihar et al. 2010). The persistence of tissue resident macrophages is due to both a prolonged lifespan and a stem-like ability to proliferate (Hashimoto et al. 2013). The persistence and fate of tumor associated macrophages has not been fully elucidated. Based on the kinetics of our in vivo experiments in mice, it is likely that the persistence of Ad5f35 transduced CAR macrophages is approximately several weeks to several months. Whether the native tissue and cytokine profile in human patients will create a more supportive niche for human macrophage persistence remains to be determined. If the persistence of macrophages is indeed limited in human patients, the safety profile of CAR macrophage treatment will be improved but the efficacy may be reduced - patients may potentially need multiple serial infusions.

In order to further enhance the potency and activity of human CAR macrophages, several rationally designed combination therapies hold promise. In this thesis, we assessed the synergy between blockade of the CD47/SIRPa axis in the THP-1 CD19 CAR model. In future work, we will assess the synergy between primary human CAR macrophages

against solid tumor targets in order to understand the potential for the combination with antibody inhibitors of either the ligand or the receptor of the anti-phagocytic axis. Furthermore, studies have shown the PDL1/PD1 interaction is anti-phagocytic, and logically, the blockade of this axis may potentially augment CAR phagocytosis (Gordon et al. 2017). In addition, the combination with T cell check point inhibitors may act to enhance the antigen presentation capacity of CAR macrophages.

Currently, CAR-T cell regimens require chemotherapeutic lymphodepletion prior to the infusion of autologous T cells. Lymphodepletion is thought to reduce regulatory T cells and increase the availability of cytokines such as IL-7 and IL-15 that promote T cell engraftment and proliferation. The precise mechanisms by which lymphodepletion acts to benefit CAR-T cell function is yet to be determined. This raises the question – will conditioning be required for macrophage adoptive transfer? Furthermore, are adoptively transferred macrophages more likely to traffic to tumors that are macrophage rich, suggesting they are actively producing myeloid chemo-attractants, or tumors that are macrophage poor, which have a greater niche for macrophages to fill? These experiments require immunocompetent models and will be the subject of future investigation.

Given that macrophages are a highly plastic cell type with the potential to adopt a broad spectrum of activation states, it is paramount that macrophages adoptively transferred in the context of cancer maintain an anti-tumor or M1 phenotype. In Chapter 4 we demonstrate that adenovirally infected macrophages adopt an irreversible M1 phenotype

and demonstrate resistance to M2 subversion. We show that upon transduction with the adenoviral vector Ad5f35, macrophages undergo a broad gene expression change associated with a strong interferon signature. Transduced macrophages upregulated cytokines, co-stimulatory ligands, antigen processing and presentation genes, and MHC molecules – suggesting that these engineered cells have passively acquired an anti-tumoral phenotype. We tested the antigen presentation and T cell priming activity of transduced macrophages and show that relative to control macrophages, activated Ad5f35 transduced CAR macrophages led to enhanced T cell proliferation in vitro and in vivo.

Macrophages are sentinel immune cells of the innate immune system and are professional antigen presenting cells. A major rationale in the choice of macrophages for CAR-based adoptive cellular immunotherapy is that after CAR-mediated phagocytosis, macrophages may process and present antigen and lead to epitope spreading. In Chapter 4, we show that Ad5f35-polarized M1 macrophages upregulate a myriad of genes that augment antigen processing, antigen presentation, and T cell stimulation. We show that macrophages up-regulate co-stimulatory ligands and that Ad5f35 transduced macrophages stimulate stronger T cell responses to artificial endogenous antigens than control untransduced T cells. A major next step will be to demonstrate MHC-II presentation and MHC-I cross-presentation of phagocytosed tumor-derived antigen. Cross-presentation assays are the subject of future research. Experimentally, this question can be approached in two ways. In one approach, immunopeptidomics can be used to measure tumor derived peptides eluted from CAR macrophage MHC-I or MHC-II. In another approach, target tumor cells could be engineered to over-express the intracellular

antigen NY-ESO-1 and CRISPR edited to induce MHC-I knockout, such that target cells cannot present endogenous antigens. Wild type or NY-ESO-1+/MHC-I- target cells can be used as phagocytic targets for control or CAR macrophages. Following an incubation period for phagocytosis and antigen presentation, the activation of NY-ESO-1 specific transgenic TCR T cells can be used to detect cross-presented NY-ESO-1 antigen on the CAR macrophage surface. These experiments are the subject of future work and will test our hypothesis that CAR mediated phagocytosis leads to the presentation of tumor neo-antigens and thus epitope spreading.

Furthermore, we tested the durability of the adenovirally induced M1 phenotype by challenging macrophages with the classic M2 inducing cytokines IL-4 and IL-13. CAR, but not control, macrophages were relatively resistant to the immunosuppressive polarization by the M2-inducing cytokines. Taken together, these results show that Ad5f35 transduced CAR macrophages have the potential to phagocytose tumor cells, process and present antigens, and actively co-stimulate tumor reactive T cells – leading to a multi-modal approach to the treatment of cancer.

The tumor microenvironment is highly variable and complex, and every tumor is unique. While we demonstrate resistance to the two canonical M2 inducing cytokines IL-4 and IL-13, the response to other immunosuppressive factors, such as interaction with eicosanoids, metabolic intermediates, hypoxic conditions, or other cytokines remains to be determined. Accurately modeling the TME *in vitro* is an outstanding challenge in the

field, and immunodeficient xenograft models lack central TME components. Future pre-clinical and clinical studies will assess the maintenance of the M1 phenotype in CAR macrophages within the tumor of syngeneic/humanized mice and in the biopsy material from human patients.

In conclusion, our findings support the concept that macrophages derived from human peripheral blood monocytes can be directed to exert potent anti-tumor activity via the introduction of a CAR, primarily through phagocytosis. We demonstrated that human macrophages can be engineered to express a CAR with high efficiency using Ad5f35, and that HER2-redirected human CAR macrophages reduced tumor burden and prolonged overall survival in xenograft models. Furthermore, our data show that Ad5f35 transduction polarized macrophages toward a unique pro-inflammatory/anti-tumor M1 phenotype, led to enhanced T-cell priming, and reduced susceptibility to immunosuppressive M2-inducing cytokines. Taken together, our results introduce CAR macrophages as a novel adoptive cellular therapy platform for the treatment of human cancer.

BIBLIOGRAPHY

Abate-Daga, D. et al., 2014. A Novel Chimeric Antigen Receptor Against Prostate Stem Cell Antigen Mediates Tumor Destruction in a Humanized Mouse Model of Pancreatic Cancer. *Human Gene Therapy*, 25(12), pp.1003–1012. Available at: http://www.ncbi.nlm.nih.gov/pubmed/24694017 [Accessed September 30, 2018].

Adusumilli, P.S. et al., 2014. Regional delivery of mesothelin-targeted CAR T cell therapy generates potent and long-lasting CD4-dependent tumor immunity. *Science Translational Medicine*, 6(261), p.261ra151-261ra151. Available at: http://www.ncbi.nlm.nih.gov/pubmed/25378643 [Accessed September 30, 2018].

Ahmed, N. et al., 2015. Human Epidermal Growth Factor Receptor 2 (HER2) -Specific Chimeric Antigen Receptor-Modified T Cells for the Immunotherapy of HER2-Positive Sarcoma. *Journal of clinical oncology : official journal of the American Society of Clinical Oncology*, 33(15), pp.1688–96. Available at: http://www.ncbi.nlm.nih.gov/pubmed/25800760.

Alvey, C.M. et al., 2017. SIRPA-Inhibited, Marrow-Derived Macrophages Engorge, Accumulate, and Differentiate in Antibody-Targeted Regression of Solid Tumors. *Current Biology*, 27(14), p.2065–2077.e6. Available at: http://www.ncbi.nlm.nih.gov/pubmed/28669759 [Accessed October 3, 2018].

An, J. et al., 2017. Targeting CCR2 with its antagonist suppresses viability, motility and invasion by downregulating MMP-9 expression in non-small cell lung cancer cells.

Oncotarget, 8(24), pp.39230–39240. Available at:

http://www.ncbi.nlm.nih.gov/pubmed/28424406 [Accessed October 1, 2018].

Andreesen, R. et al., 1990. Adoptive transfer of tumor cytotoxic macrophages generated in vitro from circulating blood monocytes: a new approach to cancer immunotherapy. *Cancer research*, 50(23), pp.7450–6. Available at: http://www.ncbi.nlm.nih.gov/pubmed/1701343 [Accessed October 1, 2018].

Ang, W.X. et al., 2017. Intraperitoneal immunotherapy with T cells stably and transiently expressing anti-EpCAM CAR in xenograft models of peritoneal carcinomatosis. *Oncotarget*, 8(8), pp.13545–13559. Available at: http://www.ncbi.nlm.nih.gov/pubmed/28088790 [Accessed September 30, 2018].

Annenkov, A.E. et al., 1998. Loss of original antigenic specificity in T cell hybridomas transduced with a chimeric receptor containing single-chain Fv of an anti-collagen antibody and Fc epsilonRI-signaling gamma subunit. *Journal of immunology (Baltimore, Md. : 1950)*, 161(12), pp.6604–13. Available at: http://www.ncbi.nlm.nih.gov/pubmed/9862688 [Accessed October 3, 2018].

Aziz, A. et al., 2009. MafB/c-Maf Deficiency Enables Self-Renewal of Differentiated Functional Macrophages. *Science*, 326(5954), pp.867–871. Available at: http://www.ncbi.nlm.nih.gov/pubmed/19892988 [Accessed October 7, 2018].

Bakalar, M.H. et al., 2018. Size-Dependent Segregation Controls Macrophage Phagocytosis of Antibody-Opsonized Targets. *Cell*, 174(1), p.131–142.e13. Available at: https://linkinghub.elsevier.com/retrieve/pii/S0092867418307220

[Accessed October 4, 2018].

Bakema, J.E. & van Egmond, M., 2014. Fc Receptor-Dependent Mechanisms of
Monoclonal Antibody Therapy of Cancer. In *Current topics in microbiology and
immunology*. pp. 373–392. Available at:
http://www.ncbi.nlm.nih.gov/pubmed/25116109 [Accessed October 19, 2018].

Ballana, E. & Esté, J.A., 2015. SAMHD1: At the Crossroads of Cell Proliferation,
Immune Responses, and Virus Restriction. *Trends in Microbiology*, 23(11), pp.680–
692. Available at: https://linkinghub.elsevier.com/retrieve/pii/S0966842X1500178X
[Accessed October 4, 2018].

Bankaitis, K.V. & Fingleton, B., 2015. Targeting IL4/IL4R for the treatment of epithelial
cancer metastasis. *Clinical & Experimental Metastasis*, 32(8), pp.847–856.
Available at: http://www.ncbi.nlm.nih.gov/pubmed/26385103 [Accessed October 1,
2018].

Baron-Bodo, V. et al., 2005. Anti-tumor properties of human-activated macrophages
produced in large scale for clinical application. *Immunobiology*, 210(2–4), pp.267–
277. Available at: http://www.ncbi.nlm.nih.gov/pubmed/16164034 [Accessed
October 1, 2018].

Baumhoer, D. et al., 2008. Glypican 3 Expression in Human Nonneoplastic,
Preneoplastic, and Neoplastic Tissues. *American Journal of Clinical Pathology*,
129(6), pp.899–906. Available at: http://www.ncbi.nlm.nih.gov/pubmed/18480006
[Accessed September 30, 2018].

Beatty, G.L. et al., 2011. CD40 Agonists Alter Tumor Stroma and Show Efficacy Against

    Pancreatic Carcinoma in Mice and Humans. *Science*, 331(6024), pp.1612–1616.

    Available at: http://www.ncbi.nlm.nih.gov/pubmed/21436454 [Accessed October 1,

    2018].

Beatty, G.L. et al., 2014. Mesothelin-Specific Chimeric Antigen Receptor mRNA-

    Engineered T Cells Induce Antitumor Activity in Solid Malignancies. *Cancer*

    Immunology Research, 2(2), pp.112–120. Available at:

    http://www.ncbi.nlm.nih.gov/pubmed/24579088 [Accessed September 30, 2018].

Beatty, G.L., Li, Y. & Long, K.B., 2017. Cancer immunotherapy: activating innate and

    adaptive immunity through CD40 agonists. *Expert Review of Anticancer Therapy*,

    17(2), pp.175–186. Available at: http://www.ncbi.nlm.nih.gov/pubmed/27927088

    [Accessed October 1, 2018].

Berger, C. et al., 2015. Safety of Targeting ROR1 in Primates with Chimeric Antigen

    Receptor-Modified T Cells. *Cancer Immunology Research*, 3(2), pp.206–216.

    Available at: http://www.ncbi.nlm.nih.gov/pubmed/25355068 [Accessed September

    30, 2018].

Bobadilla, S., Sunseri, N. & Landau, N.R., 2013. Efficient transduction of myeloid cells

    by an HIV-1-derived lentiviral vector that packages the Vpx accessory protein. *Gene*

    Therapy, 20(5), pp.514–520. Available at:

    http://www.ncbi.nlm.nih.gov/pubmed/22895508 [Accessed August 8, 2018].

Braster, R., O'Toole, T. & van Egmond, M., 2014. Myeloid cells as effector cells for

monoclonal antibody therapy of cancer. *Methods*, 65(1), pp.28–37. Available at: http://www.ncbi.nlm.nih.gov/pubmed/23811299 [Accessed August 27, 2018].

Brown, C.E. et al., 2015. Bioactivity and Safety of IL13R 2-Redirected Chimeric Antigen Receptor CD8+ T Cells in Patients with Recurrent Glioblastoma. *Clinical Cancer Research*, 21(18), pp.4062–4072. Available at: http://www.ncbi.nlm.nih.gov/pubmed/26059190 [Accessed September 30, 2018].

Brown, C.E. et al., 2018. Optimization of IL13Rα2-Targeted Chimeric Antigen Receptor T Cells for Improved Anti-tumor Efficacy against Glioblastoma. *Molecular Therapy*, 26(1), pp.31–44. Available at: http://www.ncbi.nlm.nih.gov/pubmed/29103912 [Accessed September 30, 2018].

Brown, C.E. et al., 2016. Regression of Glioblastoma after Chimeric Antigen Receptor T-Cell Therapy. *The New England journal of medicine*, 375(26), pp.2561–9. Available at: http://www.nejm.org/doi/10.1056/NEJMoa1610497 [Accessed October 6, 2018].

Burga, R.A. et al., 2015. Liver myeloid-derived suppressor cells expand in response to liver metastases in mice and inhibit the anti-tumor efficacy of anti-CEA CAR-T. *Cancer Immunology, Immunotherapy*, 64(7), pp.817–829. Available at: http://www.ncbi.nlm.nih.gov/pubmed/25850344 [Accessed September 30, 2018].

Burger, M. et al., 2010. The application of adjuvant autologous antravesical macrophage cell therapy vs. BCG in non-muscle invasive bladder cancer: a multicenter, randomized trial. *Journal of translational medicine*, 8, p.54.

Butowski, N. et al., 2016. Orally administered colony stimulating factor 1 receptor

 inhibitor PLX3397 in recurrent glioblastoma: an Ivy Foundation Early Phase

 Clinical Trials Consortium phase II study. *Neuro-Oncology*, 18(4), pp.557–564.

 Available at: http://www.ncbi.nlm.nih.gov/pubmed/26449250 [Accessed October 1,

 2018].

Caetano, M.S. et al., 2016. IL6 Blockade Reprograms the Lung Tumor

 Microenvironment to Limit the Development and Progression of K-ras-Mutant Lung

 Cancer. *Cancer Research*, 76(11), pp.3189–3199. Available at:

 http://www.ncbi.nlm.nih.gov/pubmed/27197187 [Accessed October 1, 2018].

Cameron, D. et al., 2008. A phase III randomized comparison of lapatinib plus

 capecitabine versus capecitabine alone in women with advanced breast cancer that

 has progressed on trastuzumab: updated efficacy and biomarker analyses. *Breast*

 Cancer Research and Treatment, 112(3), pp.533–543. Available at:

 http://www.ncbi.nlm.nih.gov/pubmed/18188694 [Accessed October 1, 2018].

Cannarile, M.A. et al., 2017. Colony-stimulating factor 1 receptor (CSF1R) inhibitors in

 cancer therapy. *Journal for ImmunoTherapy of Cancer*, 5(1), p.53. Available at:

 http://jitc.biomedcentral.com/articles/10.1186/s40425-017-0257-y [Accessed

 October 1, 2018].

Caruso, H.G. et al., 2016. Redirecting T-Cell Specificity to EGFR Using mRNA to Self-

 limit Expression of Chimeric Antigen Receptor. *Journal of Immunotherapy*, 39(5),

 pp.205–217. Available at: http://www.ncbi.nlm.nih.gov/pubmed/27163741

[Accessed September 30, 2018].

Chan, A. et al., 2016. Neratinib after trastuzumab-based adjuvant therapy in patients with HER2-positive breast cancer (ExteNET): a multicentre, randomised, double-blind, placebo-controlled, phase 3 trial. *The Lancet Oncology*, 17(3), pp.367–377. Available at: http://www.ncbi.nlm.nih.gov/pubmed/26874901 [Accessed October 1, 2018].

Chang, L.-S. et al., 2014. Toll-like receptor 9 agonist enhances anti-tumor immunity and inhibits tumor-associated immunosuppressive cells numbers in a mouse cervical cancer model following recombinant lipoprotein therapy. *Molecular Cancer*, 13(1), p.60. Available at: http://www.ncbi.nlm.nih.gov/pubmed/24642245 [Accessed October 1, 2018].

Chao, M.P. et al., 2010. Anti-CD47 Antibody Synergizes with Rituximab to Promote Phagocytosis and Eradicate Non-Hodgkin Lymphoma. *Cell*, 142(5), pp.699–713. Available at: http://dx.doi.org/10.1016/j.cell.2010.07.044.

Chen, K.H. et al., 2017. Preclinical targeting of aggressive T-cell malignancies using anti-CD5 chimeric antigen receptor. *Leukemia*, 31(10), pp.2151–2160. Available at: http://www.ncbi.nlm.nih.gov/pubmed/28074066 [Accessed September 30, 2018].

Chinnasamy, D. et al., 2010. Gene therapy using genetically modified lymphocytes targeting VEGFR-2 inhibits the growth of vascularized syngenic tumors in mice. *Journal of Clinical Investigation*, 120(11), pp.3953–3968. Available at: http://www.ncbi.nlm.nih.gov/pubmed/20978347 [Accessed September 30, 2018].

Cho, S.-F., Anderson, K.C. & Tai, Y.-T., 2018. Targeting B Cell Maturation Antigen (BCMA) in Multiple Myeloma: Potential Uses of BCMA-Based Immunotherapy. *Frontiers in Immunology*, 9, p.1821. Available at: http://www.ncbi.nlm.nih.gov/pubmed/30147690 [Accessed September 30, 2018].

Choi, B.D., O'Rourke, D.M. & Maus, M. V, 2017. Engineering Chimeric Antigen Receptor T cells to Treat Glioblastoma. *The journal of targeted therapies in cancer*, 6(4), pp.22–25. Available at: http://www.ncbi.nlm.nih.gov/pubmed/29167820 [Accessed September 30, 2018].

Chowdhury, D. & Lieberman, J., 2008. Death by a thousand cuts: granzyme pathways of programmed cell death. *Annual review of immunology*, 26, pp.389–420. Available at: http://www.ncbi.nlm.nih.gov/pubmed/18304003 [Accessed October 19, 2018].

D'Incalci, M. et al., 2014. Trabectedin, a drug acting on both cancer cells and the tumour microenvironment. *British Journal of Cancer*, 111(4), pp.646–650. Available at: http://www.ncbi.nlm.nih.gov/pubmed/24755886 [Accessed October 1, 2018].

Deng, Z. et al., 2015. Adoptive T-cell therapy of prostate cancer targeting the cancer stem cell antigen EpCAM. *BMC Immunology*, 16(1), p.1. Available at: http://www.ncbi.nlm.nih.gov/pubmed/25636521 [Accessed September 30, 2018].

Drent, E. et al., 2016. Pre-clinical evaluation of CD38 chimeric antigen receptor engineered T cells for the treatment of multiple myeloma. *Haematologica*, 101(5), pp.616–625. Available at: http://www.ncbi.nlm.nih.gov/pubmed/26858358 [Accessed September 30, 2018].

Dunn, G.P. et al., 2002. Cancer immunoediting: from immunosurveillance to tumor escape. *Nature Immunology*, 3(11), pp.991–998. Available at: http://www.ncbi.nlm.nih.gov/pubmed/12407406 [Accessed October 19, 2018].

Dunn, G.P., Old, L.J. & Schreiber, R.D., 2004. The Three Es of Cancer Immunoediting. *Annual Review of Immunology*, 22(1), pp.329–360. Available at: http://www.ncbi.nlm.nih.gov/pubmed/15032581 [Accessed October 19, 2018].

Ellebrecht, C.T. et al., 2016. Reengineering chimeric antigen receptor T cells for targeted therapy of autoimmune disease. *Science*, 353(6295), pp.179–184. Available at: http://www.ncbi.nlm.nih.gov/pubmed/27365313 [Accessed October 19, 2018].

Eshhar, Z. et al., 1993. Specific activation and targeting of cytotoxic lymphocytes through chimeric single chains consisting of antibody-binding domains and the gamma or zeta subunits of the immunoglobulin and T-cell receptors. *Proceedings of the National Academy of Sciences of the United States of America*, 90(2), pp.720–4. Available at: http://www.ncbi.nlm.nih.gov/pubmed/8421711 [Accessed October 3, 2018].

Eymard, J.C. et al., 1996. Phase I/II trial of autologous activated macrophages in advanced colorectal cancer. *European journal of cancer (Oxford, England : 1990)*, 32A(11), pp.1905–11. Available at: http://www.ncbi.nlm.nih.gov/pubmed/8943673 [Accessed October 1, 2018].

Faradji, A., Bohbot, A., Frost, H., et al., 1991. Phase I study of liposomal MTP-PE-activated autologous monocytes administered intraperitoneally to patients with

peritoneal carcinomatosis. *Journal of Clinical Oncology*, 9(7), pp.1251–1260. Available at: http://www.ncbi.nlm.nih.gov/pubmed/2045866 [Accessed October 1, 2018].

Faradji, A., Bohbot, A., Schmitt-Goguel, M., et al., 1991. Phase I trial of intravenous infusion of ex-vivo-activated autologous blood-derived macrophages in patients with non-small-cell lung cancer: toxicity and immunomodulatory effects. *Cancer immunology, immunotherapy : CII*, 33(5), pp.319–26. Available at: http://www.ncbi.nlm.nih.gov/pubmed/1651160 [Accessed October 1, 2018].

Feng, K. et al., 2018. Phase I study of chimeric antigen receptor modified T cells in treating HER2-positive advanced biliary tract cancers and pancreatic cancers. *Protein & Cell*, 9(10), pp.838–847. Available at: http://www.ncbi.nlm.nih.gov/pubmed/28710747 [Accessed September 30, 2018].

Forget, M.A. et al., 2014. Macrophage Colony-Stimulating Factor Augments Tie2-Expressing Monocyte Differentiation, Angiogenic Function, and Recruitment in a Mouse Model of Breast Cancer A. Valledor, ed. *PLoS ONE*, 9(6), p.e98623. Available at: http://www.ncbi.nlm.nih.gov/pubmed/24892425 [Accessed October 1, 2018].

Gao, H. et al., 2014. Development of T Cells Redirected to Glypican-3 for the Treatment of Hepatocellular Carcinoma. *Clinical Cancer Research*, 20(24), pp.6418–6428. Available at: http://www.ncbi.nlm.nih.gov/pubmed/25320357 [Accessed September 30, 2018].

Garcia, S. et al., 2016. Colony-stimulating factor (CSF) 1 receptor blockade reduces inflammation in human and murine models of rheumatoid arthritis. *Arthritis research & therapy*, 18, p.75. Available at: http://www.ncbi.nlm.nih.gov/pubmed/27036883 [Accessed October 1, 2018].

Germano, G. et al., 2013. Role of Macrophage Targeting in the Antitumor Activity of Trabectedin. *Cancer Cell*, 23(2), pp.249–262. Available at: http://www.ncbi.nlm.nih.gov/pubmed/23410977 [Accessed October 1, 2018].

Ghosh, A. & Heston, W.D.W., 2004. Tumor target prostate specific membrane antigen (PSMA) and its regulation in prostate cancer. *Journal of Cellular Biochemistry*, 91(3), pp.528–539. Available at: http://www.ncbi.nlm.nih.gov/pubmed/14755683 [Accessed September 30, 2018].

Gill, S., Tasian, S.K., Ruella, M., Shestova, O., Li, Y., Porter, D.L., Carroll, M., Danet-Desnoyers, G., et al., 2014. Preclinical targeting of human acute myeloid leukemia and myeloablation using chimeric antigen receptor-modified T cells. *Blood*, 123(15), pp.2343–54. Available at: http://www.ncbi.nlm.nih.gov/pubmed/24596416 [Accessed August 8, 2018].

Gill, S., Tasian, S.K., Ruella, M., Shestova, O., Li, Y., Porter, D.L., Carroll, M., Danet-desnoyers, G., et al., 2014. Preclinical targeting of human acute myeloid leukemia and myeloablation using chimeric antigen receptor – modi fi ed T cells. *Blood*, 123(15), pp.2343–2354.

Gomes-Silva, D. et al., 2017. Tonic 4-1BB Costimulation in Chimeric Antigen Receptors

Impedes T Cell Survival and Is Vector-Dependent. *Cell Reports*, 21(1), pp.17–26.

Available at: http://www.ncbi.nlm.nih.gov/pubmed/28978471 [Accessed October

19, 2018].

Gordon, S.R. et al., 2017. PD-1 expression by tumour-associated macrophages inhibits

phagocytosis and tumour immunity. *Nature*, 545(7655), pp.495–499. Available at:

http://www.ncbi.nlm.nih.gov/pubmed/28514441 [Accessed October 7, 2018].

Green, J. & Lipton, A., 2010. Anticancer Properties of Zoledronic Acid. *Cancer

Investigation*, 28(9), pp.944–957. Available at:

http://www.ncbi.nlm.nih.gov/pubmed/20879838 [Accessed October 1, 2018].

Gross, G. & Eshhar, Z., 1992. Endowing T cells with antibody specificity using chimeric

T cell receptors. *FASEB journal : official publication of the Federation of American

Societies for Experimental Biology*, 6(15), pp.3370–8. Available at:

http://www.ncbi.nlm.nih.gov/pubmed/1464371 [Accessed October 19, 2018].

Guedan, S. et al., 2014. ICOS-based chimeric antigen receptors program bipolar

TH17/TH1 cells. *Blood*, 124(7), pp.1070–1080. Available at:

http://www.ncbi.nlm.nih.gov/pubmed/24986688 [Accessed October 19, 2018].

Guerriero, J.L. et al., 2017. Class IIa HDAC inhibition reduces breast tumours and

metastases through anti-tumour macrophages. *Nature*, 543(7645), pp.428–432.

Available at: http://www.nature.com/articles/nature21409 [Accessed October 1,

2018].

Haldar, M. & Murphy, K.M., 2014. Origin, development, and homeostasis of tissue-resident macrophages. *Immunological reviews*, 262(1), pp.25–35. Available at: http://www.ncbi.nlm.nih.gov/pubmed/25319325 [Accessed October 19, 2018].

Hanahan, D. & Weinberg, R.A., 2000. The hallmarks of cancer. *Cell*, 100(1), pp.57–70. Available at: http://www.ncbi.nlm.nih.gov/pubmed/10647931 [Accessed September 28, 2018].

Harney, A.S. et al., 2017. The Selective Tie2 Inhibitor Rebastinib Blocks Recruitment and Function of Tie2 [Hi] Macrophages in Breast Cancer and Pancreatic Neuroendocrine Tumors. *Molecular Cancer Therapeutics*, 16(11), pp.2486–2501. Available at: http://www.ncbi.nlm.nih.gov/pubmed/28838996 [Accessed October 1, 2018].

Hartman, W.R. et al., 2010. CD38 expression, function, and gene resequencing in a human lymphoblastoid cell line-based model system. *Leukemia & lymphoma*, 51(7), pp.1315–25. Available at: http://www.ncbi.nlm.nih.gov/pubmed/20470215 [Accessed September 30, 2018].

Hashimoto, D. et al., 2013. Tissue-resident macrophages self-maintain locally throughout adult life with minimal contribution from circulating monocytes. *Immunity*, 38(4), pp.792–804.

Haso, W. et al., 2013. Anti-CD22-chimeric antigen receptors targeting B-cell precursor acute lymphoblastic leukemia. *Blood*, 121(7), pp.1165–1174. Available at: http://www.ncbi.nlm.nih.gov/pubmed/23243285 [Accessed September 30, 2018].

Heczey, A. et al., 2014. Invariant NKT cells with chimeric antigen receptor provide a

   novel platform for safe and effective cancer immunotherapy. *Blood*. Available at:

   http://www.ncbi.nlm.nih.gov/pubmed/25049283 [Accessed July 23, 2014].

Hennemann, B. et al., 1997. Adoptive immunotherapy with tumor-cytotoxic macrophages

   derived from recombinant human granulocyte-macrophage colony-stimulating factor

   (rhuGM-CSF) mobilized peripheral blood monocytes. *Journal of immunotherapy*

   (Hagerstown, Md. : 1997), 20(5), pp.365–71. Available at:

   http://www.ncbi.nlm.nih.gov/pubmed/9336743 [Accessed August 30, 2018].

Hennemann, B. et al., 1998. Effect of granulocyte-macrophage colony-stimulating factor

   treatment on phenotype, cytokine release and cytotoxicity of circulating blood

   monocytes and monocyte-derived macrophages. *British Journal of Haematology*,

   102(5), pp.1197–1203.

Hennemann, B. et al., 1995. Intrahepatic adoptive immunotherapy with autologous

   tumorcytotoxic macrophages in patients with cancer. *Journal of immunotherapy*

   with emphasis on tumor immunology : official journal of the Society for Biological

   Therapy, 18(1), pp.19–27. Available at:

   http://www.ncbi.nlm.nih.gov/pubmed/8535567 [Accessed October 1, 2018].

Hennemann, B. et al., 1998. Phase I trial of adoptive immunotherapy of cancer patients

   using monocyte-derived macrophages activated with interferon gamma and

   lipopolysaccharide. *Cancer immunology, immunotherapy : CII*, 45(5), pp.250–6.

   Available at: http://www.ncbi.nlm.nih.gov/pubmed/9439648 [Accessed October 1,

2018].

Henry, T.D. et al., 2014. Safety and efficacy of ixmyelocel-T: an expanded, autologous multi-cellular therapy, in dilated cardiomyopathy. *Circulation research*, 115(8), pp.730–7. Available at: https://www.ahajournals.org/doi/10.1161/CIRCRESAHA.115.304554 [Accessed October 1, 2018].

Hillerdal, V. et al., 2014. Systemic treatment with CAR-engineered T cells against PSCA delays subcutaneous tumor growth and prolongs survival of mice. *BMC Cancer*, 14(1), p.30. Available at: http://www.ncbi.nlm.nih.gov/pubmed/24438073 [Accessed September 30, 2018].

Hinrichs, C.S. & Rosenberg, S.A., 2014. Exploiting the curative potential of adoptive T-cell therapy for cancer. *Immunological reviews*, 257(1), pp.56–71. Available at: http://www.ncbi.nlm.nih.gov/pubmed/24329789 [Accessed October 19, 2018].

Hiroshima, Y. et al., 2014. The Tumor-Educated-Macrophage Increase of Malignancy of Human Pancreatic Cancer Is Prevented by Zoledronic Acid K. Xie, ed. *PLoS ONE*, 9(8), p.e103382. Available at: http://www.ncbi.nlm.nih.gov/pubmed/25116261 [Accessed October 1, 2018].

Holmgaard, R.B. et al., 2016. Timing of CSF-1/CSF-1R signaling blockade is critical to improving responses to CTLA-4 based immunotherapy. *OncoImmunology*, 5(7), p.e1151595. Available at: http://www.ncbi.nlm.nih.gov/pubmed/27622016 [Accessed October 1, 2018].

Hombach, A.A. et al., 2012. OX40 costimulation by a chimeric antigen receptor abrogates CD28 and IL-2 induced IL-10 secretion by redirected CD4(+) T cells. *Oncoimmunology*, 1(4), pp.458–466. Available at: http://www.ncbi.nlm.nih.gov/pubmed/22754764 [Accessed October 19, 2018].

Hong, H. et al., 2014. Diverse Solid Tumors Expressing a Restricted Epitope of L1-CAM Can Be Targeted by Chimeric Antigen Receptor Redirected T Lymphocytes. *Journal of Immunotherapy*, 37(2), pp.93–104. Available at: http://www.ncbi.nlm.nih.gov/pubmed/24509172 [Accessed September 30, 2018].

Horie, R. & Watanabe, T., 1998. CD30: expression and function in health and disease. *Seminars in Immunology*, 10(6), pp.457–470. Available at: http://www.ncbi.nlm.nih.gov/pubmed/9826579 [Accessed September 30, 2018].

Hudecek, M. et al., 2013. Receptor Affinity and Extracellular Domain Modifications Affect Tumor Recognition by ROR1-Specific Chimeric Antigen Receptor T Cells. *Clinical Cancer Research*, 19(12), pp.3153–3164. Available at: http://www.ncbi.nlm.nih.gov/pubmed/23620405 [Accessed September 30, 2018].

Hudecek, M. et al., 2010. The B-cell tumor-associated antigen ROR1 can be targeted with T cells modified to express a ROR1-specific chimeric antigen receptor. *Blood*, 116(22), pp.4532–4541. Available at: http://www.ncbi.nlm.nih.gov/pubmed/20702778 [Accessed September 30, 2018].

Hudecek, M. et al., 2015. The Nonsignaling Extracellular Spacer Domain of Chimeric Antigen Receptors Is Decisive for In Vivo Antitumor Activity. *Cancer Immunology*

Research, 3(2), pp.125–135. Available at:

http://www.ncbi.nlm.nih.gov/pubmed/25212991 [Accessed October 19, 2018].

Hussell, T. & Bell, T.J., 2014. Alveolar macrophages: plasticity in a tissue-specific

context. *Nature Reviews Immunology*, 14(2), pp.81–93. Available at:

http://www.nature.com/articles/nri3600 [Accessed October 19, 2018].

Hwu, P. et al., 1995. In vivo antitumor activity of T cells redirected with chimeric

antibody/T-cell receptor genes. *Cancer research*, 55(15), pp.3369–73. Available at:

http://www.ncbi.nlm.nih.gov/pubmed/7614473 [Accessed October 3, 2018].

Johnson, L.A. et al., 2015. Rational development and characterization of humanized anti–

EGFR variant III chimeric antigen receptor T cells for glioblastoma. *Science

Translational Medicine*, 7(275), p.275ra22-275ra22. Available at:

http://www.ncbi.nlm.nih.gov/pubmed/25696001 [Accessed September 30, 2018].

June, C.H. & Sadelain, M., 2018. Chimeric Antigen Receptor Therapy. *New England

Journal of Medicine*, 379(1), pp.64–73. Available at:

http://www.nejm.org/doi/10.1056/NEJMra1706169 [Accessed October 19, 2018].

Junghans, R.P. et al., 2016. Phase I Trial of Anti-PSMA Designer CAR-T Cells in

Prostate Cancer: Possible Role for Interacting Interleukin 2-T Cell

Pharmacodynamics as a Determinant of Clinical Response. *The Prostate*, 76(14),

pp.1257–1270. Available at: http://www.ncbi.nlm.nih.gov/pubmed/27324746

[Accessed September 30, 2018].

Kandalaft, L.E., Powell, D.J. & Coukos, G., 2012. A phase I clinical trial of adoptive

    transfer of folate receptor-alpha redirected autologous T cells for recurrent ovarian

    cancer. *Journal of Translational Medicine*, 10(1), p.157. Available at:

    http://www.ncbi.nlm.nih.gov/pubmed/22863016 [Accessed September 30, 2018].

Kaneda, M.M. et al., 2016. PI3Kγ is a molecular switch that controls immune

    suppression. *Nature*, 539(7629), pp.437–442. Available at:

    http://www.ncbi.nlm.nih.gov/pubmed/27642729 [Accessed October 1, 2018].

Katz, S.C. et al., 2015. Phase I Hepatic Immunotherapy for Metastases Study of Intra-

    Arterial Chimeric Antigen Receptor-Modified T-cell Therapy for CEA+ Liver

    Metastases. *Clinical Cancer Research*, 21(14), pp.3149–3159. Available at:

    http://www.ncbi.nlm.nih.gov/pubmed/25850950 [Accessed September 30, 2018].

Kawalekar, O.U. et al., 2016. Distinct Signaling of Coreceptors Regulates Specific

    Metabolism Pathways and Impacts Memory Development in CAR T Cells.

    Immunity, 44(3), p.712. Available at:

    http://www.ncbi.nlm.nih.gov/pubmed/28843072 [Accessed October 19, 2018].

Kelly, B. & O'Neill, L.A., 2015. Metabolic reprogramming in macrophages and dendritic

    cells in innate immunity. *Cell research*, 25(7), pp.771–84. Available at:

    http://dx.doi.org/10.1038/cr.2015.68%5Cnhttp://www.pubmedcentral.nih.gov/article

    render.fcgi?artid=4493277&tool=pmcentrez&rendertype=abstract.

Kenderian, S.S. et al., 2015. CD33-specific chimeric antigen receptor T cells exhibit

    potent preclinical activity against human acute myeloid leukemia. *Leukemia*, 29(8),

pp.1637–1647. Available at: http://www.nature.com/doifinder/10.1038/leu.2015.52.

Kloss, C.C. et al., 2018. Dominant-Negative TGF-β Receptor Enhances PSMA-Targeted

Human CAR T Cell Proliferation And Augments Prostate Cancer Eradication.

Molecular Therapy, 26(7), pp.1855–1866. Available at:

http://www.ncbi.nlm.nih.gov/pubmed/29807781 [Accessed September 30, 2018].

Kong, S. et al., 2012. Suppression of Human Glioma Xenografts with Second-Generation

IL13R-Specific Chimeric Antigen Receptor-Modified T Cells. *Clinical Cancer*

Research, 18(21), pp.5949–5960. Available at:

http://www.ncbi.nlm.nih.gov/pubmed/22966020 [Accessed September 30, 2018].

Kulemzin, S. V et al., Engineering Chimeric Antigen Receptors. *Acta naturae*, 9(1),

pp.6–14. Available at: http://www.ncbi.nlm.nih.gov/pubmed/28461969 [Accessed

October 19, 2018].

Lanitis, E. et al., 2012. Primary Human Ovarian Epithelial Cancer Cells Broadly Express

HER2 at Immunologically-Detectable Levels S. M. Hawkins, ed. *PLoS ONE*, 7(11),

p.e49829. Available at: http://www.ncbi.nlm.nih.gov/pubmed/23189165 [Accessed

September 30, 2018].

Lavin, Y. et al., 2015. Regulation of macrophage development and function in peripheral

tissues. *Nature reviews. Immunology*, 15(12), pp.731–44. Available at:

http://www.nature.com/doifinder/10.1038/nri3920%5Cnhttp://www.ncbi.nlm.nih.go

v/pubmed/26603899.

Lee, M. et al., 2014. Resiquimod, a TLR7/8 agonist, promotes differentiation of myeloid-derived suppressor cells into macrophages and dendritic cells. *Archives of Pharmacal Research*, 37(9), pp.1234–1240. Available at: http://www.ncbi.nlm.nih.gov/pubmed/24748512 [Accessed October 1, 2018].

Lee, S. et al., 2016. Macrophage-based cell therapies: The long and winding road. *Journal of Controlled Release*, 240, pp.527–540. Available at: http://dx.doi.org/10.1016/j.jconrel.2016.07.018.

Lee, S., Kivimäe, S. & Szoka, F.C., 2017. Clodronate Improves Survival of Transplanted Hoxb8 Myeloid Progenitors with Constitutively Active GMCSFR in Immunocompetent Mice. *Molecular therapy. Methods & clinical development*, 7, pp.60–73. Available at: https://linkinghub.elsevier.com/retrieve/pii/S2329050117300967 [Accessed October 7, 2018].

Lesimple, T. et al., Treatment of metastatic renal cell carcinoma with activated autologous macrophages and granulocyte--macrophage colony-stimulating factor. *Journal of immunotherapy (Hagerstown, Md. : 1997)*, 23(6), pp.675–9. Available at: http://www.ncbi.nlm.nih.gov/pubmed/11186156 [Accessed October 1, 2018].

Li, H.S. & Watowich, S.S., 2014. Innate immune regulation by STAT-mediated transcriptional mechanisms. *Immunological Reviews*, 261(1), pp.84–101. Available at: http://www.ncbi.nlm.nih.gov/pubmed/25123278 [Accessed October 1, 2018].

Li, K. et al., 2016. Adoptive immunotherapy using T lymphocytes redirected to glypican-

3 for the treatment of lung squamous cell carcinoma. *Oncotarget*, 7(3), pp.2496–507. Available at: http://www.ncbi.nlm.nih.gov/pubmed/26684028 [Accessed September 30, 2018].

Li, N. et al., 2018. Chimeric Antigen Receptor-Modified T Cells Redirected to EphA2 for the Immunotherapy of Non-Small Cell Lung Cancer. *Translational Oncology*, 11(1), pp.11–17. Available at: http://www.ncbi.nlm.nih.gov/pubmed/29132013 [Accessed September 30, 2018].

Liao, Y., Smyth, G.K. & Shi, W., 2014. featureCounts: an efficient general purpose program for assigning sequence reads to genomic features. *Bioinformatics*, 30(7), pp.923–930. Available at: http://www.ncbi.nlm.nih.gov/pubmed/24227677 [Accessed August 17, 2018].

Liu, Q. et al., 2016. Inhibition of SIRPα in dendritic cells potentiates potent antitumor immunity. *OncoImmunology*, 5(August), p.e1183850. Available at: https://www.tandfonline.com/doi/full/10.1080/2162402X.2016.1183850.

Liu, X. et al., 2015. Affinity-Tuned ErbB2 or EGFR Chimeric Antigen Receptor T Cells Exhibit an Increased Therapeutic Index against Tumors in Mice. *Cancer Research*, 75(17), pp.3596–3607. Available at: http://www.ncbi.nlm.nih.gov/pubmed/26330166 [Accessed September 30, 2018].

Lo, A. et al., 2015. Tumor-Promoting Desmoplasia Is Disrupted by Depleting FAP-Expressing Stromal Cells. *Cancer Research*, 75(14), pp.2800–2810. Available at: http://www.ncbi.nlm.nih.gov/pubmed/25979873 [Accessed September 30, 2018].

Long, A.H. et al., 2015. 4-1BB costimulation ameliorates T cell exhaustion induced by tonic signaling of chimeric antigen receptors. *Nature Medicine*, 21(6), pp.581–590. Available at: http://www.nature.com/articles/nm.3838 [Accessed October 19, 2018].

Long, A.H., Haso, W.M. & Orentas, R.J., 2013. Lessons learned from a highly-active CD22-specific chimeric antigen receptor. *OncoImmunology*, 2(4), p.e23621. Available at: http://www.ncbi.nlm.nih.gov/pubmed/23734316 [Accessed September 30, 2018].

Long, K.B. et al., 2016. IFN and CCL2 Cooperate to Redirect Tumor-Infiltrating Monocytes to Degrade Fibrosis and Enhance Chemotherapy Efficacy in Pancreatic Carcinoma. *Cancer Discovery*, 6(4), pp.400–413. Available at: http://www.ncbi.nlm.nih.gov/pubmed/26896096 [Accessed October 1, 2018].

Long, K.B. et al., 2017. IL6 Receptor Blockade Enhances Chemotherapy Efficacy in Pancreatic Ductal Adenocarcinoma. *Molecular Cancer Therapeutics*, 16(9), pp.1898–1908. Available at: http://www.ncbi.nlm.nih.gov/pubmed/28611107 [Accessed October 1, 2018].

van Lookeren Campagne, M., Wiesmann, C. & Brown, E.J., 2007. Macrophage complement receptors and pathogen clearance. *Cellular Microbiology*, 9(9), pp.2095–2102. Available at: http://doi.wiley.com/10.1111/j.1462-5822.2007.00981.x [Accessed September 18, 2018].

Louis, C.U. et al., 2011. Antitumor activity and long-term fate of chimeric antigen receptor-positive T cells in patients with neuroblastoma. *Blood*, 118(23), pp.6050–

6056. Available at: http://www.ncbi.nlm.nih.gov/pubmed/21984804 [Accessed September 30, 2018].

Lund, M.E. et al., 2016. The choice of phorbol 12-myristate 13-acetate differentiation protocol influences the response of THP-1 macrophages to a pro-inflammatory stimulus. *Journal of Immunological Methods*, 430, pp.64–70. Available at: http://www.ncbi.nlm.nih.gov/pubmed/26826276 [Accessed October 3, 2018].

Lynn, R.C. et al., 2015. Targeting of folate receptor on acute myeloid leukemia blasts with chimeric antigen receptor-expressing T cells. *Blood*, 125(22), pp.3466–3476. Available at: http://www.ncbi.nlm.nih.gov/pubmed/25887778 [Accessed September 30, 2018].

Maher, J. et al., 2016. Targeting of Tumor-Associated Glycoforms of MUC1 with CAR T Cells. *Immunity*, 45(5), pp.945–946. Available at: http://www.ncbi.nlm.nih.gov/pubmed/27851917 [Accessed September 30, 2018].

Mamonkin, M. et al., 2015. A T-cell-directed chimeric antigen receptor for the selective treatment of T-cell malignancies. *Blood*, 126(8), pp.983–992. Available at: http://www.bloodjournal.org/cgi/doi/10.1182/blood-2015-02-629527.

Maude, S.L. et al., 2015. CD19-targeted chimeric antigen receptor T-cell therapy for acute lymphoblastic leukemia. *Blood*, 125(26), pp.4017–4023. Available at: http://www.ncbi.nlm.nih.gov/pubmed/25999455 [Accessed September 30, 2018].

Maude, S.L. et al., 2018. Tisagenlecleucel in Children and Young Adults with B-Cell

Lymphoblastic Leukemia. *New England Journal of Medicine*, 378(5), pp.439–448. Available at: http://www.ncbi.nlm.nih.gov/pubmed/29385370 [Accessed August 2, 2018].

Maus, M. V. & June, C.H., 2016. Making Better Chimeric Antigen Receptors for Adoptive T-cell Therapy. *Clinical Cancer Research*, 22(8), pp.1875–1884. Available at: http://www.ncbi.nlm.nih.gov/pubmed/27084741 [Accessed October 19, 2018].

Morgan, R.A. et al., 2010. Case report of a serious adverse event following the administration of T cells transduced with a chimeric antigen receptor recognizing ERBB2. *Molecular therapy : the journal of the American Society of Gene Therapy*, 18(4), pp.843–51. Available at: http://linkinghub.elsevier.com/retrieve/pii/S1525001616323425 [Accessed October 6, 2018].

Morrison, C., 2016. Immuno-oncologists eye up macrophage targets. *Nature reviews. Drug discovery*, 15(6), pp.373–4. Available at: http://www.nature.com/articles/nrd.2016.111 [Accessed August 2, 2018].

Mosser, D.M. & Edwards, J.P., 2008. Exploring the full spectrum of macrophage activation. *Nature Reviews Immunology*, 8(12), pp.958–969. Available at: http://www.nature.com/doifinder/10.1038/nri2448.

Moyes, K.W. et al., 2017. Genetically Engineered Macrophages: A Potential Platform for Cancer Immunotherapy. *Human Gene Therapy*, 28(2), pp.200–215. Available at:

http://www.liebertpub.com/doi/10.1089/hum.2016.060 [Accessed October 4, 2018].

Mueller, K.T. et al., 2018. Clinical Pharmacology of Tisagenlecleucel in B-Cell Acute Lymphoblastic Leukemia. *Clinical cancer research : an official journal of the American Association for Cancer Research*, p.clincanres.0758.2018. Available at: http://clincancerres.aacrjournals.org/lookup/doi/10.1158/1078-0432.CCR-18-0758 [Accessed October 6, 2018].

Neelapu, S.S. et al., 2017. Axicabtagene Ciloleucel CAR T-Cell Therapy in Refractory Large B-Cell Lymphoma. *The New England journal of medicine*, 377(26), pp.2531–2544. Available at: http://www.nejm.org/doi/10.1056/NEJMoa1707447 [Accessed October 6, 2018].

Nellan, A. et al., 2018. Durable regression of Medulloblastoma after regional and intravenous delivery of anti-HER2 chimeric antigen receptor T cells. *Journal for ImmunoTherapy of Cancer*, 6(1), p.30. Available at: http://www.ncbi.nlm.nih.gov/pubmed/29712574 [Accessed September 30, 2018].

Nguyen-Lefebvre, A.T. & Horuzsko, A., 2015. Kupffer Cell Metabolism and Function. *Journal of enzymology and metabolism*, 1(1). Available at: http://www.ncbi.nlm.nih.gov/pubmed/26937490 [Accessed October 19, 2018].

Nilsson, M. et al., 2004. Development of an adenoviral vector system with adenovirus serotype 35 tropism; efficient transient gene transfer into primary malignant hematopoietic cells. *The journal of gene medicine*, 6(6), pp.631–41. Available at: http://doi.wiley.com/10.1002/jgm.543 [Accessed August 30, 2018].

Noy, R. & Pollard, J.W., 2014. Tumor-associated macrophages: from mechanisms to therapy. *Immunity*, 41(1), pp.49–61. Available at: http://www.ncbi.nlm.nih.gov/pubmed/25035953 [Accessed August 2, 2018].

Nywening, T.M. et al., 2016. Targeting tumour-associated macrophages with CCR2 inhibition in combination with FOLFIRINOX in patients with borderline resectable and locally advanced pancreatic cancer: a single-centre, open-label, dose-finding, non-randomised, phase 1b trial. *The Lancet. Oncology*, 17(5), pp.651–62. Available at: https://linkinghub.elsevier.com/retrieve/pii/S1470204516000784 [Accessed October 1, 2018].

O'Rourke, D.M. et al., 2017. A single dose of peripherally infused EGFRvIII-directed CAR T cells mediates antigen loss and induces adaptive resistance in patients with recurrent glioblastoma. *Science Translational Medicine*, 9(399), p.eaaa0984. Available at: http://www.ncbi.nlm.nih.gov/pubmed/28724573 [Accessed September 30, 2018].

O'Shea, J.J. et al., 2015. The JAK-STAT Pathway: Impact on Human Disease and Therapeutic Intervention. *Annual Review of Medicine*, 66(1), pp.311–328. Available at: http://www.ncbi.nlm.nih.gov/pubmed/25587654 [Accessed October 1, 2018].

Oldenborg, P.A. et al., 2000. Role of CD47 as a marker of self on red blood cells. *Science (New York, N.Y.)*, 288(5473), pp.2051–4. Available at: http://www.ncbi.nlm.nih.gov/pubmed/10856220 [Accessed October 3, 2018].

Oldenborg, P.A., Gresham, H.D. & Lindberg, F.P., 2001. CD47-signal regulatory protein

alpha (SIRPalpha) regulates Fcgamma and complement receptor-mediated phagocytosis. *The Journal of experimental medicine*, 193(7), pp.855–62. Available at: http://www.ncbi.nlm.nih.gov/pubmed/11283158 [Accessed October 3, 2018].

Palaiologou, M., Delladetsima, I. & Tiniakos, D., 2014. CD138 (syndecan-1) expression in health and disease. *Histology and histopathology*, 29(2), pp.177–89. Available at: http://www.ncbi.nlm.nih.gov/pubmed/24150912 [Accessed September 30, 2018].

Parihar, A., Eubank, T.D. & Doseff, A.I., 2010. Monocytes and macrophages regulate immunity through dynamic networks of survival and cell death. *Journal of innate immunity*, 2(3), pp.204–15. Available at: http://www.ncbi.nlm.nih.gov/pubmed/20375558 [Accessed October 19, 2018].

Park, Y.P. et al., 2018. CD70 as a target for chimeric antigen receptor T cells in head and neck squamous cell carcinoma. *Oral Oncology*, 78, pp.145–150. Available at: http://www.ncbi.nlm.nih.gov/pubmed/29496042 [Accessed September 30, 2018].

Pastan, I. & Hassan, R., 2014. Discovery of mesothelin and exploiting it as a target for immunotherapy. *Cancer research*, 74(11), pp.2907–12. Available at: http://www.ncbi.nlm.nih.gov/pubmed/24824231 [Accessed September 17, 2018].

Perez, E.A. et al., 2017. Trastuzumab Emtansine With or Without Pertuzumab Versus Trastuzumab Plus Taxane for Human Epidermal Growth Factor Receptor 2–Positive, Advanced Breast Cancer: Primary Results From the Phase III MARIANNE Study. *Journal of Clinical Oncology*, 35(2), pp.141–148. Available at: http://www.ncbi.nlm.nih.gov/pubmed/28056202 [Accessed October 1, 2018].

Plückthun, A., 2015. Designed Ankyrin Repeat Proteins (DARPins): Binding Proteins for

Research, Diagnostics, and Therapy. *Annual Review of Pharmacology and*

Toxicology, 55(1), pp.489–511. Available at:

http://www.annualreviews.org/doi/10.1146/annurev-pharmtox-010611-134654

[Accessed October 19, 2018].

Popivanova, B.K. et al., 2009. Blockade of a chemokine, CCL2, reduces chronic colitis-

associated carcinogenesis in mice. *Cancer research*, 69(19), pp.7884–92. Available

at: http://cancerres.aacrjournals.org/cgi/doi/10.1158/0008-5472.CAN-09-1451

[Accessed October 1, 2018].

Posey, A.D., Schwab, R.D., et al., 2016. Engineered CAR T Cells Targeting the Cancer-

Associated Tn-Glycoform of the Membrane Mucin MUC1 Control

Adenocarcinoma. *Immunity*, 44(6), pp.1444–1454. Available at:

http://www.ncbi.nlm.nih.gov/pubmed/27332733 [Accessed September 30, 2018].

Posey, A.D., Clausen, H. & June, C.H., 2016. Distinguishing Truncated and Normal

MUC1 Glycoform Targeting from Tn-MUC1-Specific CAR T Cells: Specificity Is

the Key to Safety. *Immunity*, 45(5), pp.947–948. Available at:

http://www.ncbi.nlm.nih.gov/pubmed/27851918 [Accessed September 30, 2018].

Powell, R.J. et al., 2012. Cellular therapy with Ixmyelocel-T to treat critical limb

ischemia: the randomized, double-blind, placebo-controlled RESTORE-CLI trial.

Molecular therapy : the journal of the American Society of Gene Therapy, 20(6),

pp.1280–6. Available at:

http://linkinghub.elsevier.com/retrieve/pii/S1525001616325527 [Accessed October 1, 2018].

Prapa, M. et al., 2015. A novel anti-GD2/4-1BB chimeric antigen receptor triggers neuroblastoma cell killing. *Oncotarget*, 6(28), pp.24884–94. Available at: http://www.ncbi.nlm.nih.gov/pubmed/26298772 [Accessed September 30, 2018].

Priceman, S.J., Gerdts, E.A., et al., 2018. Co-stimulatory signaling determines tumor antigen sensitivity and persistence of CAR T cells targeting PSCA+ metastatic prostate cancer. *OncoImmunology*, 7(2), p.e1380764. Available at: http://www.ncbi.nlm.nih.gov/pubmed/29308300 [Accessed September 30, 2018].

Priceman, S.J., Tilakawardane, D., et al., 2018. Regional Delivery of Chimeric Antigen Receptor–Engineered T Cells Effectively Targets HER2 [+] Breast Cancer Metastasis to the Brain. *Clinical Cancer Research*, 24(1), pp.95–105. Available at: http://www.ncbi.nlm.nih.gov/pubmed/29061641 [Accessed September 30, 2018].

Qasim, W. et al., 2017. Molecular remission of infant B-ALL after infusion of universal TALEN gene-edited CAR T cells. *Science Translational Medicine*, 9(374), p.eaaj2013. Available at: http://www.ncbi.nlm.nih.gov/pubmed/28123068 [Accessed October 7, 2018].

Qian, B.-Z., Li, J., Zhang, H., Kitamura, T., Zhang, J., Campion, L.R., Kaiser, E. a, et al., 2011. CCL2 recruits inflammatory monocytes to facilitate breast-tumour metastasis. *Nature*, 475(7355), pp.222–5.

Qian, B.-Z., Li, J., Zhang, H., Kitamura, T., Zhang, J., Campion, L.R., Kaiser, E.A., et al., 2011. CCL2 recruits inflammatory monocytes to facilitate breast-tumour metastasis. *Nature*, 475(7355), pp.222–5. Available at: http://www.nature.com/doifinder/10.1038/nature10138 [Accessed August 2, 2018].

Raikar, S.S. et al., 2018. Development of chimeric antigen receptors targeting T-cell malignancies using two structurally different anti-CD5 antigen binding domains in NK and CRISPR-edited T cell lines. *OncoImmunology*, 7(3), p.e1407898. Available at: http://www.ncbi.nlm.nih.gov/pubmed/29399409 [Accessed September 30, 2018].

Ramos, C.A. et al., 2017. Clinical and immunological responses after CD30-specific chimeric antigen receptor–redirected lymphocytes. *Journal of Clinical Investigation*, 127(9), pp.3462–3471. Available at: http://www.ncbi.nlm.nih.gov/pubmed/28805662 [Accessed September 30, 2018].

Ramos, C.A. et al., 2016. Clinical responses with T lymphocytes targeting malignancy-associated κ light chains. *Journal of Clinical Investigation*, 126(7), pp.2588–2596. Available at: http://www.ncbi.nlm.nih.gov/pubmed/27270177 [Accessed September 30, 2018].

Rapoport, A.P. et al., 2015. NY-ESO-1–specific TCR–engineered T cells mediate sustained antigen-specific antitumor effects in myeloma. *Nature Medicine*, 21(8), pp.914–921. Available at: http://www.ncbi.nlm.nih.gov/pubmed/26193344 [Accessed August 8, 2018].

Ries, C.H. et al., 2014. Targeting Tumor-Associated Macrophages with Anti-CSF-1R

Antibody Reveals a Strategy for Cancer Therapy. *Cancer Cell*, 25(6), pp.846–859. Available at: http://www.ncbi.nlm.nih.gov/pubmed/24898549 [Accessed August 2, 2018].

Ritchie, D. et al., 2007. In vivo tracking of macrophage activated killer cells to sites of metastatic ovarian carcinoma. *Cancer Immunology, Immunotherapy*, 56(2), pp.155–163.

Roblek, M. et al., 2015. Targeted delivery of CCR2 antagonist to activated pulmonary endothelium prevents metastasis. *Journal of Controlled Release*, 220(Pt A), pp.341–347. Available at: http://www.ncbi.nlm.nih.gov/pubmed/26522070 [Accessed October 1, 2018].

Romani, B. & Cohen, É.A., 2012. Lentivirus Vpr and Vpx accessory proteins usurp the cullin4–DDB1 (DCAF1) E3 ubiquitin ligase. *Current Opinion in Virology*, 2(6), pp.755–763. Available at: http://linkinghub.elsevier.com/retrieve/pii/S1879625712001563 [Accessed October 4, 2018].

Ryder, M. et al., 2013. Genetic and Pharmacological Targeting of CSF-1/CSF-1R Inhibits Tumor-Associated Macrophages and Impairs BRAF-Induced Thyroid Cancer Progression M. Ludgate, ed. *PLoS ONE*, 8(1), p.e54302. Available at: http://dx.plos.org/10.1371/journal.pone.0054302 [Accessed October 1, 2018].

Saijo, K. & Glass, C.K., 2011. Microglial cell origin and phenotypes in health and disease. *Nature Reviews Immunology*, 11(11), pp.775–787. Available at:

http://www.nature.com/articles/nri3086 [Accessed October 19, 2018].

Santoro, S.P. et al., 2015. T Cells Bearing a Chimeric Antigen Receptor against Prostate-Specific Membrane Antigen Mediate Vascular Disruption and Result in Tumor Regression. *Cancer Immunology Research*, 3(1), pp.68–84. Available at: http://www.ncbi.nlm.nih.gov/pubmed/25358763 [Accessed September 30, 2018].

Schmall, A. et al., 2015. Macrophage and Cancer Cell Cross-talk via CCR2 and CX3CR1 Is a Fundamental Mechanism Driving Lung Cancer. *American Journal of Respiratory and Critical Care Medicine*, 191(4), pp.437–447. Available at: http://www.ncbi.nlm.nih.gov/pubmed/25536148 [Accessed October 1, 2018].

Schmelzer, E. & Reid, L.M., 2008. EpCAM expression in normal, non-pathological tissues. *Frontiers in bioscience : a journal and virtual library*, 13, pp.3096–100. Available at: http://www.ncbi.nlm.nih.gov/pubmed/17981779 [Accessed September 30, 2018].

Schreiber, R.D., Old, L.J. & Smyth, M.J., 2011. Cancer Immunoediting: Integrating Immunity's Roles in Cancer Suppression and Promotion. *Science*, 331(6024), pp.1565–1570. Available at: http://www.sciencemag.org/cgi/doi/10.1126/science.1203486 [Accessed October 19, 2018].

Schutsky, K. et al., 2015. Rigorous optimization and validation of potent RNA CAR T cell therapy for the treatment of common epithelial cancers expressing folate receptor. *Oncotarget*, 6(30), pp.28911–28. Available at:

http://www.ncbi.nlm.nih.gov/pubmed/26359629%5Cnhttp://www.pubmedcentral.ni
h.gov/articlerender.fcgi?artid=PMC4745700.

Shaffer, D.R. et al., 2011. T cells redirected against CD70 for the immunotherapy of
CD70-positive malignancies. *Blood*, 117(16), pp.4304–4314. Available at:
http://www.ncbi.nlm.nih.gov/pubmed/21304103 [Accessed September 30, 2018].

Shah, M.A. et al., 2017. HELOISE: Phase IIIb Randomized Multicenter Study
Comparing Standard-of-Care and Higher-Dose Trastuzumab Regimens Combined
With Chemotherapy as First-Line Therapy in Patients With Human Epidermal
Growth Factor Receptor 2–Positive Metastatic Gastric or Gastroesophageal Junction
Adenocarcinoma. *Journal of Clinical Oncology*, 35(22), pp.2558–2567. Available
at: http://www.ncbi.nlm.nih.gov/pubmed/28574779 [Accessed October 1, 2018].

Shi, H. et al., 2018. EphA2 chimeric antigen receptor-modified T cells for the
immunotherapy of esophageal squamous cell carcinoma. *Journal of Thoracic
Disease*, 10(5), pp.2779–2788. Available at:
http://www.ncbi.nlm.nih.gov/pubmed/29997940 [Accessed September 30, 2018].

Singh, N. et al., 2014. Nature of Tumor Control by Permanently and Transiently
Modified GD2 Chimeric Antigen Receptor T Cells in Xenograft Models of
Neuroblastoma. *Cancer Immunology Research*, 2(11), pp.1059–1070. Available at:
http://www.ncbi.nlm.nih.gov/pubmed/25104548 [Accessed September 30, 2018].

Song, D.-G. et al., 2016. Effective adoptive immunotherapy of triple-negative breast
cancer by folate receptor-alpha redirected CAR T cells is influenced by surface

antigen expression level. *Journal of Hematology & Oncology*, 9(1), p.56. Available at: http://www.ncbi.nlm.nih.gov/pubmed/27439908 [Accessed September 30, 2018].

Song, D.-G. et al., 2011. In Vivo Persistence, Tumor Localization, and Antitumor Activity of CAR-Engineered T Cells Is Enhanced by Costimulatory Signaling through CD137 (4-1BB). *Cancer Research*, 71(13), pp.4617–4627. Available at: http://www.ncbi.nlm.nih.gov/pubmed/21546571 [Accessed October 19, 2018].

Di Stasi, A. et al., 2009. T lymphocytes coexpressing CCR4 and a chimeric antigen receptor targeting CD30 have improved homing and antitumor activity in a Hodgkin tumor model. *Blood*, 113(25), pp.6392–6402. Available at: http://www.ncbi.nlm.nih.gov/pubmed/19377047 [Accessed September 30, 2018].

Stasiłojć, G. et al., 2016. New perspectives on complement mediated immunotherapy. *Cancer Treatment Reviews*, 45, pp.68–75. Available at: https://linkinghub.elsevier.com/retrieve/pii/S0305737216000384 [Accessed October 19, 2018].

Steele, C.W. et al., 2016. CXCR2 Inhibition Profoundly Suppresses Metastases and Augments Immunotherapy in Pancreatic Ductal Adenocarcinoma. *Cancer cell*, 29(6), pp.832–845. Available at: http://www.ncbi.nlm.nih.gov/pubmed/27265504 [Accessed October 1, 2018].

Steele, C.W. et al., 2016. CXCR2 Inhibition Profoundly Suppresses Metastases and Augments Immunotherapy in Pancreatic Ductal Adenocarcinoma. *Cancer Cell*, 29(6), pp.832–845. Available at: http://dx.doi.org/10.1016/j.ccell.2016.04.014.

Steentoft, C. et al., 2018. Glycan-directed CAR-T cells. *Glycobiology*, 28(9), pp.656–669. Available at: http://www.ncbi.nlm.nih.gov/pubmed/29370379 [Accessed September 30, 2018].

van der Stegen, S.J.C., Hamieh, M. & Sadelain, M., 2015. The pharmacology of second-generation chimeric antigen receptors. *Nature Reviews Drug Discovery*, 14(7), pp.499–509. Available at: http://dx.doi.org/10.1038/nrd4597%5Cnhttp://www.nature.com/nrd/journal/v14/n7/pdf/nrd4597.pdf.

Stevenson, H.C. et al., 1987. Fate of gamma-interferon-activated killer blood monocytes adoptively transferred into the abdominal cavity of patients with peritoneal carcinomatosis. *Cancer research*, 47(22), pp.6100–3. Available at: http://www.ncbi.nlm.nih.gov/pubmed/3117363 [Accessed October 1, 2018].

Swain, S.M. et al., 2013. Pertuzumab, trastuzumab, and docetaxel for HER2-positive metastatic breast cancer (CLEOPATRA study): overall survival results from a randomised, double-blind, placebo-controlled, phase 3 study. *The Lancet Oncology*, 14(6), pp.461–471. Available at: http://www.ncbi.nlm.nih.gov/pubmed/23602601 [Accessed October 1, 2018].

Swain, S.M. et al., 2015. Pertuzumab, Trastuzumab, and Docetaxel in HER2-Positive Metastatic Breast Cancer. *New England Journal of Medicine*, 372(8), pp.724–734. Available at: http://www.ncbi.nlm.nih.gov/pubmed/25693012 [Accessed October 1, 2018].

Tasian, S.K. & Gardner, R.A., 2015. CD19-redirected chimeric antigen receptor-modified T cells: a promising immunotherapy for children and adults with B-cell acute lymphoblastic leukemia (ALL). *Therapeutic Advances in Hematology*, 6(5), pp.228–241. Available at: http://www.ncbi.nlm.nih.gov/pubmed/26425336 [Accessed September 30, 2018].

Tian, C. et al., 2017. Anti-CD138 chimeric antigen receptor-modified T cell therapy for multiple myeloma with extensive extramedullary involvement. *Annals of Hematology*, 96(8), pp.1407–1410. Available at: http://www.ncbi.nlm.nih.gov/pubmed/28577043 [Accessed September 30, 2018].

Till, B.G. et al., 2012. CD20-specific adoptive immunotherapy for lymphoma using a chimeric antigen receptor with both CD28 and 4-1BB domains: pilot clinical trial results. *Blood*, 119(17), pp.3940–3950. Available at: http://www.ncbi.nlm.nih.gov/pubmed/22308288 [Accessed September 30, 2018].

Tolaney, S.M. et al., 2015. Adjuvant Paclitaxel and Trastuzumab for Node-Negative, HER2-Positive Breast Cancer. *New England Journal of Medicine*, 372(2), pp.134–141. Available at: http://www.ncbi.nlm.nih.gov/pubmed/25564897 [Accessed October 1, 2018].

Tschumi, B.O. et al., 2018. CART cells are prone to Fas- and DR5-mediated cell death. *Journal for ImmunoTherapy of Cancer*, 6(1), p.71. Available at: http://www.ncbi.nlm.nih.gov/pubmed/30005714 [Accessed October 19, 2018].

Tseng, D., Vasquez-Medrano, D.A. & Brown, J.M., 2011. Targeting SDF-1/CXCR4 to

inhibit tumour vasculature for treatment of glioblastomas. *British Journal of Cancer*, 104(12), pp.1805–1809. Available at: http://www.ncbi.nlm.nih.gov/pubmed/21587260 [Accessed October 1, 2018].

Tsuchiya, S. et al., 1980. Establishment and characterization of a human acute monocytic leukemia cell line (THP-1). *International journal of cancer*, 26(2), pp.171–6. Available at: http://www.ncbi.nlm.nih.gov/pubmed/6970727 [Accessed October 3, 2018].

Varol, C., Mildner, A. & Jung, S., 2015. Macrophages: Development and Tissue Specialization. *Annual Review of Immunology*, 33(1), pp.643–675. Available at: http://www.annualreviews.org/doi/10.1146/annurev-immunol-032414-112220 [Accessed October 4, 2018].

Verma, S. et al., 2012. Trastuzumab Emtansine for HER2-Positive Advanced Breast Cancer. *New England Journal of Medicine*, 367(19), pp.1783–1791. Available at: http://www.ncbi.nlm.nih.gov/pubmed/23020162 [Accessed October 1, 2018].

Vonderheide, R.H. & Glennie, M.J., 2013. Agonistic CD40 Antibodies and Cancer Therapy. *Clinical Cancer Research*, 19(5), pp.1035–1043. Available at: http://www.ncbi.nlm.nih.gov/pubmed/23460534 [Accessed October 1, 2018].

Wallace, P.K. et al., 2001. Bispecific antibody-targeted phagocytosis of HER-2/neu expressing tumor cells by myeloid cells activated in vivo. *Journal of Immunological Methods*, 248(1–2), pp.167–182.

Wallace, P.K. et al., 2000. Production of macrophage-activated killer cells for targeting
of glioblastoma cells with bispecific antibody to FcgammaRI and the epidermal
growth factor receptor. *Cancer immunology, immunotherapy : CII*, 49(9), pp.493–
503. Available at: papers3://publication/uuid/9C003159-D4D8-4DA9-8AE3-
C01481E9FB23.

Wang, L.-C.S. et al., 2014. Targeting Fibroblast Activation Protein in Tumor Stroma with
Chimeric Antigen Receptor T Cells Can Inhibit Tumor Growth and Augment Host
Immunity without Severe Toxicity. *Cancer Immunology Research*, 2(2), pp.154–
166. Available at: http://www.ncbi.nlm.nih.gov/pubmed/24778279 [Accessed
September 30, 2018].

Wang, L. et al., 2016. Efficient tumor regression by adoptively transferred CEA-specific
CAR-T cells associated with symptoms of mild cytokine release syndrome.
OncoImmunology, 5(9), p.e1211218. Available at:
http://www.ncbi.nlm.nih.gov/pubmed/27757303 [Accessed September 30, 2018].

Wang, Y. et al., 2018. Blockade of CCL2 enhances immunotherapeutic effect of anti-
PD1 in lung cancer. *Journal of bone oncology*, 11, pp.27–32. Available at:
https://linkinghub.elsevier.com/retrieve/pii/S2212137417301422 [Accessed October
1, 2018].

Wang, Y. et al., 2014. Effective response and delayed toxicities of refractory advanced
diffuse large B-cell lymphoma treated by CD20-directed chimeric antigen receptor-
modified T cells. *Clinical Immunology*, 155(2), pp.160–175. Available at:

http://www.ncbi.nlm.nih.gov/pubmed/25444722 [Accessed September 30, 2018].

Weiskopf, K., 2017. Cancer immunotherapy targeting the CD47/SIRPα axis. *European Journal of Cancer*, 76, pp.100–109. Available at: http://www.ncbi.nlm.nih.gov/pubmed/28286286 [Accessed August 2, 2018].

Weiskopf, K. et al., 2016. CD47-blocking immunotherapies stimulate macrophage-mediated destruction of small-cell lung cancer. *Journal of Clinical Investigation*, 126(7), pp.2610–2620.

Weiskopf, K. et al., 2014. Engineered SIRP a Variants as. , 88(2013).

Weiskopf, K. & Weissman, I.L., 2015. Macrophages are critical effectors of antibodies therapies for cancer. *mABs*, (June 2015), pp.37–41.

Whitmore, M.M. et al., 2004. Synergistic Activation of Innate Immunity by Double-Stranded RNA and CpG DNA Promotes Enhanced Antitumor Activity. *Cancer Research*, 64(16), pp.5850–5860. Available at: http://www.ncbi.nlm.nih.gov/pubmed/15313929 [Accessed October 1, 2018].

Willingham, S.B. et al., 2012. The CD47-signal regulatory protein alpha (SIRPa) interaction is a therapeutic target for human solid tumors. *Proceedings of the National Academy of Sciences*, 109(17), pp.6662–6667. Available at: http://www.ncbi.nlm.nih.gov/pubmed/22451913 [Accessed October 3, 2018].

Wunderlich, M. et al., 2010. AML xenograft efficiency is significantly improved in NOD/SCID-IL2RG mice constitutively expressing human SCF, GM-CSF and IL-3.

Leukemia, 24(10), pp.1785–1788. Available at:

http://www.ncbi.nlm.nih.gov/pubmed/20686503 [Accessed August 6, 2018].

Yoshida, T. et al., 2016. All-trans retinoic acid enhances cytotoxic effect of T cells with

an anti-CD38 chimeric antigen receptor in acute myeloid leukemia. *Clinical &*

Translational Immunology, 5(12), p.e116. Available at:

http://www.ncbi.nlm.nih.gov/pubmed/28090317 [Accessed September 30, 2018].

Zhao, Y. et al., 2010. Multiple Injections of Electroporated Autologous T Cells

Expressing a Chimeric Antigen Receptor Mediate Regression of Human

Disseminated Tumor. *Cancer Research*, 70(22), pp.9053–9061. Available at:

http://www.ncbi.nlm.nih.gov/pubmed/20926399 [Accessed September 30, 2018].

Zheng, W. & Pollard, J.W., 2016. Inhibiting macrophage PI3Kγ to enhance

immunotherapy. *Cell Research*, 26(12), pp.1267–1268. Available at:

http://www.ncbi.nlm.nih.gov/pubmed/27834344 [Accessed October 1, 2018].

Zuccolotto, G. et al., 2014. PSMA-Specific CAR-Engineered T Cells Eradicate

Disseminated Prostate Cancer in Preclinical Models N. Lapteva, ed. *PLoS ONE*,

9(10), p.e109427. Available at: http://www.ncbi.nlm.nih.gov/pubmed/25279468

[Accessed September 30, 2018].